

ISTANBUL TECHNICAL UNIVERSITY ★ GRADUATE SCHOOL OF SCIENCE
ENGINEERING AND TECHNOLOGY

**STRUCTURAL ANALYSIS OF THIN/THICK COMPOSITE BOX BEAMS
USING FINITE ELEMENT METHOD**



M.Sc. THESIS

Buse Tuğçe TEMUÇİN

Department of Aeronautics and Astronautics

Aeronautical and Astronautical Engineering Programme

JULY 2020

ISTANBUL TECHNICAL UNIVERSITY ★ GRADUATE SCHOOL OF SCIENCE
ENGINEERING AND TECHNOLOGY

**STRUCTURAL ANALYSIS OF THIN/THICK COMPOSITE BOX BEAMS
USING FINITE ELEMENT METHOD**



M.Sc. THESIS

Buse Tuğçe TEMUÇİN

(511171105)

Department of Aeronautics and Astronautics

Aeronautical and Astronautical Engineering Programme

Thesis Advisor: Assist. Prof. Dr. Özge ÖZDEMİR

JULY 2020

İSTANBUL TEKNİK ÜNİVERSİTESİ ★ FEN BİLİMLERİ ENSTİTÜSÜ

**İNCE/KALIN KOMPOZİT KUTU KİRİŞLERİN SONLU ELEMANLAR
YÖNTEMİ İLE YAPISAL ANALİZİ**

YÜKSEK LİSANS TEZİ

Buse Tuğçe TEMUÇİN

(511171105)

Uçak ve Uzay Mühendisliği Anabilim Dalı

Uçak ve Uzay Mühendisliği Programı

Tez Danışmanı: Dr. Öğr. Üyesi Özge ÖZDEMİR

TEMMUZ 2020

Buse Tuğçe Temuçin, a M.Sc. student of İTÜ Graduate School of Science Engineering and Technology student ID 511171105, successfully defended the thesis entitled “STRUCTURAL ANALYSIS OF THE THIN/THICK COMPOSITE BOX BEAMS USING FINITE ELEMENT METHOD”, which she prepared after fulfilling the requirements specified in the associated legislations, before the jury whose signatures are below.

Thesis Advisor : **Assist. Prof. Dr. Özge ÖZDEMİR**
İstanbul Technical University

Jury Members : **Prof. Dr. Metin Orhan KAYA**

Prof. Dr. Osman Ergüven VATANDAŞ

Date of Submission : 15 June 2020

Date of Defense : 13 July 2020





To my family,



FOREWORD

First of all, I would like to offer my sincerest gratitude to my thesis advisor, Assist. Prof. Dr. Özge Özdemir who helped me to prepare and finish this project successfully. She has always been supportive leader for me to my academic progress and life. She also always encouraged me to come to better places in the future and helped me continue my studies, love my job and my life.

I am truly indebted thanks to Prof. Dr. Metin O. Kaya, who shared his knowledge of the plate finite element methods, for his guidance. He has created an important milestone in my academic life by encouraging me to research, work and not give up.

I thank my jury members, for taking their time to evaluate my thesis. Their ideas and suggestions were valuable and important to improve of this work.

Also, I would like to thank to my friend Hasan Kıyık for his support to me during my thesis process academically and morally. I would like to express thanks to my friends and colleagues who were with me in my graduate program and did not lose faith in me.

Above all, I would like to thank my dear family who has always been with me for years and empowers me to continue. Without them, I would not have been able to come to this point and be proud of the person I am. They supported me in every decision and shed light on my way with their ideas. I hope that the completion of my thesis will enable them to live this happiness and pride with me.

July 2020

Buse Tuğçe TEMUÇİN

Aeronautical Engineer



TABLE OF CONTENTS

	<u>Page</u>
FOREWORD	ix
TABLE OF CONTENTS	xi
ABBREVIATIONS	xiii
SYMBOLS	xv
LIST OF TABLES	xvii
LIST OF FIGURES	xix
SUMMARY	xxi
ÖZET	xxv
1. INTRODUCTION	1
1.1. Purpose of Thesis and Overview	1
1.2. Literature Review	2
2. EQUATIONS OF MOTION AND VIBRATION	5
2.1. Equations of Motion	5
2.2. Vibration	7
3. FINITE ELEMENT METHOD	11
3.1. Process of Obtaining Shape Functions	12
3.2. Shape functions for membrane element	13
3.3. Shape functions for thin plate bending element	15
3.4. Shape functions for thick plate bending element	18
4. PLATE TEORIES AND FORMULATIONS	21
4.1. The Kirchhoff-Love Theory	22
4.2. The Reissner-Mindlin Theory	26
5. COMPOSITE PLATES	35
6. FOLDED PLATES AND BOX BEAM	45
6.1. Folded Plates and Results	47
6.1.1. The isotropic plates	48
6.1.2. The composite laminated folded plates	53
6.2. Box Beams and Results	58

6.2.1. The isotropic box beam.....	59
6.2.2. The composite laminated box beam	62
7. CONCLUSIONS AND RECOMMENDATION	69
REFERENCES.....	71
CURRICULUM VITAE.....	73



ABBREVIATIONS

CPT	: Classical Plate Theory
DOF	: Degree of Freedom
EOM	: Equation of Motion
FEM	: Finite Element Method
FSDT	: First-Order Shear Deformation Theory
HSDT	: Higher-Order Shear Deformation Theory
KLPT	: Kirchhoff-Love Plate Theory
QLLL	: Quadrilateral, Bilinear Deflection, Bilinear Rotations and Linear Transverse Shear Strain Fields
RMPT	: Reissner-Mindlin Plate theory
SYM	: Symmetric



SYMBOLS

a	: Half Length of a Plate at X Axis
A	: Cross-sectional Area
b	: Half Length of a Plate at Y Axis
E	: Elastic Modulus of Material
G	: Shear Modulus of Material
L	: Length of a Plate/Box Beam
α	: Crank Angle
β	: Ratio of Plate Dimensions at Y/X axes/Crank Angle/Shear Stiffness Coefficient Constant
γ	: Shear Strain
δ	: Coefficient Matrix
ϵ	: Strain
η	: Dimensionless Y Axis of an Element
θ	: Ply Orientation Angle
θ_x	: Rotation about X Axis
θ_y	: Rotation about Y Axis
θ_z	: Rotation about Z Axis
κ	: Shear Correction Factor
λ	: Non-dimensional Natural Frequency
ν	: Poisson' Ratio
ξ	: Dimensionless X Axis of an Element
ρ	: Density of Material
ϱ	: Ratio of Plate Dimensions at X/Y axes
σ	: Stress
ϕ	: Rotation Angle
ω	: Natural Frequency



LIST OF TABLES

	<u>Page</u>
Table 4.1 : The square plate properties (Petty, 1990).	26
Table 4.2 : Comparison of natural frequencies (Hz) of the square plate.	26
Table 4.3 : The simply supported plate properties (Petty, 1990).	34
Table 4.4 : Comparison of non-dimensional $\lambda^{0.5} = h\omega\sqrt{(\rho/G)}$ natural frequencies of the square plate.	34
Table 5.1 : Comparison of non-dimensional $\lambda = \omega (L^2/h)\sqrt{(\rho/E_2)}$ natural frequencies of the composite simply supported square plate with $[0^\circ/90^\circ]_s$	44
Table 6.1 : The thin plate properties (Niyogi, et al, 1999).	49
Table 6.2 : Comparison of non-dimensional $\lambda = L\omega\sqrt{(\rho(1-\nu^2)/E)}$ natural frequencies of the 90° one folded thin clamped plate ($L=1.5m$).	49
Table 6.3 : Comparison of the non-dimensional $\lambda = L\omega\sqrt{(\rho(1-\nu^2)/E)}$ natural frequencies of the 90° two folded thin clamped plate ($L=2m$).	50
Table 6.4 : Comparison of natural frequencies (Hz) of the folded thin plates.	51
Table 6.5 : Comparison of natural frequencies (Hz) of the folded thick plates.	51
Table 6.6 : The composite plate properties with Material I (Niyogi, et al, 1999).	53
Table 6.7 : Comparison of non-dimensional natural frequencies of the composite $[30^\circ/-30^\circ/30^\circ]$ clamped thin plate with Material I.	54
Table 6.8 : Comparison of natural frequencies (Hz) of the composite clamped thin plate with Material I $[30^\circ/-30^\circ/30^\circ]$ stacking sequence.	54
Table 6.9 : The composite plate properties with Material II (Haldar & Sheikh, 2005).	56
Table 6.10 : Comparison of non-dimensional natural frequencies ($\lambda = L^2\omega\sqrt{(\rho/E_2)/h}$) of the one folded cantilever scomposite plate with Material II.	56
Table 6.11 : Comparison of natural frequencies (Hz) of the composite cantilever thick plate with Material I $[30^\circ/-30^\circ/30^\circ/30^\circ/-30^\circ/30^\circ]$ sequence.	57
Table 6.12 : The isotropic thin box beam properties with Material III (Ramkumar & Kang, 2013).	59
Table 6.13 : Comparison of natural frequencies (Hz) of the thin isotropic box beam with Material III.	60
Table 6.14 : Comparison of natural frequencies (Hz) of the thick isotropic box beam with Material III.	61
Table 6.15 : The composite laminated thin box beam properties with Material IV (Ramkumar & Kang, 2013).	63

Table 6.16 : Comparison of natural frequencies (Hz) of the composite thin box beam with Material IV.	64
Table 6.17 : The composite laminated box beam properties with Material V.	66
Table 6.18 : Comparison of natural frequencies (Hz) of the composite thin box beam with Material V $[0_3/90_2/0_3]$	67
Table 6.19 : Comparison of natural frequencies of the composite thick box beam with Material V $[0_3/90_2/0_3]$	68



LIST OF FIGURES

	<u>Page</u>
Figure 2.1 : Mass motion and its path.....	6
Figure 2.2 : Multi degree of freedom spring-mass-damper system (Rao, 1993).....	8
Figure 3.1 : Element and node numbering on box beam and plate.....	12
Figure 3.2 : 4-node quadrilateral element and node numbering (Augarde, 2004)....	12
Figure 3.3 : Polynomial coefficients of different type elements (Cook, et al., 2001).	13
Figure 3.4 : Membrane element (Petyt, 1990).	13
Figure 3.5 : Thin plate bending element (Oñate, 2013).....	16
Figure 3.6 : Thick plate bending elements representation (Oñate, 2013).	18
Figure 4.1 : Boundary conditions in plates (Oñate, 2013).....	22
Figure 4.2 : Kirchhoff-Love plate representation (Oñate, 2013).	22
Figure 4.3 : Bending element of plate (Petyt, 1990).....	23
Figure 4.4 : RMPT displacements and rotations (Oñate, 2013).....	27
Figure 4.5 : Gauss integration schemes based on elements (Hinton & Bicanic, 1979).	30
Figure 4.6 : Gauss sampling points and weight factors (Cook, et al., 2001).	31
Figure 4.7 : Assumed shear strain field (Oñate, 2013).	32
Figure 4.8 : The non-dimensional frequency convergence (Petyt, 1990).....	34
Figure 5.1 : Lamination representation with thicknesses (Oñate, 2013).	36
Figure 5.2 : Membrane element of plate (Petyt, 1990).	38
Figure 6.1 : Clamped one and two folded plate with crank angle α/β (Liu & Huang, 1992).	48
Figure 6.2 : Mode shapes of the cantilever one folded isotropic thin plate.	49
Figure 6.3 : Mode shapes of the cantilever two folded isotropic thin plate.....	50
Figure 6.4 : Mode shapes of the cantilever one folded isotropic thick plate.	52
Figure 6.5 : Mode shapes of the cantilever two folded isotropic thick plate.	52
Figure 6.6 : Ply stacking $[30^\circ/-30^\circ/30^\circ]$ of one fold and two folded composite thin plate with reference surface ($z=0$) and thickness respectively.....	54
Figure 6.7 : Mode shapes of the one fold composite plate with Material I.	55

Figure 6.8 : Mode shapes of two fold composite plate with Material I.	55
Figure 6.9 : The box beam representation.....	58
Figure 6.10 : Mode shapes of the clamped-free thin Material III isotropic box beam with deformed and undeformed shapes.....	60
Figure 6.11 : Mode shapes of the clamped-clamped thin isotropic box beam with Material III.	61
Figure 6.12 : Mode shapes of the thick clamped-free Material III isotropic box beam.	62
Figure 6.13 : Mode shapes of thick clamped-clamped Material III isotropic box beam.	62
Figure 6.14 : Mode shapes of the [45/45/45/45/45] composite clamped-free box beam.	65
Figure 6.15 : Mode shapes of the [45/45/45/45/45] composite clamped-clamped box beam.	65
Figure 6.16 : Mode shapes of the [90/90/90/90/90] composite clamped-free box beam.	65
Figure 6.17 : Mode shapes of the [90/90/90/90/90] composite clamped-clamped box beam.	66
Figure 6.18 : Mode shapes of the thin cantilever Material V composite box beam with undeformed and deformed shapes.....	67
Figure 6.19 : Mode shapes of the thick cantilever Material V composite box beam with undeformed and deformed shapes.....	68

STRUCTURAL ANALYSIS OF THIN/THICK COMPOSITE BOX BEAMS USING FINITE ELEMENT METHOD

SUMMARY

The aim of this master's thesis is to evaluate thin and thick composite box beams, which are accepted as folded plates, using the finite element method in terms of vibration and to develop a computer code. In order to make this assessment, folded plates and box beams were analyzed with certain plate theories using different materials, boundary conditions and variable plate thicknesses. This thesis consists of introduction, equation of motion and vibration, finite element method, plate theories, composite plates and folded plates and box beam formulation sections.

The introduction part is about general information of plates, box beams, vibration, materials and the use of finite elements method and the historical process of these studies. The literature studies on the emergence and development of plate theories are intended to provide the reader with a preliminary knowledge of their different uses. In addition, a general framework has been attempted to use Kirchhoff-Love and Reissner-Mindlin plate theories based on the length to thickness ratio of the plates.

Vibration is an important phenomenon in terms of structural integrity, strength and efficiency for box beams, shells and panels that make up the majority of aircraft today. It is therefore significant that natural frequencies can be obtained and evaluated. Especially, accepting composite beams as folded plates in obtaining process of natural frequency values will be a basic and different approach for composite thin walled beam theories.

The equation of motion and vibration section includes that the equation of motion (EOM) of different systems, the extraction of the characteristic equation that provides the frequencies of the systems from the EOMs, the phenomenon of vibration and its types. Thus, the necessity of using energy equations to find the mass and stiffness matrices which are required to obtain the natural frequency is explained through formulations. In this thesis, free vibration is discussed and structures are evaluated in this context.

Finite element method section describes the element selection, creating nodes and determining degrees of freedom to obtain the shape functions of the elements. Shape functions are defined as the displacement relationship between an element and the nodes. The displacements are expressed with polynomials based on the dimensionless coordinates of the element. In this study, the finite element method (FEM) was applied to the structure by selecting a four-node quadrilateral element. Besides, this element type was evaluated as a membrane, thin bending or thick bending element with different degree of freedom (DOF) and shape functions were found for them.

The plate theories form the basis of the finite element code and analysis in this study. Kirchhoff-Love Plate Theory (KLPT) is applied to thin plates, which has a length-to-thickness ratio greater than 10, comes more suitable form for isotropic homogeneous materials, since shear effects are neglected. According to KLPT, the in-plane displacements of material particles in the plate middle surface are smaller than the displacements in other direction. At the same time, the normal of the middle surface remains on the same curve and perpendicular to the plane throughout the movement. So, this theory is applied using a thin bending element and rotational displacements are dependent on vertical displacement.

The shape functions have been used to equalize the potential energy, which includes strain formulas of the bending element, and the classical energy equation from EOM. The same method was followed to equalize two different form of kinetic energy equations. Thus, the stiffness and mass matrices of an element are derived from the potential energy and kinetic energy expressions. A thin metal flat plate was considered as a case study and divided into elements, matrices for one element were transformed into general matrices with the summation method of the finite element method, and the stiffness and mass values of the entire structure were obtained. Then, boundary conditions were applied to these matrices and a reduction was made. The reduced global matrices were solved by applying Modal Analysis and the results obtained were compared with the experimental, analytical and FEM results in the literature to confirm the accuracy of the applied finite element formulation and the results were seen to converge.

Reissner-Mindlin plate theory (RMPT) takes into account the transverse shear effects and rotary inertia, unlike KLPT, so it is applied to thick plates which have length-to-thickness ratio is less than 10. As a reflection of transverse shear effects, it is as good in orthotropic material as in isotropic homogeneous materials. RMPT assumes that the normal of the mid surface is not perpendicular to the surface throughout the movement. This assumption makes rotational displacements independent from vertical displacement. The shape functions of the thick bending element have been used to obtain stiffness and mass matrices from energy equations.

While the structure becomes thinner, it is seen that a case called as shear locking, which makes the shear stiffness dominant, occurs in RMPT application. To overcome this case, shear stiffness must be reduced by methods such as Gauss reduced integration or use of Quadrilateral, Bilinear Deflection, Bilinear Rotations and Linear Transverse Shear Strain Fields (QLLL) elements that are based transverse shear strain fields. This makes the Mindlin theory applicable to thin plates. In the comparison study, the global matrices of a metal flat plate were obtained by adding two different stiffness matrices (bending and shearing) for one element, and the QLLL method was applied prior to the shear stiffness term. With the application of boundary conditions, the natural frequencies were found using the achieved code and the dimensionless results are compared with the analytical and FEM results in literature, and the commercial finite element program ABAQUS results where the same mesh size was used with the achieved code. It has been seen that the results are very close in this comparison.

The composite plates section mentioned the necessity of membrane effects in plate due to its material properties. Due to the existence of axial displacement, the DOF is taken to be 5. Thus, it was observed that bending, shear and membrane stiffness appeared to be depending on the layouts and angular orientations. In cases where the sequence is not balanced and symmetrical, the axial and bending forces act on each other and may form the membrane bending coupling stiffness.

Both Kirchhoff and Mindlin theories have been applied to the composite plates by adding in-plane stiffness and mass matrices. It was compared with the dimensionless frequency values in the literature and it was seen that Mindlin theory gave good results for thick plates but Kirchhoff was not sufficient. Similarly, close results were obtained from both theories in comparison of thin plate, but the code applied based on Mindlin theory converged more due to the shear effect along the cross section of the layers.

In the last part, thin/thick metal and composite folded plates and the box beams which are accepted as 4-folded plates, were analyzed with the codes obtained by the finite element method in the light of the information from the previous sections. The data were compared with the studies in the literature in order to verify and if the study was not found, it was modeled with the help of ABAQUS and compared with the results obtained here. The crank angle is considered as 90° in this thesis. The local axes of each face of the folded plates should be converted to a global axis to analyze easily. In order to get a suitable transformation, in-plane displacements and rotational movement on the vertical axis (drilling degree) are also considered as DOF. Thus, the structure had 6 degrees of freedom and their elements were transformed so that their stiffness and mass matrices were on the global axis. Thin/thick one and two folded composite and metal plates were evaluated, mode shapes and natural frequency values were calculated. Then, two theories were compared on different sizes of thin/thick composite and metal box beams.

As a result, it has been revealed that the frequency values decrease with decreasing thickness, the restricted degrees of freedom increase the frequency values and the different sequences affect the frequency values. Moreover, the membrane effects and the transverse shear effects are important in the folded and composite structures. In several comparisons, it was seen that these codes, which were created based on the finite element method in the Mathematica program, converge as ABAQUS package program. Thus, it has been shown that beams can be considered as folded plates and the main purpose of this thesis is to be able to analyze the structures with different plate theories and to obtain better results in terms of vibration. Many computer code have been written on this subject with different theories and application methods.



İNCE/KALIN KOMPOZİT KUTU KİRİŞLERİN SONLU ELEMANLAR YÖNTEMİ İLE YAPISAL ANALİZİ

ÖZET

Bu yüksek lisans tezinin amacı katlanmış plaka olarak kabul edilen ince ve kalın kompozit kutu kirişlerinin plaka teorileri ile titreşim açısından sonlu elemanlar yöntemi kullanılarak değerlendirilmesi ve bunu yapmayı sağlayan bir bilgisayar kodunun geliştirilmesidir. Bu değerlendirmenin yapılabilmesi için farklı malzemeler, sınır koşulları ve değişken plaka kalınlıkları kullanılarak öncelikli olarak plakalar, katlanmış plakalar ve kutu kirişler belirli plaka teorileri ile analiz edilmiştir.

Bu çalışmada; giriş bölümü, hareket denklemleri ve titreşime genel bakış, sonlu elemanlar formülasyonları, plaka teorileri yapısal formülasyonu, kompozit plaka formülasyonları ve katlanmış plakalar ile kutu kiriş formülasyonları olmak üzere altı ana bölüm yer almaktadır.

Giriş bölümünde genel olarak plakalar, kutu kirişler, titreşim, malzemeler ve sonlu elemanlar yönteminin kullanımından ve bu çalışmaların tarihsel süreci hakkında bilgi verilmektedir. Plaka teorilerinin ortaya çıkışı ve geliştirilmesi ile ilgili literatür çalışmalarına yer verilerek farklı kullanımları hakkında okuyucunun ön bilgiye sahip olması amaçlanmıştır. Ayrıca bu bölümde, plakaların kalınlıklarına göre sınıflandırılması ve bu sınıflandırmaya bağlı olarak farklı deplasman teorilerine ihtiyaç duyulduğu, Kirchhoff-Love ve Reissner-Mindlin plaka teorileri olarak bilinen teorilerin kullanım alanları hakkında genel bir çerçeve oluşturulmaya çalışılmıştır.

Günümüzde hava araçlarının büyük bir kısmını kutu kirişler, kabuklar ve paneller oluşturmaktadır. Bu nedenle, bunlar gibi özellikle kontrol yüzeylerinde ve aerodinamik yüzeylerde kullanılan yapılarda titreşim yapısal bütünlük, dayanım ve verimlilik açısından önemli bir olgudur. Titreşim yorulmaya ve çatlaklar gibi yapısal zararlara neden olabildiği için çoğunlukla hava aracında kaçınılmak istenen bir olay olarak kendini gösterebilir. Doğal frekansların elde edilerek değerlendirilebilmesi bu nedenle önem taşımaktadır. Özellikle ince/kalın cidarlı kompozit kirişlerin plakalar gibi değerlendirilerek sonlu elemanlar yöntemi ile bir bilgisayar kodu kullanılarak doğal frekans değerlerinin elde edilmesi ince cidarlı kompozit kiriş teorilerine temel ve alternatif bir yaklaşım olacaktır.

Hareket denklemleri ve titreşim bölümünün, ilk alt bölümünde enerji denklemlerinin bir cismin hareketine bağlı olarak elde edilmesi ve farklı serbestlik dereceli sistemlerin Hamilton prensibi ile hareket denklemlerinin çıkarılması gösterilmiştir. İkinci alt bölümünde ise sistemlerin frekanslarının elde edilmesini sağlayan karakteristik denklemin hareket denklemlerinden çıkartılması, titreşim olgusu ve tipleri anlatılmıştır.

Böylece doğal frekansı sonlu elemanlar yöntemi mantığına uygun olarak elde edebilmek için gereken kütle ve katılık matrislerinin sistemin hareketinden kaynaklı meydana geldiği ve bu değerlerin bulunabilmesi için enerji denklemlerinin kullanılması gerekliliği formülasyonlar aracılığıyla anlatılmıştır. Bu tez içerisinde serbest titreşim ele alınmış ve yapılar bu bağlamda değerlendirilmiştir.

Sonlu elemanlar yöntemi bölümünde eleman seçimi, düğüm noktalarının oluşturulması ve serbestlik derecelerinin belirlenmesi ile elemanların şekil fonksiyonlarının elde edilmesine yer verilmiştir. Şekil fonksiyonları bir elemanın deplasmanlarının düğüm noktalarındaki deplasman değerleri ile ilişkisini ifade eder. Bunu yaparken de elemanın boyutsuz eksenini baz alan polinomlarla deplasmanları tanımlar. Böylece daha önceki kısımlarda bahsedilen potansiyel ve kinetik enerji denklemlerinden çıkarılan katılık ve kütle matrislerinin, düğüm noktalarındaki değerlere göre açılımı sağlanmış olur ve seçilen elemanın matrisleri oluşturulabilir. Bu çalışmada, dört düğüm noktalı dörtgen eleman seçilerek yapıya sonlu elemanlar yöntemi uygulanmıştır. Ancak bu eleman farklı serbestlik dereceleri için membran, ince eğilme ve kalın eğilme elemanı olarak değerlendirilip şekil fonksiyonları bulunmuştur.

Plaka teorilerinin yapısal formülasyonları bu çalışmadaki sonlu elemanlar kodunun ve analizin temelini oluşturmaktadır. Kirchhoff-Love Plaka Teorisi (KLPT) yanal kayma deformasyonu etkileri ihmal edildiği için ince plakalara uygulanan bir plaka teorisidir ve bu ihmalden dolayı daha çok izotropik homojen malzemelere uygundur. Uzunluğunun kalınlığına oranı 10 dan büyük olan plakalar ince plaka olarak adlandırılmaktadır. Öncelikli olarak Kirchhoff-Love plaka teorisine (KLPT) göre plakanın orta yüzeyindeki malzeme tanecikleri dikey yönde hareket etmekte ve eksenel hareketleri diğer yöndeki hareketine göre küçük olduğu için ihmal edilmektedir.

Aynı zamanda hareket boyunca orta yüzeyin normalinin aynı eğri üzerinde ve yüzeye dik olarak kaldığı varsayılır. Bu yüzden, teori ince eğilme elemanı kullanılarak uygulanır ve dönme deplasmanları dikey yöndeki deplasmana bağlı olarak tanımlıdır. Eğilme elemanının şekil fonksiyonları ve düğüm noktalarındaki deplasmanları, gerinim formüllerini içeren potansiyel enerji denklemi ile hareket denklemlerinden gelen klasik potansiyel enerji denkleminin eşitlenmesinde kullanılmıştır. Kinetik enerji denklemlerinin eşitlenmesinde de aynı yöntem izlenmiştir. Böylece bu teori için bir elemanın katılık ve kütle matrisleri çıkartılmıştır. İnce, metal ve düz bir plaka örnek çalışma olarak ele alınarak elemanlara bölünmüş, bir eleman için tanımlanan matrisler sonlu elemanlar yönteminin toplama metodu ile global matrisler haline getirilmiş ve tüm yapının katılık ve kütle değerleri elde edilmiştir. Ardından sınır koşulları bu matrislere uygulanarak indirgeme yapılmıştır. İndirgenmiş global matrisler Modal Analiz uygulanarak çözülmüş ve elde edilen sonuçlar, uygulanan sonlu elemanlar yönteminin doğruluğunu teyit etmek amacıyla literatürdeki deneysel, analitik ve FEM sonuçları ile karşılaştırılmıştır ve sonuçların yakınsadığı görülmüştür.

Diğer bir plaka teorisi olan Reissner-Mindlin plaka teorisi (RMPT), KLPT den farklı olarak yanal kayma deformasyonu etkilerini ve dönme ataletini de hesaba katar bu nedenle de yanal kayma deformasyonu etkisinin kalınlık boyunca önemli olduğu kalın plakalara uygulanan bir plaka teorisidir. Kayma deformasyonu etkilerinin bir yansıması olarak ortotropik malzemede de izotropik homojen malzemelerde olduğu kadar iyi sonuç vermektedir. Uzunluğunun kalınlığına oranı 10 dan küçük olan plakalar kalın plaka olarak adlandırılmaktadır.

RMPT, Kirchhoff teorisindeki ana özellikleri aynen kabul etmesi ile birlikte, hareket boyunca orta yüzeyin normalinin yüzeye dik kalmadığını varsayar. Bu varsayım dönme deplasmanlarını dikey yöndeki deplasmandan bağımsız hale getirir. Bu teoride kalın eğilme elemanı kullanılmıştır. Kalın eğilme elemanının şekil fonksiyonları ve düğüm noktalarındaki deplasmanları, eksenel ve kayma gerinim formüllerini içeren potansiyel enerji denklemi ile hareket denklemlerinden gelen klasik potansiyel enerji denkleminin eşitlenmesinde kullanılmıştır. Kütle matrisinin eldesi için de kinetik enerji denklemleri eşitlenmiş ve bu kez dönme deplasmanından kaynaklanan etkiler de ortaya çıkmıştır. Böylece bu teori için bir elemanın hem eğilme hem de ve göz önünde bulundurulmuş yanal kayma deformasyonu etkilerinden dolayı oluşan katılık ve kütle matrisleri çıkartılmıştır.

Aynı zamanda yapı incelidikçe RMPT uygulamasında sorunlar olduğu ve frekans değerlerinin iyi sonuçlar vermediği görülür. Bunun nedeni kayma kilitlemesi olarak adlandırılan bir durumdur. Bu durum, azalan plaka kalınlığı sonucunda kayma katılığının dominant hale gelmesinden kaynaklanmaktadır.

Bu durumu engellemek için kayma katılığının indirgenmesi gerekir. Kayma kilitlemesini aşmak için Gauss integral indirgeme yöntemleri ya da QLLL adı verilen yanal kayma gerinim alanlarına bağlı eleman yapısı metodu kullanılmıştır. Böylece Mindlin teorisi ince plakalara da uygulanabilir hale getirilmiştir. Karşılaştırma çalışmasında metal düz bir plakanın global matrisleri KLPT ile aynı şekilde elde edilmiştir. Ancak bu sefer bir eleman için iki farklı katılık matrisi (eğilme ve kayma) bulunarak toplanmıştır ve kayma katılığı için öncesinde QLLL metodu uygulanmıştır. Aynı şekilde bağımsız dönme deplasmanları da kütle matrisini farklılaştırmıştır. Sınır şartlarının bu matrislere uygulanarak indirgenmesi ile yapının doğal frekansları hazırlanan modal analiz kodu uygulanarak bulunmuş ve boyutsuzlaştırılmış sonuçlar, literatürdeki analitik, FEM sonuçları ve ticari sonlu elemanlar programı ABAQUS ile aynı ağ boyutunda modellenerek buradan da alınan boyutsuz frekans değerleri ile karşılaştırılmıştır ve sonuçların çok yakın olduğu görülmüştür.

Kompozit plakalar bölümünde; kompozit malzemelerin özelliklerinden, katmanların diziliminden ve kompozit malzeme yapısından kaynaklı olarak membran etkilerinin görüldüğünden yani eksenel yer değiştirmenin ihmal edilemediği ve eğilme etkisinin daha baskın olmadığından bahsedilmiştir. Böylece katman dizilimlerine ve açısal yönelimlerine bağlı olarak eğilme, kayma, eksenel katılıklarının ortaya çıktığı görülmüştür. Dizilimin dengeli ve simetrik olmaması gibi durumlarda eksenel ve eğilme kuvvetleri birbirleri üzerine etki ederler ve membran eğilme birleşik katılığını oluşturabilirler. Bu katılıklar katman dizilimlerine bağlı olarak hem eğilme hem de membran elemanının beraber kullanılması ile elde edilmişlerdir. Serbestlik derecesi, eksenel yer değiştirme kabulü nedeniyle diğer plakalardan farklı olarak 5 olarak alınmıştır. Hem Kirchhoff hem de Mindlin teorileri, bu plakalara eksenel katılık ve kütle matrisleri de hesaplanıp toplanarak uygulanmıştır. Bunun sonucu olarak değişken kalınlıklarda kompozit plakalar iki teori ile modal analiz yapılarak değerlendirilmiştir. Literatürdeki boyutsuz frekans değerleri ile karşılaştırılmış ve kalın plakalar için Mindlin teorisinin iyi sonuç verdiği ancak Kirchhoff 'un yeterli olmadığı görülmüştür. Aynı şekilde ince plaka için yapılan kıyaslamada da iki teoriden de yakın sonuçlar alınmış ancak katmanların yanal kesiti boyunca kayma etkisinden dolayı Mindlin teorisine bağlı uygulanan kod daha fazla yakınsamıştır.

Son bölümde ince/kalın metal ve kompozit katlanmış plakalar ve 4 katlamalı plaka gibi kabul edilmiş olan kutu kirişler daha önceki bölümlerden elde edilen bilgiler ışığında sonlu elemanlar yöntemi ile elde edilen kodlarla analiz edilmiştir. Veriler doğrulamak amacı ile literatürdeki çalışmalarla karşılaştırılmış, çalışma bulunamadığı takdirde ABAQUS yardımı ile modellenerek buradan alınan sonuçlarla kıyaslanmıştır.

Belirli bir açı ile katlanmış plakalarda, plakalar farklı lokal eksenlerde yer aldıkları için sonlu elemanlarla analiz yöntemi uygulanırken açık bir zar gibi düşünülerek katlanmış plakanın açıldığı var sayılmalı ve global bir eksen baz alınarak katlanmış plakaların her yüzünün lokal eksenlerinin bu global eksene dönüşümü yapılmalıdır. Bu dönüşümün sağlıklı olabilmesi açısından düzlem içi yer değiştirmeleri ve dikey eksenlerdeki dönme hareketi de serbestlik derecesi olarak dikkate alınmıştır. Bu dönme hareketi beraberinde tekillik problemi getirirse de sıfır olan ve z eksenine etrafındaki dönme etkisinden gelen köşegen elemanlarının çok küçük değerlere eşitlenmesi ile bu durum giderilmiştir. Böylece yapı 6 serbestlik derecesine sahip olmuş ve plakalar arasındaki açıyla ilişkilendirilen bir dönüşüm matrisi yardımı ile plaka elemanlarının katılık ve kütle matrisleri global eksende olacak şekilde dönüştürülmüştür. Ardından, yukarıda bahsedilen düz plakalarda izlenen yol izlenmiştir.

Bu tezde katlama açısı 90° olarak kabul edilmiş ince/kalın tek ve çift katlamalı kompozit ve metal plakalar değerlendirilmiş, mod şekilleri ve doğal frekans değerleri çıkartılmıştır. Ardından farklı boyutlarda ince/kalın kompozit ve metal kutu kirişler üzerinde iki teori de kıyaslanmıştır. Farklı sınır koşulları, malzeme özellikleri, katman dizilimleri ve kalınlık değişiminin titreşime etkisi gösterilmiştir. Farklı boyutlardaki kutu kirişlerin mod şekilleri değerlendirildiğinde, kısa kirişlerin daha erken burulma moduna girdiği ve yapısının bozulduğu gözlemlenmiştir.

Sonuç olarak, yapı inceldikçe frekanslarda düşüş olduğu, kısıtlanan serbestlik derecelerinin frekansı arttırdığı, farklı dizilimlerin frekans değerlerini etkilediği, membran etkilerinin ve yanal kayma etkilerinin katlanmış yapılarda önemli olduğu ortaya çıkmıştır. Birçok kıyaslamada Mathematica programında sonlu elemanlar yöntemine dayalı olarak oluşturulan bu kodların, ABAQUS paket programı kadar iyi yakınsadığı görülmüştür. Böylece, kirişlerin katlanmış plakalar olarak kabul edilerek değerlendirilebildiği gösterilmiş ve bu tezin asıl amacı olan yapıların farklı plaka teorileri ile analiz edilebilmesi ve titreşim açısından daha iyi sonuçlar elde edilebilmesi konusunda başarılı olunmuştur. Bu konuda çok sayıda farklı teori ve uygulama yöntemleri ile bilgisayar kodu yazılmıştır.





1. INTRODUCTION

Plates are flat structures which has thickness is smaller than other dimensions. They are used for many structure by folding such as skins or boxes and panels of air vehicle. All plate theories provide help to understand thin or thick walled frameworks.

Box beams can be considered as a four-fold plate or four plates joined by their edges. The box beam structures are generally used in aviation especially in terms of wings and helicopter blades.

The changeable structural properties of composites provide them privilege to be elected in terms of performance. It has been possible to gain advantage about weight and strength in fiber reinforced layer composite applications by controlling the layer angle and order, and with this adaptive structure, the folded plate structure applications have increased. The use of lighter and higher-strength structures, by evaluating the strength and vibration aspects of the structures in aircraft, has gained more importance from the past to the present.

1.1. Purpose of Thesis and Overview

The main purpose of this study is to examine the box beams structurally and evaluate them in terms of vibration using a folded plate approach by FEM coding. In this study, a box beam is considered as a four folded plate and vibration properties were examined with the use of different materials. Frequencies are used when describing dynamic properties of structure and efficiency is connected these values. Therefore, mode shapes and natural frequencies are evaluated in this study.

Thickness to length ratios and material properties of plates play an important role in deciding which theory to choose. Noor (1972) suggested Reissner-Mindlin method for composite structures especially in the case of thick plates. At the same time, Oñate (2013) classify plates according to their length-to-thickness ratio and while Kirchhoff-Love assumptions are suitable for thin plates, Reissner-Mindlin assumptions are suitable for thick ones.

In this thesis, Kirchhoff-Love plate theory (KLPT) is applied to thin isotropic homogenous and to composite plates. Also, Reissner-Mindlin plate theory (RMPT) is applied to plates that have different thicknesses and materials. These plate theories are used to analyze the box beam structures. The Reissner-Mindlin theory is actually suitable for thick plates and box beams because shear locking problems begin to appear as the plate becomes thinner. It is aimed to get better results by using some reduction methods like shear strain area assumptions. Examining the vibration characteristics of both thin and thick box beams was a priority. Since these structures are used at key points in an aircraft, they may be exposed to various aero elastic effects such as flutter. For this reason, it is important to obtain the vibration values.

Both plate theories are assumed to have three DOF, since the middle surface accepts the reference plane as homogeneous and isotropic plates and the axial stresses at this surface are accepted to be zero for flat plates (Oñate, 2013).

Folded plates lie at different planes in space. Due to the use of different local axes in the folded or joined plates, it has been observed that the in-plane effects should also be taken into account and axial stresses are also taken into consideration. As a result, a system with 5 DOF was reached and the general mass and stiffness matrices were expanded to 6 DOF by adding the degree of rotation, which is the rotation about the vertical axis. The flat, one folded, two folded plates and box beam natural frequencies are obtained for isotropic, homogeneous material. Then, the same procedure is repeated for composite laminated plate.

A FEM approach code is written by using Wolfram Mathematica program to calculate natural frequencies of the different models of plates and box beams. Besides, the structures are modeled and analyzed by using ABAQUS package program. Obtained results from present code are compared with ABAQUS results and literature data.

1.2. Literature Review

The first studies are about vibration of thin plates by Euler at the 17th century and this studies have been improved by Bernoulli with only considered membrane effects. The first theory of plate bending is developed by Gustav R. Kirchhoff at the 18th century using Bernoulli's beam approaches.

Also, Love was working about elasticity theory at the same time. Reissner improved these studies by the shear effects, when Mindlin added a rotary inertia. Generation to generation, these theories tried to be developed with different solution methods such as finite difference, finite strip etc. (Szilard, 2004).

According to Nguyen-Van, et al. (2008), dynamic characteristics are very significant for structures in aerospace applications especially for control surfaces of air vehicles. The plates play increasingly significant role, so their natural frequencies also need to be analyzed and evaluated for proper design. Petyt (1990), performed vibration analysis of stiffened plates and folded plate structures, which include box beam structure.

Vibration is the mechanical oscillation of a body from equilibrium condition. It is a very significant phenomena for engineering structures. Especially, extreme values of vibration create devastating cases. So, most of the vibration studies are tend to reduce vibration. Under these conditions, engineers need vibration data of the systems before finalizing the design of the structures to achieve appropriate structure designs (Chakraverty, 2009).

Actually plates vibrate in-plane and also out of plane (flexural), although the plate theories neglect membrane effects. This is because bending is more dominant than membrane effects created by in-plane vibration (Petyt, 1990).

Thin walled cantilever folded plates are studied by Irie, et al. (1984) according to Love theory and compare Ritz method by the way of mode shapes. Besides, Niyogi, et al. (1999) studied on folded laminated plates and their vibration characteristics based on Irie and friends' results. They analyzed by using finite element method with first order shear deformation theory which is called as Reissner-Mindlin approach.

The Reissner-Mindlin approach has some deviations which is called as shear locking problem on thin structures owing to domination of shear and over stiffness. In another study, splines were used to apply the used elements, but it was observed that the shear-locking problem continued. In order to overcome this problem, some kind of stabilization technique has been applied in theory. This technique is a study with reduced integrations (Thai, et al., 2012).

It has been observed in studies with different materials that mechanics of composites effect the behavior of plates or shells and the theories that are currently in use need to be arranged and studied accordingly. The laminated structures are formulated different from isotropic and homogenous materials. Because the points of plate middle plane can move in the plane direction and this creates membrane results and coupling between bending and axial effects. So, in-plane displacements are taken into account (Oñate, 2013).

In different work, the Kirchhoff-Love theory, is called as classical plate theory, has been compared with the FSDT according to accuracy of fundamental frequencies of skew-symmetric laminations. Different thickness ratios are evaluated and Reissner method was found to be better because of shear deformations on lamina (Noor, 1972). All of these studies can be based on different solution and analysis methods but generally, finite element method is the most widely used in engineering problems.

Finite element method (FEM) is a numerical process used in engineering studies such as fluid mechanics, solid mechanics etc. It is used to obtained approximate solutions or forces and displacements of frameworks with respect to discrete and continuum elements. This method provides so many advantages for asymmetrical shaped, different materials or complex boundary conditions to reduced simple works (Segerlind, 1984).

FEM, separate the region which are finite elements between nodes. Then, equation of system specified, developed and solved. According to Petyt (1990) studies, the plate divided into finite elements are triangles, rectangles and quadrilaterals to analyze frequencies of complex structures such as aircraft and ships. These elements are used to synthesize axial forces and dynamic loads normal to middle plane.

2. EQUATIONS OF MOTION AND VIBRATION

2.1. Equations of Motion

The equations of motion are obtained from Newton's second law where the rate of change of momentum of a body is directly proportional to the force acted and it is given by

$$m \frac{d^2 u}{dt^2} = f \quad (2.1a)$$

$$f - m\ddot{u} = 0 \quad (2.1b)$$

where, u is the displacement, m is a mass, t is the time and f is the force. The system is represented in Figure 2.1.

According to Hamilton's principle, the work is to move a body of mass m from one point to another. If this work is done with a conservative force, it depends on the position of the two location points, but if it is done with non-conservative forces, it depends on the path of the body. The conservative force work is obtained by potential energy change of a system like shown in equations (2.2), (2.3) and (2.4);

$$U(\vec{r}) = \int_{\vec{r}}^{\vec{r}_0} \vec{f} \cdot d\vec{r} \quad (2.2)$$

$$W_c = \int_{\vec{r}_1}^{\vec{r}_2} \vec{f} \cdot d\vec{r} = \int_{\vec{r}_1}^{\vec{r}_0} \vec{f} \cdot d\vec{r} - \int_{\vec{r}_2}^{\vec{r}_0} \vec{f} \cdot d\vec{r} = -(U(\vec{r}_2) - U(\vec{r}_1)) \quad (2.3)$$

$$\delta W_c = -\delta U \quad (2.4)$$

where U is the potential energy, W_c is the conservative work and r_0 , r_1 and r_2 are position vectors (Petyt, 1990). If an elastic spring stretched to enough to displace by a force,

$$f = -ku \quad (2.5)$$

$$U = \int_u^0 f \cdot du \quad (2.6a)$$

$$U = \int_u^0 -k \cdot u \cdot du = \frac{1}{2} ku^2 \quad (2.6b)$$

where k is the stiffness of spring.

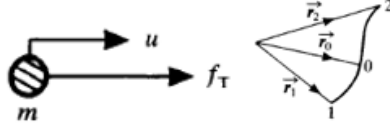


Figure 2.1 : Mass motion and its path.

The equilibrium condition is defined by Newton's first law as an object which is rest will be at rest or if it is in motion, it will continue moving. So, external forces on body are balanced. Petyt (1990) mentioned that if the system is in equilibrium condition, based on virtual displacements principle, total work will be zero. When applying the principle of virtual displacements to the system in Figure 2.1, and the following equations are obtained

$$f\delta u - m\ddot{u}\delta u = 0 \quad (2.7)$$

$$m\ddot{u}\delta u = m \frac{d}{dt}(\dot{u}\delta u) - m\dot{u}\delta\dot{u} = m \frac{d}{dt}(\dot{u}\delta u) - \delta\left(\frac{1}{2}m\dot{u}^2\right) \quad (2.8)$$

$$T = \frac{1}{2}m\dot{u}^2 \quad (2.9)$$

where T is the kinetic energy of the system. So,

$$\delta W - m \frac{d}{dt}(\dot{u}\delta u) + \delta T = 0 \quad (2.10)$$

$$\delta u = 0 \text{ at } t = t_1 = t_2 \quad (2.11)$$

$$\int_{t_1}^{t_2} (\delta W + \delta T) dt = \int_{t_1}^{t_2} m \frac{d}{dt}(\dot{u}\delta u) dt = 0 \quad (2.12a)$$

$$\int_{t_1}^{t_2} (\delta W + \delta T) dt = \int_{t_1}^{t_2} (\delta W_c + \delta W_{nc} + \delta T) dt \quad (2.12b)$$

where W_{nc} is the work done by non-conservative forces.

$$\delta W_{nc} = (f - c\dot{u})\delta u \quad (2.13)$$

$$\int_{t_1}^{t_2} (-\delta U + \delta W_{nc} + \delta T) dt = 0 \quad (2.14)$$

It gives the equations of motion of the system when c is the damping coefficient. If equation 2.14 is combined with energy equations,

$$\int_{t_1}^{t_2} \left(-\frac{\partial U}{\partial u}\delta u + (f - c\dot{u})\delta u + \frac{\partial T}{\partial \dot{u}}\delta\dot{u}\right) dt = 0 \quad (2.15)$$

$$\int_{t_1}^{t_2} \frac{\partial T}{\partial \dot{u}} \delta \dot{u} dt = \left[\frac{\partial T}{\partial \dot{u}} \delta u \right]_{t_1}^{t_2} - \int_{t_1}^{t_2} \frac{d}{dt} \left(\frac{\partial T}{\partial \dot{u}} \right) \delta u dt = - \int_{t_1}^{t_2} \frac{d}{dt} \left(\frac{\partial T}{\partial \dot{u}} \right) \delta u dt \quad (2.16)$$

$$\int_{t_1}^{t_2} \left(-\frac{\partial U}{\partial u} + (f - c\dot{u}) - \frac{d}{dt} \left(\frac{\partial T}{\partial \dot{u}} \right) \right) \delta u dt = 0 \quad (2.17)$$

Total work equations turn,

$$\frac{\partial U}{\partial u} + (c\dot{u}) + \frac{d}{dt} \left(\frac{\partial T}{\partial \dot{u}} \right) = f \quad (2.18)$$

Lagrange equation and it gives

$$m\ddot{u} + c\dot{u} + ku = f \quad (2.19)$$

as equation of system.

At multi-DOF system, the displacements are described as independent generalized coordinates q and kinetic energy and strain energy (potential energy) can be written in matrix format as shown

$$T = \frac{1}{2} [\dot{q}]^T [M] [\dot{q}] \quad (2.20)$$

$$U = \frac{1}{2} [q]^T [K] [q] \quad (2.21)$$

$$\delta W_{nc} = ([F] - [C][\dot{q}]) \delta q \quad (2.22)$$

where $[q]$, $[\dot{q}]$, $[F]$, $[M]$ and $[K]$ are displacement vector, velocity vector, external forces, mass and stiffness matrices, respectively (Petyt, 1990). Lagrange equation of multi DOF system is expressed as

$$[M][\ddot{q}] + [C][\dot{q}] + [K][q] = [F] \quad (2.23)$$

2.2. Vibration

If the system vibrates after the first disturbance without any external force effect, vibration type is called as free vibration. If any external force acts on the system repeatedly, this type is called as forced vibration. Depending on the energy lost during oscillation, vibration is classified as two types, damped and undamped. It is also classified according to whether it is linear or random (Rao, 1993).

The analysis of vibration begins with mathematical modelling and then continues with evaluating governing equations. Generally, the vibration systems are modelled as spring-mass-damper systems because modeling complex systems with simple approaches is important in terms of ease of solution.

The multi DOF systems are shown as Figure 2.2 and equations of motion 2.9, 2.6b and 2.13 are obtained as mentioned in the previous chapter.

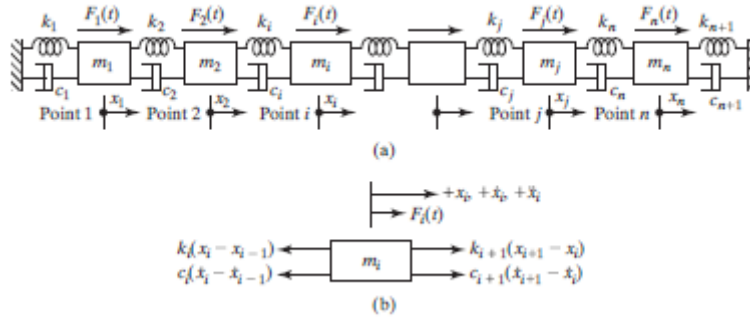


Figure 2.2 : Multi degree of freedom spring-mass-damper system (Rao, 1993).

The equations of motion can be written as follows

$$T = \frac{1}{2} m_1 \dot{u}_1^2 + \frac{1}{2} m_2 \dot{u}_2^2 + \dots + \frac{1}{2} m_n \dot{u}_n^2 \quad (2.24)$$

$$U = \frac{1}{2} k_1 \dot{u}_1^2 + \frac{1}{2} k_2 \dot{u}_2^2 + \dots + \frac{1}{2} k_n \dot{u}_n^2 \quad (2.25)$$

$$\delta W_{nc} = ((f_1 - c_1 \dot{u}_1) + (f_2 - c_2 \dot{u}_2) + \dots + (f_n - c_n \dot{u}_n)) \delta u \quad (2.26)$$

Lagrange equation and it gives

$$\sum m_i \ddot{u}_i + c_i \dot{u}_i + k_i u_i = \sum f_i \quad (2.27)$$

as equation of system.

In this thesis, undamped free vibration is examined to obtain natural frequencies of system. Lagrange equation of multi DOF system under free vibration is converted from equation 2.23 to

$$[M][\ddot{q}] + [K][q] = 0 \quad (2.28)$$

Laplace transforms are used for this equation to obtain natural frequency and characteristic equation of system. The displacement is assumed to be

$$q(t) = Ae^{st} \quad (2.29)$$

where A and s are constants. Substitution of assumption into EOM (equation of motion) gives characteristic equation

$$Ae^{st}([M]s^2 + [K]) = 0 \quad (2.30a)$$

$$([M]s^2 + [K]) = 0 \quad (2.30b)$$

The natural frequencies are ω_n (Rao, 1993);

$$s = \mp i \omega_n \text{ and } s^2 = -\omega_n^2 \quad (2.31)$$

$$|[K] - [M] \omega_n^2| = 0 \quad (2.32a)$$

$$[K]^{-1}[M] = \omega_n^2 \text{ and } \omega_n = \sqrt{[K]^{-1}[M]} \quad (2.32b)$$

The n DOF brings n natural frequency and a mode shape will be obtained for each natural frequency.



3. FINITE ELEMENT METHOD

Finite element displacement method has more common usage field in engineering applications when compare with analytical methods because of defining complex structures easily. Especially, vibration problems often use this method to obtain mode shapes and natural frequencies.

This method models the structure by following these steps respectively;

- Divide the structure into equal parts called elements and create points which are called nodes on the structure. Number the elements and nodes on the structure. An example of dividing and numbering the plate and box-beam elements for a 4-noded quadrilateral element is given in Figure 3.1.
- Assign a certain DOF to each node to specify displacement and rotations of the structure.
- Define functions for each of DOF. Each displacement of the structure will have been expressed using these defined functions at node points. These expressions are called shape functions.
- Solve the problems by applying shape functions to the energy expressions.

This method also forms the basis of various computer package programs such as ABAQUS, NASTRAN/PATRAN etc. For instance, in ABAQUS after modeling the structures the values such as vibration, displacement and stresses can be obtained by dividing them into elements.

At the same time, in this thesis, while the frequencies are obtained through the mentioned package programs, the code is developed in Mathematica program based on the finite element method and the model is analyzed in the light of these information. For the modelling of the plates, 4-noded quadrilateral 2D elements are used and their shape functions are obtained based on types of elements.

Following the steps of the finite element method, stiffness and mass are obtained by taking an element as a reference. After that, the summation method helps adding the matrices calculated for an element as reference for each element in the same plane and adding them to each other with the necessary operations so that the matrices turn into the global stiffness and mass matrix of the entire structure.

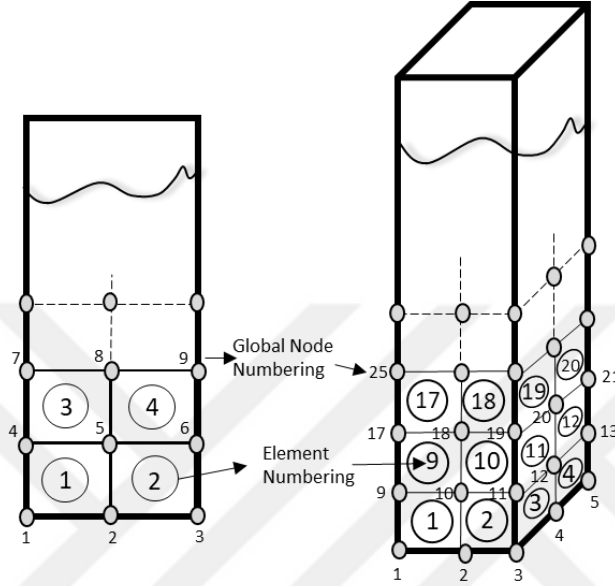


Figure 3.1 : Element and node numbering on box beam and plate.

3.1. Process of Obtaining Shape Functions

In this thesis, one of the 4-noded-quadrilateral element is used for analysis of the plates fundamentally like in Figure 3.2. It is called Q4 element and has four nodes which are placed at the corners and rectangular shape. When the X axis is associated with dimensionless ξ axis, the Y axis is associated with dimensionless η axis and the relationship between these axes can be given in equation 3.1. Also, different types of elements use different polynomials while describing DOF at dimensionless axes like given in Figure 3.3.

$$\xi = \frac{x}{a} \quad \text{and} \quad \eta = \frac{y}{b} \quad (3.1)$$

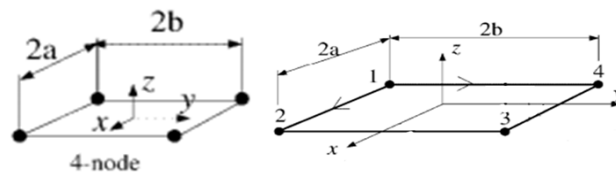


Figure 3.2 : 4-node quadrilateral element and node numbering (Augarde, 2004).

Different types of quadrilateral elements are also used in special cases of plates such as shear locking phenomena. For this study, QLLL (quadrilateral, bilinear deflection, bilinear rotations and linear transverse shear strain fields) method and Gauss integration method are chosen for application on Q4 element during reduced integration process of shear element stiffness for isotropic and composite structures respectively. Detailed information on the use of this element will be described in Section 4.

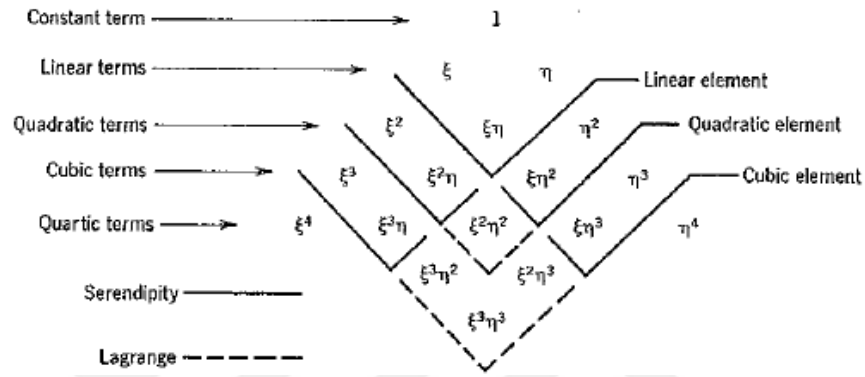


Figure 3.3 : Polynomial coefficients of different type elements (Cook, et al., 2001).

3.2. Shape functions for membrane element

Firstly, when the element is considered in-plane, it can easily be seen that the membrane effects are dominant. There are 2 DOF which are u and v displacements, on each node for in-plane plate analysis and it can be seen in Figure 3.4 for membrane element.

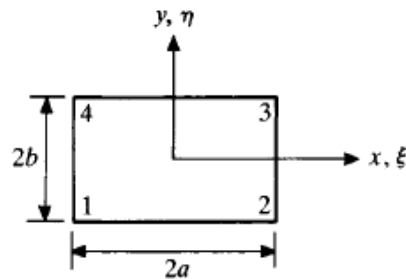


Figure 3.4 : Membrane element (Petyt, 1990).

Cook, et al. (2001) stated that for the 4-node quadrilateral element, total DOF is eight and it requires functions that have 8 unknowns. Each displacement must have bilinear functions with 4 terms as equations 3.2a and 3.2b.

$$u = a_1 + a_2\xi + a_3\eta + a_4\xi\eta = [1 \quad \xi \quad \eta \quad \xi\eta] \begin{Bmatrix} a_1 \\ a_2 \\ a_3 \\ a_4 \end{Bmatrix} \quad (3.2a)$$

$$v = a_5 + a_6\xi + a_7\eta + a_8\xi\eta = [1 \quad \xi \quad \eta \quad \xi\eta] \begin{Bmatrix} a_5 \\ a_6 \\ a_7 \\ a_8 \end{Bmatrix} \quad (3.2b)$$

Equations can be expanded for 4 node displacements as follows,

$$\begin{Bmatrix} u_1 \\ u_2 \\ u_3 \\ u_4 \end{Bmatrix} = \begin{bmatrix} 1 & \xi_1 & \eta_1 & \xi_1\eta_1 \\ 1 & \xi_2 & \eta_2 & \xi_2\eta_2 \\ 1 & \xi_3 & \eta_3 & \xi_3\eta_3 \\ 1 & \xi_4 & \eta_4 & \xi_4\eta_4 \end{bmatrix} \cdot \begin{Bmatrix} a_1 \\ a_2 \\ a_3 \\ a_4 \end{Bmatrix} \quad (3.3a)$$

$$\{u\} = [Rm] \cdot \{a\} \quad (3.3b)$$

$$\{a\} = [Rm]^{-1} \cdot \{u\} \quad (3.3c)$$

$$u = [1 \quad \xi \quad \eta \quad \xi\eta] [Rm]^{-1} \{u\} \quad (3.3d)$$

where $\xi = -1$ and $\eta = -1$ at node 1, $\xi = 1$ and $\eta = -1$ at node 2, $\xi = 1$ and $\eta = 1$ at node 3, $\xi = -1$ and $\eta = 1$ at node 4. Rm coefficient matrix can be obtained as,

$$[Rm] = \begin{bmatrix} 1 & -1 & -1 & 1 \\ 1 & 1 & -1 & -1 \\ 1 & 1 & 1 & 1 \\ 1 & -1 & 1 & -1 \end{bmatrix} \quad (3.4)$$

Secondly, the displacements u and v can be written using N_i shape functions,

$$u = \sum_{i=1}^4 N_i u_i \quad \text{and} \quad v = \sum_{i=1}^4 N_i v_i \quad (3.5)$$

If these expressions are expanded to matrix forms,

$$u = [N_1 \quad N_2 \quad N_3 \quad N_4] \begin{Bmatrix} u_1 \\ u_2 \\ u_3 \\ u_4 \end{Bmatrix} \quad (3.6a)$$

$$v = [N_1 \quad N_2 \quad N_3 \quad N_4] \begin{Bmatrix} v_1 \\ v_2 \\ v_3 \\ v_4 \end{Bmatrix} \quad (3.6b)$$

$$\begin{Bmatrix} u \\ v \end{Bmatrix} = \begin{bmatrix} N_1 & 0 & N_2 & 0 & N_3 & 0 & N_4 & 0 \\ 0 & N_1 & 0 & N_2 & 0 & N_3 & 0 & N_4 \end{bmatrix} \begin{Bmatrix} u_1 \\ v_1 \\ u_2 \\ v_2 \\ u_3 \\ v_3 \\ u_4 \\ v_4 \end{Bmatrix} \quad (3.6c)$$

Shape function relations are obtained and it can be seen that the displacements use the same shape functions. Combining u expressions give the shape functions as,

$$[N_1 \ N_2 \ N_3 \ N_4] = [1 \ \xi \ \eta \ \xi\eta][Rm]^{-1} \quad (3.7)$$

So, general shape function terms can be given like below.

$$N_i = \frac{1}{4}(1 + \xi_i \xi)(1 + \eta_i \eta) \quad (3.8)$$

Finally, if dimensionless coordinates of nodes at X and Y axis are substituted into general equation, shape functions for each node can be seen like

$$N_1 = \frac{1}{4}(1 - \xi)(1 - \eta) \quad (3.9a)$$

$$N_2 = \frac{1}{4}(1 + \xi)(1 - \eta) \quad (3.9b)$$

$$N_3 = \frac{1}{4}(1 + \xi)(1 + \eta) \quad (3.9c)$$

$$N_4 = \frac{1}{4}(1 - \xi)(1 + \eta) \quad (3.9d)$$

where $\xi_1 = -1$ and $\eta_1 = -1$ at node 1, $\xi_2 = 1$ and $\eta_2 = -1$ at node 2, $\xi_3 = 1$ and $\eta_3 = 1$ at node 3, $\xi_4 = -1$ and $\eta_4 = 1$ at node 4.

$$[N] = \begin{bmatrix} N_1 & 0 & N_2 & 0 & N_3 & 0 & N_4 & 0 \\ 0 & N_1 & 0 & N_2 & 0 & N_3 & 0 & N_4 \end{bmatrix} \quad (3.10)$$

3.3. Shape functions for thin plate bending element

The KLPT, depending on thin plate bending elements, aims to evaluate rotation free plates. The thin plate element is assumed to have only out of plane displacements, because in-plane displacements are less than displacements in other direction. So, it can easily be seen that the bending effects are dominant in Figure 3.5. There are 3 DOF which are w , θ_x and θ_y displacement and rotations respectively, on each node for out of plane plate analysis.

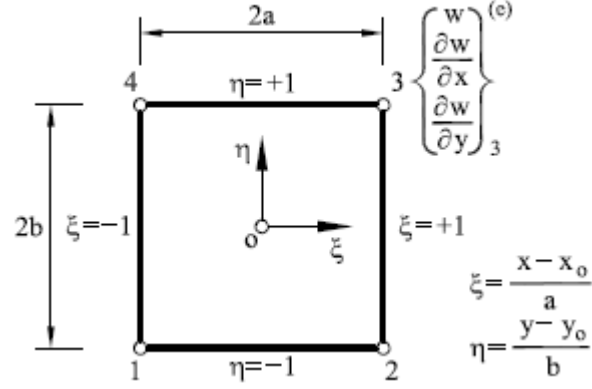


Figure 3.5 : Thin plate bending element (Oñate, 2013).

When a and b are dimensions of element shown in Figure 3.5 and rotations are given in equation 3.11 in terms of displacement relationships,

$$\theta_x = \frac{\partial w}{\partial y} = \frac{1}{b} \frac{\partial w}{\partial \eta} \quad \text{and} \quad \theta_y = -\frac{\partial w}{\partial x} = -\frac{1}{a} \frac{\partial w}{\partial \xi} \quad (3.11)$$

Cook, et al. (2001) stated that for the 4-node quadrilateral element, total DOF is 12 and it requires functions have 12 unknowns. The displacement, w , must have cubic functions depend on Figure 3.3 with 12 terms as following situations because of rotations are dependent to displacement at Z axis.

$$w = a_9 + a_{10}\xi + a_{11}\eta + a_{12}\xi^2 + a_{13}\xi\eta + a_{14}\eta^2 + a_{15}\xi^3 + a_{16}\xi^2\eta + a_{17}\xi\eta^2 + a_{18}\eta^3 + a_{19}\xi^3\eta + a_{20}\xi\eta^3 \quad (3.12a)$$

$$\theta_x = \frac{1}{b} (a_{11} + a_{13}\xi + 2a_{14}\eta + a_{16}\xi^2 + 2a_{17}\xi\eta + 3a_{18}\eta^2 + a_{19}\xi^3 + 3a_{20}\xi\eta^2) \quad (3.12b)$$

$$\theta_y = -\frac{1}{a} (a_{10} + 2a_{12}\xi + a_{13}\eta + 3a_{15}\xi^2 + 2a_{16}\xi\eta + a_{17}\eta^2 + 3a_{19}\xi^2\eta + a_{20}\eta^3) \quad (3.12c)$$

$$\begin{Bmatrix} w \\ b\theta_x \\ a\theta_y \end{Bmatrix} = \begin{bmatrix} 1 & \xi & \eta & \xi^2 & \xi\eta & \eta^2 & \xi^3 & \xi^2\eta & \xi\eta^2 & \eta^3 & \xi^3\eta & \xi\eta^3 \\ 0 & 0 & 1 & 0 & \xi & 2\eta & 0 & \xi^2 & 2\xi\eta & 3\eta^2 & \xi^3 & 3\xi\eta^2 \\ 0 & -1 & 0 & -2\xi & -\eta & 0 & 3\xi^2 & -2\xi\eta & -\eta^2 & 0 & -3\xi^2\eta & -\eta^3 \end{bmatrix} \begin{Bmatrix} a_9 \\ a_{10} \\ a_{11} \\ a_{12} \\ a_{13} \\ a_{14} \\ a_{15} \\ a_{16} \\ a_{17} \\ a_{18} \\ a_{19} \\ a_{20} \end{Bmatrix} \quad (3.12d)$$

Equations can be expanded for 4 node displacements,

$$\{w\} = [w_1 \quad b\theta_{x1} \quad a\theta_{y1} \quad w_2 \quad b\theta_{x2} \quad a\theta_{y2} \quad w_3 \quad b\theta_{x3} \quad a\theta_{y3} \quad w_4 \quad b\theta_{x4} \quad a\theta_{y4}]^T \quad (3.13a)$$

$$\{w\} = [Rb]\{a\} \quad (3.13b)$$

$$\{a\} = [Rb]^{-1}\{w\} \quad (3.13c)$$

where $\xi = -1$ and $\eta = -1$ at node 1, $\xi = 1$ and $\eta = -1$ at node 2, $\xi = 1$ and $\eta = 1$ at node 3, $\xi = -1$ and $\eta = 1$ at node 4. Rb coefficient matrix can be obtained as,

$$[Rb] = \begin{Bmatrix} 1 & -1 & -1 & 1 & 1 & 1 & -1 & -1 & -1 & -1 & 1 & 1 \\ 0 & 0 & 1 & 0 & -1 & -2 & 0 & 1 & 2 & 3 & -1 & -3 \\ 0 & -1 & 0 & 2 & 1 & 0 & -3 & -2 & -1 & 0 & 3 & 1 \\ 1 & 1 & -1 & 1 & -1 & 1 & 1 & -1 & 1 & -1 & -1 & -1 \\ 0 & 0 & 1 & 0 & 1 & -2 & 0 & 1 & -2 & 3 & 1 & 3 \\ 0 & -1 & 0 & -2 & 1 & 0 & -3 & 2 & -1 & 0 & 3 & 1 \\ 1 & 1 & 1 & 1 & 1 & 1 & 1 & 1 & 1 & 1 & 1 & 1 \\ 0 & 0 & 1 & 0 & 1 & 2 & 0 & 1 & 2 & 3 & 1 & 3 \\ 0 & -1 & 0 & -2 & -1 & 0 & -3 & -2 & -1 & 0 & -3 & -1 \\ 1 & -1 & 1 & 1 & -1 & 1 & -1 & 1 & -1 & 1 & -1 & -1 \\ 0 & 0 & 1 & 0 & -1 & 2 & 0 & 1 & -2 & 3 & -1 & -3 \\ 0 & -1 & 0 & 2 & -1 & 0 & 3 & 2 & -1 & 0 & -3 & -1 \end{Bmatrix} \quad (3.14)$$

The displacements w can be written using N_i shape functions.

$$w = \sum_{i=1}^4 N_i w_i \quad (3.15a)$$

If these expression is expanded to matrix forms,

$$w = [N_1 \ N_2 \ N_3 \ N_4] \{w\} \quad (3.15b)$$

shape function relation is obtained and it can be seen that the displacements use the same shape functions. Combining u expressions give the shape functions as,

$$[N_1 \ N_2 \ N_3 \ N_4] = [1 \ \xi \ \eta \ \xi^2 \ \xi\eta \ \eta^2 \ \xi^3 \ \xi^2\eta \ \xi\eta^2 \ \eta^3 \ \xi^3\eta \ \xi\eta^3][Rb]^{-1} \quad (3.16)$$

Finally, general shape function terms for w displacement can be given like below.

$$[N_i]^T = \begin{bmatrix} \frac{1}{8}(1 + \xi_i\xi)(1 + \eta_i\eta)(2 + \xi_i\xi + \eta_i\eta - \xi^2 - \eta^2) \\ \frac{b}{8}(1 + \xi_i\xi)(\eta_i + \eta)(\eta^2 - 1) \\ \frac{a}{8}(\xi_i + \xi)(1 + \eta_i\eta)(\xi^2 - 1) \end{bmatrix} \quad (3.17)$$

If dimensionless coordinates of nodes at X and Y axis are substituted into general equation, shape functions for each node can be seen like

$$N_1^T = \begin{bmatrix} \frac{1}{4} - \frac{3\eta}{8} + \frac{\eta^3}{8} - \frac{3\xi}{8} + \frac{\eta\xi}{2} - \frac{\eta^3\xi}{8} + \frac{\xi^3}{8} - \frac{\eta\xi^3}{8} \\ \frac{b}{8} - \frac{b\eta}{8} - \frac{b\eta^2}{8} + \frac{b\eta^3}{8} - \frac{b\xi}{8} + \frac{b\eta\xi}{8} + \frac{1}{8}b\eta^2\xi - \frac{1}{8}b\eta^3\xi \\ -\frac{a}{8} + \frac{a\eta}{8} + \frac{a\xi}{8} - \frac{a\eta\xi}{8} + \frac{a\xi^2}{8} - \frac{1}{8}a\eta\xi^2 - \frac{a\xi^3}{8} + \frac{1}{8}a\eta\xi^3 \end{bmatrix} \quad (3.18a)$$

$$N_2^T = \begin{bmatrix} \frac{1}{4} - \frac{3\eta}{8} + \frac{\eta^3}{8} + \frac{3\xi}{8} - \frac{\eta\xi}{2} + \frac{\eta^3\xi}{8} - \frac{\xi^3}{8} + \frac{\eta\xi^3}{8} \\ \frac{b}{8} - \frac{b\eta}{8} - \frac{b\eta^2}{8} + \frac{b\eta^3}{8} + \frac{b\xi}{8} - \frac{b\eta\xi}{8} - \frac{1}{8}b\eta^2\xi + \frac{1}{8}b\eta^3\xi \\ \frac{a}{8} - \frac{a\eta}{8} + \frac{a\xi}{8} - \frac{a\eta\xi}{8} - \frac{a\xi^2}{8} + \frac{1}{8}a\eta\xi^2 - \frac{a\xi^3}{8} + \frac{1}{8}a\eta\xi^3 \end{bmatrix} \quad (3.18b)$$

$$N_3^T = \begin{bmatrix} \frac{1}{4} + \frac{3\eta}{8} - \frac{\eta^3}{8} + \frac{3\xi}{8} + \frac{\eta\xi}{2} - \frac{\eta^3\xi}{8} - \frac{\xi^3}{8} - \frac{\eta\xi^3}{8} \\ -\frac{b}{8} - \frac{b\eta}{8} + \frac{b\eta^2}{8} + \frac{b\eta^3}{8} - \frac{b\xi}{8} - \frac{b\eta\xi}{8} + \frac{1}{8}b\eta^2\xi + \frac{1}{8}b\eta^3\xi \\ \frac{a}{8} + \frac{a\eta}{8} + \frac{a\xi}{8} + \frac{a\eta\xi}{8} - \frac{a\xi^2}{8} - \frac{1}{8}a\eta\xi^2 - \frac{a\xi^3}{8} - \frac{1}{8}a\eta\xi^3 \end{bmatrix} \quad (3.18c)$$

$$N_4^T = \begin{bmatrix} \frac{1}{4} + \frac{3\eta}{8} - \frac{\eta^3}{8} - \frac{3\xi}{8} - \frac{\eta\xi}{2} + \frac{\eta^3\xi}{8} + \frac{\xi^3}{8} + \frac{\eta\xi^3}{8} \\ -\frac{b}{8} - \frac{b\eta}{8} + \frac{b\eta^2}{8} + \frac{b\eta^3}{8} + \frac{b\xi}{8} + \frac{b\eta\xi}{8} - \frac{1}{8}b\eta^2\xi - \frac{1}{8}b\eta^3\xi \\ -\frac{a}{8} - \frac{a\eta}{8} + \frac{a\xi}{8} + \frac{a\eta\xi}{8} + \frac{a\xi^2}{8} + \frac{1}{8}a\eta\xi^2 - \frac{a\xi^3}{8} - \frac{1}{8}a\eta\xi^3 \end{bmatrix} \quad (3.18d)$$

where $\xi_1 = -1$ and $\eta_1 = -1$ at node 1, $\xi_2 = 1$ and $\eta_2 = -1$ at node 3, $\xi_3 = 1$ and $\eta_3 = 1$ at node 3, $\xi_4 = -1$ and $\eta_4 = 1$ at node 4.

$$[N] = [N_1 \quad N_2 \quad N_3 \quad N_4] \quad (3.19)$$

3.4. Shape functions for thick plate bending element

Initially, the thick plate element is assumed to have only out of plane displacements, because in-plane displacements are less than displacements in other direction. But also, the bending and shear effects work together on this element and this element represented in Figure 3.6. There are 3 DOF which are w , θ_x and θ_y displacement and rotations respectively, for each node for out of plane plate analysis like thin plate but these deformations are not dependent to each other.

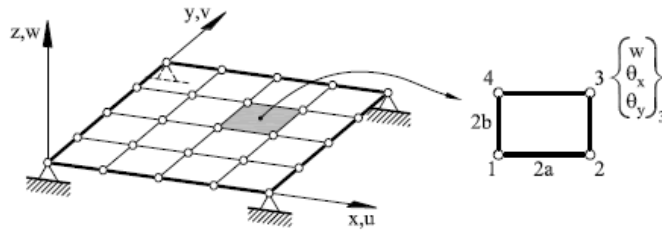


Figure 3.6 : Thick plate bending elements representation (Oñate, 2013).

The θ_x and θ_y rotations are independent variables with ϕ_x and ϕ_y rotation angles. This assumption can be seen as below.

$$\theta_x = \frac{\partial w}{\partial x} + \phi_x \text{ and } \theta_y = \frac{\partial w}{\partial y} + \phi_y \quad (3.20)$$

According to Cook, et al. (2001) for the 4-node quadrilateral element, total DOF is 12 and it requires functions have 12 unknowns. Each of displacement must have bilinear functions with 4 terms as following equations 3.21a, 3.21b and 3.21c depending on Figure 3.3.

$$w = a_9 + a_{10}\xi + a_{11}\eta + a_{12}\xi\eta = [1 \quad \xi \quad \eta \quad \xi\eta] \begin{Bmatrix} a_9 \\ a_{10} \\ a_{11} \\ a_{12} \end{Bmatrix} \quad (3.21a)$$

$$\theta_x = a_{13} + a_{14}\xi + a_{15}\eta + a_{16}\xi\eta = [1 \quad \xi \quad \eta \quad \xi\eta] \begin{Bmatrix} a_{13} \\ a_{14} \\ a_{15} \\ a_{16} \end{Bmatrix} \quad (3.21b)$$

$$\theta_y = a_{17} + a_{18}\xi + a_{19}\eta + a_{20}\xi\eta = [1 \quad \xi \quad \eta \quad \xi\eta] \begin{Bmatrix} a_{17} \\ a_{18} \\ a_{19} \\ a_{20} \end{Bmatrix} \quad (3.21c)$$

Equations can be expanded for 4 node displacements as follows,

$$\{w\} = [Rb] \cdot \{a\} \quad (3.22a)$$

$$\{a\} = [Rb]^{-1} \cdot \{w\} \quad (3.22b)$$

$$w = [1 \quad \xi \quad \eta \quad \xi\eta][Rb]^{-1}\{w\} \quad (3.22c)$$

where $\xi = -1$ and $\eta = -1$ at node 1, $\xi = 1$ and $\eta = -1$ at node 2, $\xi = 1$ and $\eta = 1$ at node 3, $\xi = -1$ and $\eta = 1$ at node 4. Also, the θ_x and θ_y are written as w . Therefore, it is possible to obtain a Rb coefficient matrix only through one.

$$[Rb] = \begin{bmatrix} 1 & -1 & -1 & 1 \\ 1 & 1 & -1 & -1 \\ 1 & 1 & 1 & 1 \\ 1 & -1 & 1 & -1 \end{bmatrix} \quad (3.23)$$

where the w , θ_x and θ_y are written using N_i shape functions,

$$w = \sum_{i=1}^4 N_i w_i \quad \theta_x = \sum_{i=1}^4 N_i \theta_{x_i} \text{ and } \theta_y = \sum_{i=1}^4 N_i \theta_{y_i} \quad (3.24a)$$

If these expressions are expanded to matrix forms,

$$\begin{Bmatrix} w \\ \theta_x \\ \theta_y \end{Bmatrix} = \begin{bmatrix} N_1 & 0 & 0 & N_2 & 0 & 0 & N_3 & 0 & 0 & N_4 & 0 & 0 \\ 0 & N_1 & 0 & 0 & N_2 & 0 & 0 & N_3 & 0 & 0 & N_4 & 0 \\ 0 & 0 & N_1 & 0 & 0 & N_2 & 0 & 0 & N_3 & 0 & 0 & N_4 \end{bmatrix} \begin{Bmatrix} w_1 \\ \theta_{x_1} \\ \theta_{y_1} \\ w_2 \\ \theta_{x_2} \\ \theta_{y_2} \\ w_3 \\ \theta_{x_3} \\ \theta_{y_3} \\ w_4 \\ \theta_{x_4} \\ \theta_{y_4} \end{Bmatrix} \quad (3.24b)$$

shape function relations are obtained and it can be seen that the displacements use the same shape functions. Combining u expressions give the shape functions as,

$$[N_1 \ N_2 \ N_3 \ N_4] = [1 \ \xi \ \eta \ \xi\eta][Rb]^{-1} \quad (3.25)$$

So, general shape function terms can be given like membrane element.

$$N_i = \frac{1}{4}(1 + \xi_i \xi)(1 + \eta_i \eta) \quad (3.26)$$

If dimensionless coordinates of nodes at X and Y axis are substituted into general equation, shape functions for each node can be seen like

$$N_1 = \frac{1}{4}(1 - \xi)(1 - \eta) \quad (3.27a)$$

$$N_2 = \frac{1}{4}(1 + \xi)(1 - \eta) \quad (3.27b)$$

$$N_3 = \frac{1}{4}(1 + \xi)(1 + \eta) \quad (3.27c)$$

$$N_4 = \frac{1}{4}(1 - \xi)(1 + \eta) \quad (3.27d)$$

where $\xi_1 = -1$ and $\eta_1 = -1$ at node 1, $\xi_2 = 1$ and $\eta_2 = -1$ at node 2, $\xi_3 = 1$ and $\eta_3 = 1$ at node 3, $\xi_4 = -1$ and $\eta_4 = 1$ at node 4.

$$[N] = \begin{bmatrix} N_1 & 0 & 0 & N_2 & 0 & 0 & N_3 & 0 & 0 & N_4 & 0 & 0 \\ 0 & N_1 & 0 & 0 & N_2 & 0 & 0 & N_3 & 0 & 0 & N_4 & 0 \\ 0 & 0 & N_1 & 0 & 0 & N_2 & 0 & 0 & N_3 & 0 & 0 & N_4 \end{bmatrix} \quad (3.28)$$

4. PLATE TEORIES AND FORMULATIONS

Flat structures with smaller thickness values than other dimensions are called plates. Like beams, plates have some theories about their structural analysis. Szilard (2004) mentioned that the plates can have different boundary conditions, support types statically or loadings dynamically and these constraints affect their cases. For instance, the shear affects can be seen as bending or torsion on plate. The governing equations, are obtained from statically or dynamically constraints, are used to analyze of plate structures based on elasticity theory.

While comparing Kirchhoff-Love and Reissner-Mindlin theories, that the two most well-known plate theory, the RMPT was emphasized in terms of its use and approach on both thick and thin plates with some modifications. Plates with high length-to-thickness ratio ($L / h > 10$) are called thin plates. If this ratio is lower ($L / h < 10$), they are called thick (Petyt, 1990). The KLPT is applicable on thin plates for isotropic and composite materials. However, the application of the RMPT produces closer results on thick plates and composite materials, because these plates also have transverse shear effect cross their thickness. Various transverse shear stress fields are accepted or reduced integration method is used to eliminate the shear locking which is the disadvantage of using this theory on thin plates (Oñate, 2013).

The plates can be restricted under different boundary conditions. Basically, these conditions affect behavior, natural frequency values and mode shapes of plates. They can be applied on plates as restricted some DOF according to their boundary conditions. In this thesis, three main boundary conditions are considered with different applications and these restrictions are shown in the Figure 4.1 with DOF effects. At the same time, the box beams are accepted as folded plates in thick or thin walled cases. Due to similarity of plates and thin walled structures, the plate theories are suitable for box beams in many cases. Their DOF, boundary conditions and extra techniques are mentioned in following sections 5 and 6.

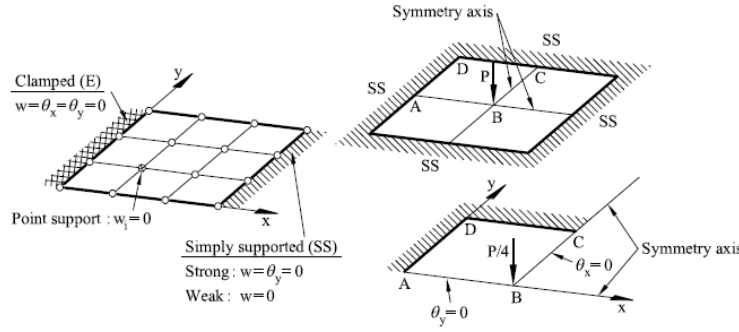


Figure 4.1 : Boundary conditions in plates (Oñate, 2013)

4.1. The Kirchhoff-Love Theory

The Kirchhoff-Love plate is represented in Figure 4.2 with deformation data and KLPT is explained with three assumptions as follows (Oñate, 2013);

- The particles of middle plane move vertically. Actually, middle plane ($z = 0$) in plane movement is smaller than movement through thickness of plate.
- The plate middle surface has the identical vertical displacement through the normal line.
- The normal stress σ_z is negligible.
- The normal line points of the plate middle plane stay same spline as orthogonal to middle plane.

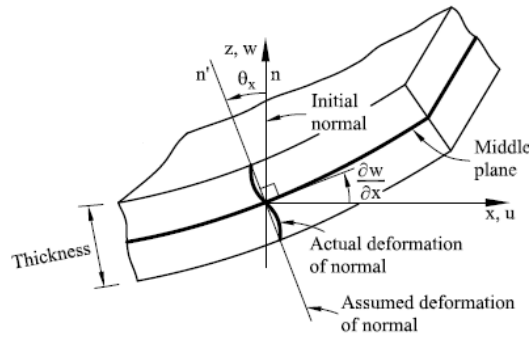


Figure 4.2 : Kirchhoff-Love plate representation (Oñate, 2013).

So, displacement functions for isotropic and homogenous materials, when evaluated thin plate element based on first, second and fourth assumptions obtain as in below:

$$u(x, y, z) = z\theta_y(x, y) \quad (4.1a)$$

$$v(x, y, z) = -z\theta_x(x, y) \quad (4.1b)$$

$$w(x, y, z) = w \quad (4.1c)$$

$$\theta_x = \frac{\partial w}{\partial y} \text{ and } \theta_y = -\frac{\partial w}{\partial x} \quad (4.1d)$$

From these functions, u and v are in-plane displacements which are parallel to plate middle surface and w is normal to the middle surface at z directions. Besides, θ_x and θ_y are rotations about x and y axis respectively. In Figure 3.5, it can be seen that thin plate element has 3 DOF at each node.

The KLPT refers to thin plate bending element and their displacement and rotations with shape functions as mentioned at section 3.3. The Figure 4.3 shows the plate with normal to the middle surface direction loads.

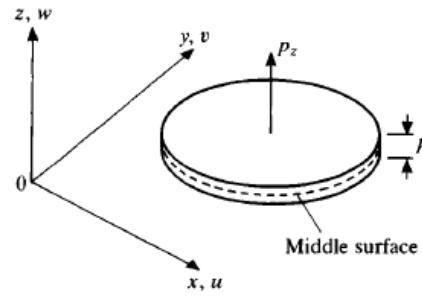


Figure 4.3: Bending element of plate (Petyt, 1990).

For thin plates, transverse shear stress is assumed as zero because of lower thickness to length ratio. The energy equations can be expressed as again,

$$U = \frac{1}{2} \int \{\varepsilon\}^T [D] \{\varepsilon\} dV \quad (4.2)$$

$$T = \frac{1}{2} \int h \rho (\dot{w}^2) dA \quad (4.3)$$

But, strain matrix is

$$\{\varepsilon\} = -z\{X\} \quad (4.4)$$

where

$$\{X\} = \begin{bmatrix} \partial^2 w / \partial x^2 \\ \partial^2 w / \partial y^2 \\ 2 \partial^2 w / \partial x \partial y \end{bmatrix} \quad (4.5)$$

Combining these equations, the strain energy function is obtained as below.

$$U = \frac{1}{2} \int \frac{h^3}{12} \{X\}^T [D] \{X\} dA \quad (4.6)$$

For isotropic materials, elastic property is

$$[D] = \begin{bmatrix} E & Ev & 0 \\ Ev & E & 0 \\ 0 & 0 & G \end{bmatrix} \quad (4.7)$$

where, E is the modulus of elasticity, ν is the Poisson's ratio and $G = \frac{E}{2(1-\nu)}$ is the shear modulus.

If classical equation of kinetic energy becomes equal to obtained thin plate kinetic energy function, it gives the mass matrix of the element as,

$$T_e = \frac{1}{2} [M]_b \{\dot{w}\}_e^2 \quad (4.8)$$

$$[M]_b = \int h \rho [N]^T [N] dA = \rho h \int_{-1}^1 \int_{-1}^1 ([N]^T [N] \det J d\eta) d\xi \quad (4.9)$$

where N is the shape function matrix that mentioned in section 3.3, M_b is the mass matrix for thin bending element from combination of equations 3.15a, 4.3 and 4.8 and J is the jacobian matrix of the element which can be formulated as

$$\det J = \begin{vmatrix} \frac{\partial x}{\partial \xi} & \frac{\partial y}{\partial \xi} \\ \frac{\partial x}{\partial \eta} & \frac{\partial y}{\partial \eta} \end{vmatrix} = \left| \sum_{i=1}^4 \begin{bmatrix} \frac{\partial N_i}{\partial \xi} \\ \frac{\partial N_i}{\partial \eta} \end{bmatrix} \begin{bmatrix} x_i \\ y_i \end{bmatrix} \right| = ab \quad (4.10)$$

The Jacobian matrix is constant for plates, which have $2a \times 2b$ dimension, and equals ab where x and y is coordinates of corner point of element.

The mass matrix dimension is 12x12 and its relation with plate properties can be seen like below (Petyt, 1990).

$$[M]_b = \frac{\rho_{\text{hab}}}{6300} \begin{bmatrix} [\text{m}11] & [\text{m}21]^T \\ [\text{m}21] & [\text{m}22] \end{bmatrix} \quad (4.11)$$

$$[M]_b = \frac{\text{phab}}{6300} * \begin{bmatrix} 3454 & 922b & -922a & 1226 & 398b & 548a & 394 & -232b & 232a & 1226 & -548b & -398a \\ & 320b^2 & -252ab & 398b & 160b^2 & 168ab & 232b & -120b^2 & 112ab & 548b & -240b^2 & -168ab \\ & & 320a^2 & -548a & -168ab & -240a^2 & -232a & 112ab & -120a^2 & -398a & 168ab & 160a^2 \\ & & & 3454 & 922b & 922a & 1226 & -548b & 398a & 394 & -232b & -232a \\ & & & & 320b^2 & 252ab & 548b & -240b^2 & 168ab & 232b & -120b^2 & -112ab \\ & & & & & 320a^2 & 398a & -168ab & 160a^2 & 232a & -112ab & -120a^2 \\ & & & & & & 3454 & -922b & 922a & 1226 & -398b & -548a \\ & & & & & & & 320b^2 & -252ab & -398b & 160b^2 & 168ab \\ & & & & & & & & 320a^2 & 548a & -168ab & -240a^2 \\ & & & & & & & & & 3454 & -922b & -922a \\ & & & & & & & & & & 320b^2 & 252ab \\ & & & & & & & & & & & 320a^2 \end{bmatrix}$$

(4.12)

Generation of the element stiffness matrix has same procedure with mass matrix but this time, the strain energy equations are used for obtaining process.

$$U_e = \frac{1}{2} [K]_e \{w\}_e^2 \quad (4.13)$$

$$[K]_e = \int \frac{h^3}{12} [B_e]^T [D] [B_e] = \rho \frac{h^3}{12} ab \int_{-1}^1 \int_{-1}^1 ([B_e]^T [D] [B_e] d\eta) d\xi \quad (4.14)$$

where K_e is the stiffness matrix and B_e is the strain matrix. The stiffness matrix consists of bending part only because of neglected transverse shear stresses. Where B_e is given by,

$$[B_e] = \begin{bmatrix} \frac{\partial^2 N}{\partial x^2} \\ \frac{\partial^2 N}{\partial y^2} \\ 2 \frac{\partial^2 N}{\partial x \partial y} \end{bmatrix} = \begin{bmatrix} \frac{1}{a^2} \frac{\partial^2 N}{\partial \xi^2} \\ \frac{1}{b^2} \frac{\partial^2 N}{\partial \eta^2} \\ \frac{1}{2ab} \frac{\partial^2 N}{\partial \xi \partial \eta} \end{bmatrix} \quad (4.15)$$

The stiffness matrix dimension is 12x12 and its relation with plate properties can be seen like below.

$$[K]_e = \frac{Eh^3}{48ab(1-\nu^2)} * \begin{bmatrix} [k_{11}] & [k_{21}] & [k_{31}] & [k_{41}] \\ [k_{21}] & [k_{22}] & [k_{23}] & [k_{24}] \\ [k_{31}] & [k_{23}] & [k_{33}] & [k_{34}] \\ [k_{41}] & [k_{24}] & [k_{34}] & [k_{44}] \end{bmatrix} \quad (4.16a)$$

$$[k_{11}] = \begin{bmatrix} 2.8 + 4\beta^2 + 4Q^2 - 0.8\nu & 4\beta a + b(0.4 + 1.6\nu) & -4Q^2 a + a(-0.4 - 1.6\nu) \\ & \frac{16}{3}a^2 + \frac{16}{15}b^2(1 - \nu) & -4.ab\nu \\ \text{symmetrical} & & \frac{16}{3}b^2 + \frac{16}{15}a^2(1 - \nu) \end{bmatrix} \quad (4.16b)$$

$$[k_{21}] = \begin{bmatrix} -2.8 + 2\beta^2 - 4Q^2 + 0.8\nu & 2\beta a - b(0.4 + 1.6\nu) & -4Q^2 a + a(-0.4 + 0.4\nu) \\ 2\beta a - b(0.4 + 1.6\nu) & \frac{8}{3}a^2 + \frac{16}{15}b^2(-1 + \nu) & 0. \\ 4Q^2 a + a(0.4 - 0.4\nu) & 0. & \frac{8}{3}b^2 + \frac{4}{15}a^2(-1 + \nu) \end{bmatrix} \quad (4.16c)$$

$$[k_{31}] = \begin{bmatrix} 2.8 - 2\beta^2 - 2Q^2 - 0.8\nu & -2\beta a + b(0.4 - 0.4\nu) & 2Q^2 a - a(0.4 - 0.4\nu) \\ 2\beta a + b(-0.4 + 0.4\nu) & \frac{4}{3}a^2 + \frac{4}{15}b^2(1 - \nu) & 0. \\ -2Q^2 a + a(0.4 - 0.4\nu) & 0 & \frac{4}{3}b^2 + \frac{4}{15}a^2(1 - \nu) \end{bmatrix} \quad (4.16d)$$

$$[k_{41}] = \begin{bmatrix} -2.8 + 2\beta^2 - 2Q^2 + 0.8\nu & -2\beta a + b(-0.4 + 0.4\nu) & -2Q^2 a + a(0.4 + 0.4\nu) \\ 2\beta a + b(0.4 - 0.4\nu) & \frac{4}{3}a^2 \pm \frac{4}{15}b^2(1 - \nu) & 0. \\ -2Q^2 a + a(0.4 + 0.4\nu) & 0 & \frac{4}{3}b^2 - \frac{4}{15}a^2(1 - \nu) \end{bmatrix} \quad (4.16e)$$

$$\beta = \frac{b}{a}, Q = \frac{a}{b} \quad (4.16f)$$

$$I_1 = \begin{bmatrix} -1 & 0 & 0 \\ 0 & 1 & 0 \\ 0 & 0 & 1 \end{bmatrix}, I_2 = \begin{bmatrix} 1 & 0 & 0 \\ 0 & -1 & 0 \\ 0 & 0 & 1 \end{bmatrix}, I_3 = \begin{bmatrix} 1 & 0 & 0 \\ 0 & 1 & 0 \\ 0 & 0 & -1 \end{bmatrix} \quad (4.16g)$$

$$[k_{22}] = I_3^T [k_{11}] I_3, [k_{32}] = I_3^T [k_{41}] I_3, [k_{33}] = I_1^T [k_{11}] I_1, [k_{42}] = I_3^T [k_{31}] I_3, \\ [k_{43}] = I_1^T [k_{21}] I_1, [k_{22}] = I_2^T [k_{11}] I_2 \quad (4.16h)$$

The first six natural frequencies of square plate which is point supported at its corners are validated with 16x16 mesh code developed in Mathematica and Q4 element. Its material and dimension properties are shown in Table 4.1 and code results compare with analytical, experimental and FEM results in Table 4.2.

Table 4.1 : The square plate properties (Petyt, 1990).

Plate Properties	Values
E	73.084*10 ⁹ N/m ²
ρ	2821 kg/m ³
v	0.3
h	0.0032766 m
2a	0.3048 m

Table 4.2 : Comparison of natural frequencies (Hz) of the square plate.

Modes	Present	FEM (Petyt, 1990)	Analytical (Reed, 1965)	Experimental (Reed, 1965)
1	61.58	62.09	61.40	62
2 (a)	136.44	138.5	136	134
2 (b)	136.44	138.5	136	134
3	169.47	169.7	170	169
4	333.15	340.0	333	330
5	382.98	396.0	385	383

4.2. The Reissner-Mindlin Theory

Transverse shear and rotation effects are important for thick plates and deep beams. Therefore, changes in thickness must be taken into account as differ from thin plates. Figure 4.3 also shows a thick plate bending element but the Reissner-Mindlin plate shape and their deformation can be seen in Figure 4.4. The RMPT has same first three assumptions with KLPT but fourth assumption is differentiated classical theory in the following statement;

- The normal line points of the plate middle plane stay same spline but does not have to orthogonal under deformation.

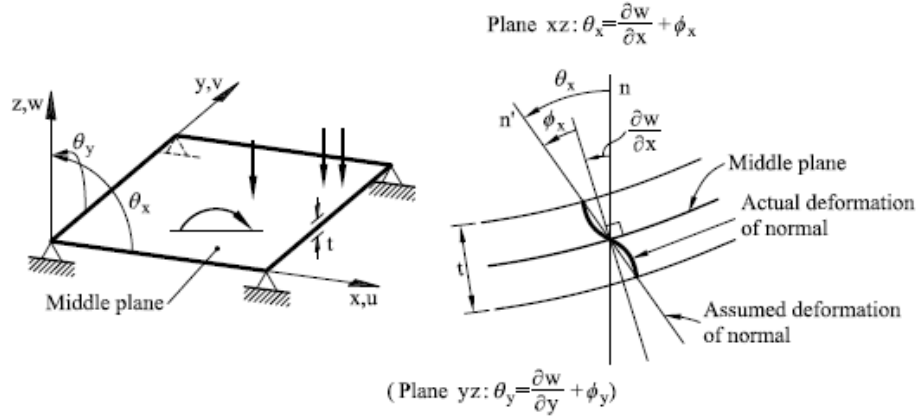


Figure 4.4 : RMPT displacements and rotations (Oñate, 2013).

For thick plates, transverse shear and rotary effects are taken into account because of higher thickness to length ratio. So, displacement functions for isotropic and homogenous materials, when evaluated thick plate element based on transverse shear deformations, obtain as follows:

$$u(x, y, z) = z\theta_y(x, y) \quad (4.17a)$$

$$v(x, y, z) = -z\theta_x(x, y) \quad (4.17b)$$

$$w(x, y, z) = w \quad (4.17c)$$

$$\theta_x = \frac{\partial w}{\partial x} + \phi_x \text{ and } \theta_y = \frac{\partial w}{\partial y} + \phi_y \quad (4.17d)$$

From these functions, u and v are in-plane displacements which are parallel to plate middle surface and w is normal to middle surface at z directions. Besides, θ_x and θ_y are rotations about x and y axis respectively.

The strain matrix is

$$\{\varepsilon\} = -z\{\chi\} \quad (4.18)$$

$$\{\chi\} = \begin{bmatrix} -\partial\theta_y/\partial x \\ \partial\theta_x/\partial y \\ -\partial\theta_y/\partial y + \partial\theta_x/\partial x \end{bmatrix} \quad (4.19a)$$

$$\{\gamma\} = \begin{bmatrix} \theta_y + \partial w/\partial x \\ -\theta_x + \partial w/\partial y \end{bmatrix} \quad (4.19b)$$

where γ is the shear strains and combination of these equations give the new potential energy equation as,

$$U = \frac{1}{2} \int \{\varepsilon\}^T [D] \{\varepsilon\} dV + \frac{1}{2} \int \{\tau\}^T \{\gamma\} dV \quad (4.20)$$

where τ is the shear stresses and shear stress-strain relationship according to Hooke's law can be given by

$$\{\tau\} = \kappa [D^s] \{\gamma\} \quad (4.21)$$

where κ is the shear correction factor and for isotropic materials elastic property is,

$$[D^s] = \begin{bmatrix} G & 0 \\ 0 & G \end{bmatrix} \quad (4.22)$$

Finally, the energy equations can be expressed as,

$$T_e = \frac{1}{2} \int \rho (\dot{w}^2 + \dot{v}^2 + \dot{u}^2) dV = \frac{1}{2} \int \rho \left(h \dot{w}^2 + \frac{h^3}{12} \dot{\theta}_x^2 + \frac{h^3}{12} \dot{\theta}_y^2 \right) dA \quad (4.23a)$$

$$U_e = \frac{1}{2} \int \frac{h^3}{12} \{\chi\}^T [D] \{\chi\} dA + \frac{1}{2} \int \kappa h \{\gamma\}^T [D^s] \{\gamma\} dA \quad (4.23b)$$

ρ , h , T_e and U_e are density of material, thickness of plate, kinetic energy and potential energy formulations respectively. T_e and U_e have classical formulations so, these are used for stiffness and mass matrix obtain process with energy formulas based on displacement.

RMPT refers thick plate bending element and their displacement and rotations are explained in section 3.4. Combination of classical equation 2.20 of kinetic energy and obtained thick plate energy function give the mass matrix of the element as,

$$T_e = \frac{1}{2} [M]_{bs} \{\dot{w}\}_e^2 \quad (4.24)$$

$$[M]_{bs} = \int \rho [N]^T \begin{bmatrix} h & 0 & 0 \\ 0 & \frac{h^3}{12} & 0 \\ 0 & 0 & \frac{h^3}{12} \end{bmatrix} [N] dA \quad (4.25)$$

where N is the shape function matrix that mentioned in section 3.4 and M_{bs} is the mass matrix for thick bending element.

$$[M]_{bs} = \rho h a b \begin{bmatrix} \frac{4}{9} & 0 & 0 & \frac{2}{9} & 0 & 0 & \frac{1}{9} & 0 & 0 & \frac{2}{9} & 0 & 0 \\ 0 & \frac{h^2}{27} & 0 & 0 & \frac{h^2}{54} & 0 & 0 & \frac{h^2}{108} & 0 & 0 & \frac{h^2}{54} & 0 \\ 0 & 0 & \frac{h^2}{27} & 0 & 0 & \frac{h^2}{54} & 0 & 0 & \frac{h^2}{108} & 0 & 0 & \frac{h^2}{54} \\ \frac{2}{9} & 0 & 0 & \frac{4}{9} & 0 & 0 & \frac{2}{9} & 0 & 0 & \frac{1}{9} & 0 & 0 \\ 0 & \frac{h^2}{54} & 0 & 0 & \frac{h^2}{27} & 0 & 0 & \frac{h^2}{54} & 0 & 0 & \frac{h^2}{108} & 0 \\ 0 & 0 & \frac{h^2}{54} & 0 & 0 & \frac{h^2}{27} & 0 & 0 & \frac{h^2}{54} & 0 & 0 & \frac{h^2}{108} \\ \frac{1}{9} & 0 & 0 & \frac{2}{9} & 0 & 0 & \frac{4}{9} & 0 & 0 & \frac{2}{9} & 0 & 0 \\ 0 & \frac{h^2}{108} & 0 & 0 & \frac{h^2}{54} & 0 & 0 & \frac{h^2}{27} & 0 & 0 & \frac{h^2}{54} & 0 \\ 0 & 0 & \frac{h^2}{108} & 0 & 0 & \frac{h^2}{54} & 0 & 0 & \frac{h^2}{27} & 0 & 0 & \frac{h^2}{54} \\ \frac{2}{9} & 0 & 0 & \frac{1}{9} & 0 & 0 & \frac{2}{9} & 0 & 0 & \frac{4}{9} & 0 & 0 \\ 0 & \frac{h^2}{54} & 0 & 0 & \frac{h^2}{108} & 0 & 0 & \frac{h^2}{54} & 0 & 0 & \frac{h^2}{27} & 0 \\ 0 & 0 & \frac{h^2}{54} & 0 & 0 & \frac{h^2}{108} & 0 & 0 & \frac{h^2}{54} & 0 & 0 & \frac{h^2}{27} \end{bmatrix} \quad (4.26)$$

The stiffness matrix of the element is generated by combination of classical equation of 2.21 strain energy with obtained thick plate energy function and given by

$$U_e = \frac{1}{2} [K]_e \{w\}_e^2 \quad (4.27)$$

$$[K]_e = \int [B_e]^T [D_e] [B_e] \quad (4.28)$$

where D_e represents the elastic property matrices. The stiffness matrix has two part: bending stiffness and shear stiffness matrices. This result can be seen in strain energy function.

$$[K]_e = [K^b] + [K^s] \quad (4.29)$$

$$[K^b] = \int \frac{h^3}{12} [B^b]^T [D] [B^b] dA \quad (4.30a)$$

$$[K^s] = \int \kappa h [B^s]^T [D_s] [B^s] dA \quad (4.30b)$$

When B^b and B^s are bending and shear strain matrices respectively and given by,

$$[B^b] = \begin{bmatrix} 0 & 0 & -\frac{\partial N}{\partial x} \\ 0 & \frac{\partial N}{\partial y} & 0 \\ 0 & \frac{\partial N}{\partial x} & -\frac{\partial N}{\partial y} \end{bmatrix} \quad (4.31a)$$

$$[B^s] = \begin{bmatrix} \frac{\partial N}{\partial x} & 0 & N \\ \frac{\partial N}{\partial y} & -N & 0 \end{bmatrix} \quad (4.31b)$$

Petyt (1990) states that both bending and shear stiffness matrices can be created using 2x2 Gauss quadrature. Also, this technique is called as full integration for 4-noded quadrilateral elements and helps to evaluate integral of strain and elasticity matrices with summation method.

Gauss integration schemes can be grouped under three main heading as full, selective and reduced integrations like seen in the Figure 4.5 where K_f and K_s are bending and shear stiffness respectively. The full integration application on Mindlin plates gives exact result with integral of matrices because of constant jacobian value. Generally reduced integration usage is preferred to improve element for different cases and prevents some problems on element. But, if 4 noded element is chosen, selective integration is suggested instead of reduced (Hinton & Bicanic, 1979).

	Integration Gauss-Legendre product rules					
	Full		Selective		Reduced	
Element	K_f	K_s	K_f	K_s	K_f	K_s
4 noded	2×2	2×2	2×2	1×1	1×1	1×1
8 noded	3×3	3×3	3×3	2×2	2×2	2×2
9 noded	3×3	3×3	3×3	2×2	2×2	2×2
12 noded	4×4	4×4	4×4	3×3	3×3	3×3
16 noded	4×4	4×4	4×4	3×3	3×3	3×3

Figure 4.5 : Gauss integration schemes based on elements (Hinton & Bicanic, 1979).

Nevertheless, as the plate becomes thinner, taking transverse shear terms into account makes the element and plate over-stiff. This called as the shear locking. The shear locking is occurred while h goes to zero, equation 2.5 combining with equations 4.29, 4.30a, 4.30b and stiffness are written with elastic properties,

$$f = ([K^b] + [K^s])u = \left(\frac{Eh^3}{12(1-\nu^2)} [\overline{K^b}] + Gh[\overline{K^s}] \right) u \quad (4.32a)$$

$$k\beta = \frac{Eh^2}{12(1-\nu^2)G} \quad (4.32b)$$

$$f = \left([\overline{K^b}] + \frac{1}{k\beta} [\overline{K^s}] \right) u \quad (4.32c)$$

$k\beta$ goes zero also, but $1/k\beta$ goes to infinity and this causes dominant shear stiffness on plate. If u should not be equal to zero, the term of shear stiffness becomes singular. The shear locking problem converts singularity problem and reduced integrations can be used to overcome it. Different solution methods are used to eliminate shear locking effect such as; assumed shear strain fields, reduced integration of stiffness and linked interpolation (Oñate, 2013). The one point Gauss quadrature may be used for shear stiffness term like suggested in Figure 4.5 selective integration to handle this problem. According to Cook, et al (2001), gauss quadrature application expressed by

$$I = \int_{x_1}^{x_2} f dA = \iint_{-1}^1 \phi(\xi, \eta) \det J d\eta d\xi = \sum_i \sum_j W_i W_j \phi(\xi_i, \eta_j) \quad (4.33)$$

where W is the weight factor, ξ and η are sampling points which are given in Figure 4.6.

Order n	Location ξ_i of Sampling Point	Weight Factor W_i
1	0.	2.
2	$\pm 0.57735 02691 89626 = \pm 1/\sqrt{3}$	1.
3	$\pm 0.77459 66692 41483 = \pm \sqrt{0.6}$	$0.55555 55555 55555 = \frac{5}{9}$
	0.	$0.88888 88888 88888 = \frac{8}{9}$

Figure 4.6 : Gauss sampling points and weight factors (Cook, et al., 2001).

Oñate (2013), aims that achieve exact solution on thin plates with RMPT based on assumed shear strain fields method. Four noded plate quadrilateral element with linear shear field is named as QLLL method. From shear strain equation,

$$\gamma_{xz} = -\theta_x + \partial w / \partial y = \sum_{i=1}^4 \frac{\partial N_i}{\partial \xi} \frac{\partial \xi}{\partial x} w_i - N_i \theta_{xi} = a_1(w_i, \theta_i) + a_2(w_i, \theta_i)\eta + a_3(\theta_i)\xi + a_4(\theta_i)\xi\eta \quad (4.34)$$

If $\gamma_{xz} = 0$ assumes based on KLPT, this gives $\alpha_1 = \alpha_2 = \alpha_3 = \alpha_4 = 0$ from equation 4.34. This leads $\theta_{xi} = 0$ as a result of its coefficients α_3, α_4 are equal to zero. But this causes to $w_i = 0$ for $\alpha_1 = \alpha_2 = 0$. So, this brings the locking. To overcome problem, for γ_{xz} , $\xi=0$ and for γ_{yz} , $\eta=0$ assumed and $\alpha_3 = \alpha_4 = 0$ condition is obtained respectively,

$$\varepsilon^s = \overline{B^s} a^e = \gamma = \begin{Bmatrix} \gamma_{xz} \\ \gamma_{yz} \end{Bmatrix} = \begin{Bmatrix} a_1(w_i, \theta_i) + a_2(w_i, \theta_i)\eta \\ \overline{a_1}(w_i, \theta_i) + \overline{a_2}(w_i, \theta_i)\xi \end{Bmatrix} \quad (4.35)$$

where the $\overline{B^s}$ new shear strain term based on assumed strain fields. Assumed shear strain field are represented in Figure 4.7 for one 4-noded element.

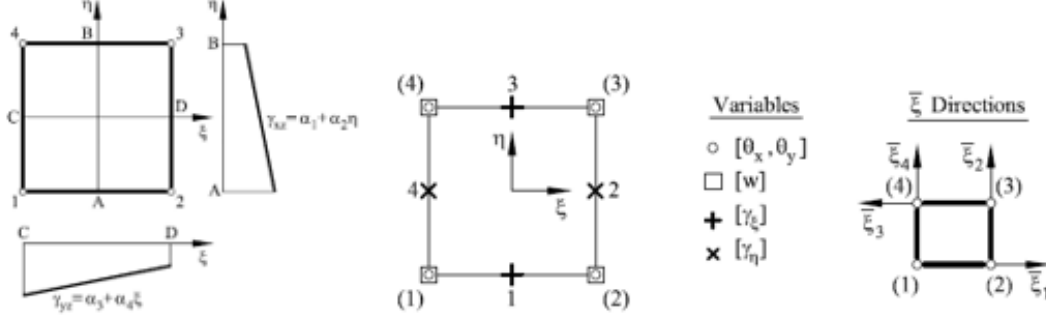


Figure 4.7 : Assumed shear strain field (Oñate, 2013).

The quadrature points are used along the lines $\xi = 0$ and $\eta = 0$ as seen in the Figure 4.7 and states

$$\varepsilon^s = \bar{B}^s a^e = \sum_{k=1}^m N_{\gamma k} B_k^s a_k = \sum_{k=1}^m N_{\gamma k} \hat{\gamma}_k \quad (4.36)$$

$$\gamma = J^{-1} \gamma' = J^{-1} \begin{Bmatrix} \gamma_{\xi} \\ \gamma_{\eta} \end{Bmatrix} \quad (4.37)$$

where $N_{\gamma k}$ is the interpolation function matrix, m is the shear strain points, γ_{ξ} and γ_{η} are shear strains at natural system and $\gamma_{\bar{\xi}_i}$ is the shear strains at middle points of plate in Figure 4.7.

$$\gamma' = \begin{Bmatrix} \gamma_{\xi} \\ \gamma_{\eta} \end{Bmatrix} = \begin{Bmatrix} a_1 + a_2 \eta \\ a_3 + a_4 \xi \end{Bmatrix} = Aa \quad (4.38a)$$

$$A = \begin{bmatrix} 1 & \eta & 0 & 0 \\ 0 & 0 & 1 & \xi \end{bmatrix} \quad (4.38b)$$

$$\gamma_{\bar{\xi}_i} = (a_1 + a_2 \eta) \cos \beta_i + (a_3 + a_4 \xi) \sin \beta_i; \quad i = 1, \dots, 4 \quad (4.39)$$

where β_i is the angle between the $\bar{\xi}_i$ and ξ axis. So,

$$[P]\{a\} = \begin{bmatrix} 1 & -1 & 0 & 0 \\ 0 & 0 & 1 & 1 \\ -1 & -1 & 0 & 0 \\ 0 & 0 & 1 & -1 \end{bmatrix} \begin{Bmatrix} a_1 \\ a_2 \\ a_3 \\ a_4 \end{Bmatrix} = \begin{Bmatrix} \gamma_{\bar{\xi}_1} \\ \gamma_{\bar{\xi}_2} \\ \gamma_{\bar{\xi}_3} \\ \gamma_{\bar{\xi}_4} \end{Bmatrix} \quad (4.40)$$

$$\begin{Bmatrix} \gamma_{\bar{\xi}_1} \\ \gamma_{\bar{\xi}_2} \\ \gamma_{\bar{\xi}_3} \\ \gamma_{\bar{\xi}_4} \end{Bmatrix} = \begin{bmatrix} 1 & 0 & \dots & \dots & 0 \\ \vdots & 0 & 1 & \vdots & \vdots \\ \vdots & \vdots & \vdots & -1 & 0 \\ 0 & \dots & \dots & 0 & 1 \end{bmatrix} \begin{Bmatrix} \gamma_{\xi_1} \\ \gamma_{\eta_1} \\ \gamma_{\xi_2} \\ \gamma_{\eta_2} \\ \gamma_{\xi_3} \\ \gamma_{\eta_3} \\ \gamma_{\xi_4} \\ \gamma_{\eta_4} \end{Bmatrix} = [T]\{\hat{\gamma}'\} \quad (4.41)$$

$$\{\widehat{\gamma'}\} = \begin{bmatrix} J_1 & \dots & \dots & 0 \\ \vdots & J_2 & \vdots & \vdots \\ \vdots & \vdots & J_3 & \vdots \\ 0 & \dots & \dots & J_4 \end{bmatrix} \begin{Bmatrix} \widehat{\gamma^1} \\ \vdots \\ \vdots \\ \widehat{\gamma^4} \end{Bmatrix} = [C]\widehat{\gamma} = [C]B^s a^e = [C] \begin{Bmatrix} B^{s1} \\ \vdots \\ \vdots \\ B^{s4} \end{Bmatrix} a^e \quad (4.42)$$

All equations from 4.35 to 4.42 inserting each other shear strain occurs as,

$$\gamma = J^{-1}AP^{-1}TC\widehat{\gamma} = N_\gamma\widehat{\gamma} \quad (4.43)$$

$$N_\gamma = J^{-1}AP^{-1}TC \quad (4.44)$$

$$\gamma = J^{-1}AP^{-1}TCB^s a^e = \overline{B^s} a^e \quad (4.45)$$

$$\overline{B^s} = N_\gamma B^s \quad (4.46)$$

The $\overline{B^s}$ new shear strain term can be used instead of B^s in K^s and provides to prevent locking like one point gauss integration. When these steps are applied on Q4 element new shear strain term is found equal to below term,

$$\overline{B^s}^T = \begin{bmatrix} \frac{-1+\eta}{4a} & \frac{-1+\xi}{4b} \\ \frac{1}{4}(-1+\eta) & 0 \\ 0 & \frac{1}{4}(-1+\xi) \\ -\frac{-1+\eta}{4a} & -\frac{1+\xi}{4b} \\ \frac{1}{4}(-1+\eta) & 0 \\ 0 & \frac{1}{4}(-1-\xi) \\ \frac{1+\eta}{4a} & \frac{1+\xi}{4b} \\ \frac{1}{4}(-1-\eta) & 0 \\ 0 & \frac{1}{4}(-1-\xi) \\ -\frac{1+\eta}{4a} & -\frac{-1+\xi}{4b} \\ \frac{1}{4}(-1-\eta) & 0 \\ 0 & \frac{1}{4}(-1+\xi) \end{bmatrix} \quad (4.47)$$

All these methods are made applicable RMPT to thin plates. In this thesis, QLLL method and Gauss method are applied separately on thin plates during usage of RMPT. The first six non-dimensional natural frequencies of square plate which is simply supported at four side are validated with 16x16 mesh developed code in Mathematica and 4 noded quadrilateral-QLLL element.

At the same time, the natural frequencies of plate are obtained from 16x16 mesh mathematical modal on ABAQUS package program. Its material and dimension properties are shown in Table 4.3 and code results compare with ABAQUS, analytical and FEM results in Table 4.4.

Table 4.3 : The simply supported plate properties (Petyt, 1990).

Plate Properties	Values
E	10920 N/m ²
ρ	1 kg/m ³
ν	0.3
h	0.1 m
2a	1 m

Table 4.4 : Comparison of non-dimensional $\lambda^{0.5} = h\omega\sqrt{(\rho/G)}$ natural frequencies of the square plate.

Modes	Present	Present-ABAQUS	HTK element-FEM (Petyt, 1990)	Analytical (Petyt, 1990)
(1,1)	0.0934	0.0933	0.0945	0.0930
(2,1)	0.2250	0.2247	0.2347	0.2218
(2,2)	0.3456	0.3443	0.3597	0.3402
(3,1)	0.4286	0.4279	0.4729	0.4144
(3,2)	0.5347	0.5318	0.5746	0.5197
(3,3)	0.6894	0.6882	0.7520	0.6821

The non-dimensional natural frequencies converge with increasing number of used elements for this plate example and it can be seen in Figure 4.8.

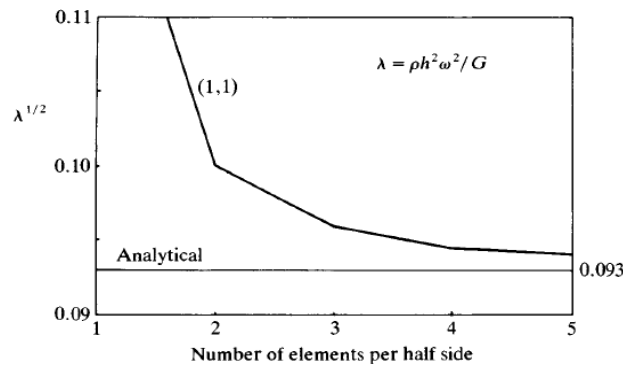


Figure 4.8 : The non-dimensional frequency convergence (Petyt, 1990).

5. COMPOSITE PLATES

Fundamentally, composite is combination of different type materials in a specific form to obtain new improved properties than singular usage. Its type is called as the anisotropic material due to have different material properties in all directions of body. Composite structures are more popular than isotropic materials in aviation especially in consequence of their higher stiffness and strength characteristics.

In contrast to plate bending theories, in plane displacements on mid plane of composite plates are effective more than the homogeneous materials because of axial forces which are named as membrane effects. This change brings the membrane element effect on mass and stiffness of the plate. Besides, membrane effect creates coupling with bending element depending on stacking and sequence of laminas. This coupling can cause some problems are called as membrane locking like shear locking phenomena.

The laminated plates have in plane and out of plane elongations so, there are 5 DOF, u , v , w , θ_x and θ_y for each node of the accepted element. So, for 4-noded quadrilateral element, total DOF is twenty and this requires twenty unknowns for five displacement equations. As a result, dimensions of the mass and stiffness matrices are 20x20. The laminated composite plates have cross section area as seen in Figure 5.1.

Niyogi, et. al. (1999), states that the relationship between displacements can be expressed as follow.

$$\begin{Bmatrix} u \\ v \\ w \\ \theta_x \\ \theta_y \end{Bmatrix} = \sum_{j=1}^4 N_j [I_5] \begin{Bmatrix} u_j \\ v_j \\ w_j \\ \theta_{xj} \\ \theta_{yj} \end{Bmatrix} \quad (5.1)$$

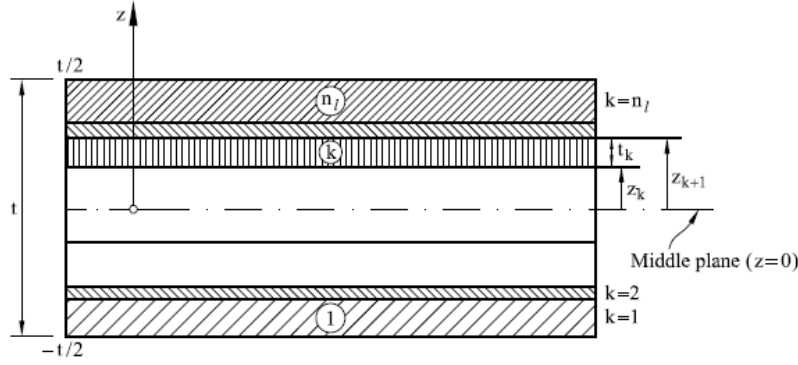


Figure 5.1 : Lamination representation with thicknesses (Oñate, 2013).

Initially, if the composite plates are investigated in terms of their stiffness and elastic properties, the necessary matrices are obtained as

$$D_e = \begin{bmatrix} A_{11} & A_{12} & A_{16} & B_{11} & B_{12} & B_{16} & 0 & 0 \\ A_{21} & A_{22} & A_{26} & B_{21} & B_{22} & B_{26} & 0 & 0 \\ A_{16} & A_{26} & A_{66} & B_{16} & B_{26} & B_{66} & 0 & 0 \\ B_{11} & B_{12} & B_{16} & D_{11} & D_{12} & D_{16} & 0 & 0 \\ B_{21} & B_{22} & B_{26} & D_{21} & D_{22} & D_{26} & 0 & 0 \\ B_{16} & B_{26} & B_{66} & D_{16} & D_{26} & D_{66} & 0 & 0 \\ 0 & 0 & 0 & 0 & 0 & 0 & A_{44} & A_{45} \\ 0 & 0 & 0 & 0 & 0 & 0 & A_{45} & A_{55} \end{bmatrix} \quad (5.2)$$

$$[A_{ij}] = \sum_{k=1}^n [\bar{Q}_{ij}]^k (z_k - z_{k-1}) \quad i, j = 1, 2, 6 \quad (5.3a)$$

$$[A_{ij}] = \sum_{k=1}^n [\bar{Q}_{ij}]^k \kappa (z_k - z_{k-1}) \quad i, j = 4, 5 \quad \kappa = 5/6 \quad (5.3b)$$

$$[B_{ij}] = \frac{1}{2} \sum_{k=1}^n [\bar{Q}_{ij}]^k (z_k^2 - z_{k-1}^2) \quad i, j = 1, 2, 6 \quad (5.3c)$$

$$[D_{ij}] = \frac{1}{3} \sum_{k=1}^n [\bar{Q}_{ij}]^k (z_k^3 - z_{k-1}^3) \quad i, j = 1, 2, 6 \quad (5.3d)$$

where \bar{Q}_{ij} is the stiffness matrix of lamina depends of angles of layers, A_{ij} is the in plane stiffness, B_{ij} is the axial bending coupling stiffness, D_{ij} is the bending stiffness, D_e is the elastic property matrices of laminate respectively. The κ is the laminate curvature, z is the distance from middle plane, k is the number of layer and n is the total number of layer in laminate. A_{ij} , B_{ij} , D_{ij} and \bar{Q}_{ij} matrices are symmetric for laminate (Nettles, 1994).

$$Q_{11} = \frac{E_L}{1 - \nu_{LT} \nu_{TL}} \quad (5.4a)$$

$$Q_{12} = \nu_{TL} * \frac{E_T}{1 - \nu_{LT} \nu_{TL}} \quad (5.4b)$$

$$Q_{22} = \frac{E_T}{1-\nu_{LT}\nu_{TL}} \quad (5.4c)$$

$$Q_{66} = G_{LT} \quad Q_{44} = G_{Lz} \quad Q_{55} = G_{Tz} \quad (5.4d)$$

$$\bar{Q}_{11} = Q_{11}(\cos[\theta])^4 + 2(Q_{12} + 2Q_{66})(\sin[\theta])^2(\cos[\theta])^2 + Q_{22}(\sin[\theta])^4 \quad (5.4e)$$

$$\bar{Q}_{12} = ((Q_{11} + Q_{22} - 4Q_{66})(\sin[\theta])^2(\cos[\theta])^2) + Q_{12}((\sin[\theta])^4 + (\cos[\theta])^4) \quad (5.4f)$$

$$\bar{Q}_{22} = Q_{11}(\sin[\theta])^4 + 2(Q_{12} + 2Q_{66})(\sin[\theta])^2(\cos[\theta])^2 + Q_{22}(\cos[\theta])^4 \quad (5.4g)$$

$$\bar{Q}_{16} = ((Q_{11} - Q_{12} - 2Q_{66})\sin[\theta](\cos[\theta])^3) + ((Q_{12} - 2Q_{66})\cos[\theta](\sin[\theta])^3) \quad (5.4h)$$

$$\bar{Q}_{26} = ((Q_{11} - Q_{12} - 2Q_{66})\cos[\theta](\sin[\theta])^3) + ((Q_{12} - 2Q_{66})\sin[\theta](\cos[\theta])^3) \quad (5.4i)$$

$$\bar{Q}_{66} = ((Q_{11} + Q_{22} - 2Q_{12}) - 2Q_{66})(\sin[\theta])^2(\cos[\theta])^2 + Q_{66}((\sin[\theta])^4 + (\cos[\theta])^4) \quad (5.4j)$$

$$\begin{aligned} \bar{Q}_{44} &= Q_{55}(\sin[\theta])^2 + Q_{44}(\cos[\theta])^2 & \bar{Q}_{45} &= (Q_{55} - Q_{44})(\sin[\theta])(\cos[\theta]) \\ \bar{Q}_{55} &= Q_{44}(\sin[\theta])^2 + Q_{55}(\cos[\theta])^2 \end{aligned} \quad (5.4k)$$

where Q_{ij} terms represent reduced stiffness, E_L , E_T , G_{LT} , G_{Lz} , G_{Tz} , ν_{LT} , ν_{TL} and θ are L direction elastic modulus, T direction elastic modulus, LT direction shear modulus, Lz direction shear modulus, Tz direction shear modulus, LT direction Poisson's ratio, TL direction Poisson's ratio and layer fiber orientation angle respectively. The L expresses the direction of the longitudinal fibers and T is opposite direction.

Both of the plate theories can be applicable for composite laminated plate out of plane displacements and rotations. In composite plate examination process, the KLPT and the RMPT converge by membrane element adding. But, the RMPT approach more precise as a result of considering of transverse shear effect cross the thickness of laminate.

Second part is achieving membrane element energy functions to add bending elements. Figure 5.2 shows a plate with in-plane direction loads and h is the thickness of the plate. When u , v , σ and ϵ represent displacement components of x and y directions, plane stress and strains respectively, energy equations can be expressed as

$$U = \frac{1}{2} \int \{\sigma\}^T \{\epsilon\} dV \quad (5.5a)$$

$$T = \frac{1}{2} \int h \rho (\dot{u}^2 + \dot{v}^2) dA \quad (5.5b)$$

where stress-strain relationship is given by

$$\{\sigma\} = [D]\{\varepsilon\} \quad (5.6)$$

$$\{\varepsilon\} = \begin{bmatrix} \partial u / \partial x \\ \partial v / \partial y \\ \partial v / \partial x + \partial u / \partial y \end{bmatrix} \quad (5.7)$$

from Hooke's law.

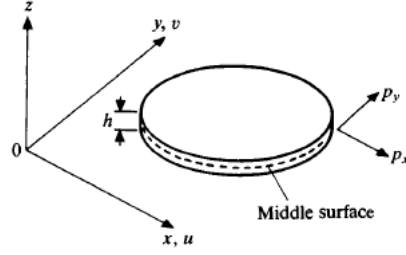


Figure 5.2 : Membrane element of plate (Petyt, 1990).

So, strain energy is

$$U = \frac{1}{2} \int \{\varepsilon\}^T [D] \{\varepsilon\} dV = \frac{1}{2} \int h \{\varepsilon\}^T [D] \{\varepsilon\} dA \quad (5.8)$$

This theory refers membrane element and their displacement and rotations are explained in section 3.2. Combining classical equation of kinetic energy with obtained membrane element energy function gives the mass matrix of the element as,

$$T_e = \frac{1}{2} [M]_m \{\dot{u}\}_e^2 \quad (5.9)$$

$$[M]_m = \int \rho h [N]^T [N] dA = \rho h a b \int_{-1}^1 \int_{-1}^1 ([N]^T [N] d\eta) d\xi \quad (5.10)$$

where N is the shape function matrix that mentioned in section 3.2 and M_m is the mass matrix for membrane element and \dot{u} is the in plane velocity vector.

$$[M]_m = \rho h a b \begin{bmatrix} \frac{4}{9} & 0 & \frac{2}{9} & 0 & \frac{1}{9} & 0 & \frac{2}{9} & 0 \\ 0 & \frac{4}{9} & 0 & \frac{2}{9} & 0 & \frac{1}{9} & 0 & \frac{2}{9} \\ \frac{2}{9} & 0 & \frac{4}{9} & 0 & \frac{2}{9} & 0 & \frac{1}{9} & 0 \\ 0 & \frac{2}{9} & 0 & \frac{4}{9} & 0 & \frac{2}{9} & 0 & \frac{1}{9} \\ \frac{1}{9} & 0 & \frac{2}{9} & 0 & \frac{4}{9} & 0 & \frac{2}{9} & 0 \\ 0 & \frac{1}{9} & 0 & \frac{2}{9} & 0 & \frac{4}{9} & 0 & \frac{2}{9} \\ \frac{2}{9} & 0 & \frac{1}{9} & 0 & \frac{2}{9} & 0 & \frac{4}{9} & 0 \\ 0 & \frac{2}{9} & 0 & \frac{1}{9} & 0 & \frac{2}{9} & 0 & \frac{4}{9} \end{bmatrix} \quad (5.11)$$

The stiffness matrix of the element is generated with combination of classical strain energy equation with obtained membrane element energy function given by

$$U_e = \frac{1}{2} [K]_m \{u\}_e^2 \quad (5.12)$$

When u is the in plane displacements, K_m is the membrane element stiffness and B_m is the in plane strain matrices respectively and for isotropic homogeneous plates given by,

$$[K]_m = \int h [B_m]^T [D] [B_m] \quad (5.13)$$

$$B_m = \begin{bmatrix} \frac{\partial N}{\partial x} & 0 \\ 0 & \frac{\partial N}{\partial y} \\ \frac{\partial N}{\partial y} & \frac{\partial N}{\partial x} \end{bmatrix} \quad (5.14)$$

$$[K]_m = \frac{Eh}{6ab(1-\nu^2)} \begin{bmatrix} [k_{11}] & [k_{12}] \\ [k_{12}] & [k_{22}] \end{bmatrix} \quad (5.15)$$

$$[k_{11}] = \begin{bmatrix} 2b^2 + a^2(1-\nu) & ab(0.75 + 0.75\nu) & -2b^2 + a^2(0.5 - 0.5\nu) & ab(-0.75 + 2.25\nu) \\ \text{symmetric} & 2a^2 + b^2(1-\nu) & ab(0.75 - 2.25\nu) & a^2 + b^2(-1 + \nu) \\ & & 2b^2 + a^2(1-\nu) & ab(-0.75 - 0.75\nu) \\ & & & 2a^2 + b^2(1-\nu) \end{bmatrix} \quad (5.16a)$$

$$[k_{12}] = \begin{bmatrix} -b^2 + a^2(-0.5 + 0.5\nu) & ab(-0.75 - 0.75\nu) & b^2 + a^2(-1 + \nu) & ab(0.75 - 2.25\nu) \\ \text{symmetric} & -a^2 + b^2(-0.5 + 0.5\nu) & ab(-0.75 + 2.25\nu) & -2a^2 + b^2(0.5 - 0.5\nu) \\ & & -b^2 + a^2(-0.5 + 0.5\nu) & ab(0.75 + 0.75\nu) \\ & & & -a^2 + b^2(-0.5 + 0.5\nu) \end{bmatrix} \quad (5.16b)$$

$$[k_{22}] = \begin{bmatrix} 2b^2 + a^2(1-\nu) & ab(0.75 + 0.75\nu) & -2b^2 + a^2(0.5 - 0.5\nu) & ab(-0.75 + 2.25\nu) \\ \text{symmetric} & 2a^2 + b^2(1-\nu) & ab(0.75 - 2.25\nu) & a^2 + b^2(-1 + \nu) \\ & & 2b^2 + a^2(1-\nu) & ab(-0.75 - 0.75\nu) \\ & & & 2a^2 + b^2(1-\nu) \end{bmatrix} \quad (5.16c)$$

After that, out of plane displacement case is calculated and added to membrane effect. The coupling between membrane and bending also takes into account. According to chosen plate theory mass matrices can be expanded to 5 DOF. For the KLPT application to composite plates element mass matrix is given by

$$[M]_e = [M]_m + [M]_b \quad (5.17)$$

$$[M]_e = \int \rho h [N_m]_u^T [N_m]_u + \rho h [N_m]_v^T [N_m]_v + \rho h [N_b]^T [N_b] dA \quad (5.18)$$

Where N_m is the expanded version of membrane element shape functions which are mentioned in section 3.2, N_b is the expanded version of thin plate bending element shape functions mentioned before in section 3.3. The coefficient matrices of membrane and thin bending element are combined as R matrix,

$$[R] = \begin{bmatrix} 1 & -1 & -1 & 1 & 0 & 0 & 0 & 0 & 0 & 0 & 0 & 0 & 0 & 0 & 0 & 0 & 0 & 0 & 0 \\ 0 & 0 & 0 & 0 & 1 & -1 & -1 & 1 & 0 & 0 & 0 & 0 & 0 & 0 & 0 & 0 & 0 & 0 & 0 \\ 0 & 0 & 0 & 0 & 0 & 0 & 0 & 0 & 1 & -1 & -1 & 1 & 1 & 1 & -1 & -1 & -1 & 1 & 1 \\ 0 & 0 & 0 & 0 & 0 & 0 & 0 & 0 & 0 & 0 & 1 & 0 & -1 & -2 & 0 & 1 & 2 & 3 & -1 & -3 \\ 0 & 0 & 0 & 0 & 0 & 0 & 0 & 0 & 0 & -1 & 0 & 2 & 1 & 0 & -3 & -2 & -1 & 0 & 3 & 1 \\ 1 & 1 & -1 & -1 & 0 & 0 & 0 & 0 & 0 & 0 & 0 & 0 & 0 & 0 & 0 & 0 & 0 & 0 & 0 \\ 0 & 0 & 0 & 0 & 1 & 1 & -1 & -1 & 0 & 0 & 0 & 0 & 0 & 0 & 0 & 0 & 0 & 0 & 0 \\ 0 & 0 & 0 & 0 & 0 & 0 & 0 & 0 & 1 & 1 & -1 & 1 & -1 & 1 & 1 & -1 & 1 & -1 & -1 & -1 \\ 0 & 0 & 0 & 0 & 0 & 0 & 0 & 0 & 0 & 0 & 1 & 0 & 1 & -2 & 0 & 1 & -2 & 3 & 1 & 3 \\ 0 & 0 & 0 & 0 & 0 & 0 & 0 & 0 & 0 & -1 & 0 & -2 & 1 & 0 & -3 & 2 & -1 & 0 & 3 & 1 \\ 1 & 1 & 1 & 1 & 0 & 0 & 0 & 0 & 0 & 0 & 0 & 0 & 0 & 0 & 0 & 0 & 0 & 0 & 0 \\ 0 & 0 & 0 & 0 & 1 & 1 & 1 & 1 & 0 & 0 & 0 & 0 & 0 & 0 & 0 & 0 & 0 & 0 & 0 \\ 0 & 0 & 0 & 0 & 0 & 0 & 0 & 0 & 1 & 1 & 1 & 1 & 1 & 1 & 1 & 1 & 1 & 1 & 1 \\ 0 & 0 & 0 & 0 & 0 & 0 & 0 & 0 & 0 & 0 & 1 & 0 & 1 & 2 & 0 & 1 & 2 & 3 & 1 & 3 \\ 0 & 0 & 0 & 0 & 0 & 0 & 0 & 0 & 0 & -1 & 0 & -2 & -1 & 0 & -3 & -2 & -1 & 0 & -3 & -1 \\ 1 & -1 & 1 & -1 & 0 & 0 & 0 & 0 & 0 & 0 & 0 & 0 & 0 & 0 & 0 & 0 & 0 & 0 & 0 \\ 0 & 0 & 0 & 0 & 1 & -1 & 1 & -1 & 0 & 0 & 0 & 0 & 0 & 0 & 0 & 0 & 0 & 0 & 0 \\ 0 & 0 & 0 & 0 & 0 & 0 & 0 & 0 & 1 & -1 & 1 & 1 & -1 & 1 & -1 & 1 & -1 & 1 & -1 & -1 \\ 0 & 0 & 0 & 0 & 0 & 0 & 0 & 0 & 0 & 0 & 1 & 0 & -1 & 2 & 0 & 1 & -2 & 3 & -1 & -3 \\ 0 & 0 & 0 & 0 & 0 & 0 & 0 & 0 & 0 & -1 & 0 & 2 & -1 & 0 & -3 & 2 & -1 & 0 & -3 & -1 \end{bmatrix} \quad (5.19)$$

$$\delta = [1 \quad 1 \quad 1 \quad \xi \quad \eta \quad \xi \quad \xi \quad \xi^2 \quad \xi\eta \quad \eta^2 \quad \eta \quad \eta \quad \xi^3 \quad \xi^2\eta \quad \xi\eta^2 \quad \xi\eta \quad \xi\eta \quad \eta^3 \quad \xi^3\eta \quad \xi\eta^3] \quad (5.20)$$

$$[N_b] = [N_1 \quad N_2 \quad N_3 \quad N_4] = \delta[R]^{-1} \quad (5.21)$$

$$[N_m] = [N_m]_u = [N_1 \quad N_2 \quad N_3 \quad N_4] \text{ for } u \text{ displacement} \quad (5.22a)$$

$$[N_m] = [N_m]_v = [N_1 \quad N_2 \quad N_3 \quad N_4] \text{ for } v \text{ displacement} \quad (5.22b)$$

Finally, the mass matrix is obtained as,

$$[M]_e = \rho h a b \int_{-1}^1 \int_{-1}^1 ([N_m]_u^T [N_m]_u + [N_m]_v^T [N_m]_v + [N_b]^T [N_b]) d\eta d\xi \quad (5.23)$$

$$[M]_e = \frac{\rho h a b}{6300} \begin{bmatrix} [m_{11}] & [m_{12}] \\ [m_{21}] & [m_{22}] \end{bmatrix} \quad (5.24)$$

$$[m_{11}] = \begin{bmatrix} 2800 & 0 & 0 & 0 & 0 & 1400 & 0 & 0 & 0 & 0 \\ 0 & 2800 & 0 & 0 & 0 & 0 & 1400 & 0 & 0 & 0 \\ 0 & 0 & 3454 & 922b & -922a & 0 & 0 & 1226 & 398b & 548a \\ 0 & 0 & 922b & 320b^2 & -252ab & 0 & 0 & 398b & 160b^2 & 168ab \\ 0 & 0 & -922a & -252ab & 320a^2 & 0 & 0 & -548a & -168ab & -240a^2 \\ 1400 & 0 & 0 & 0 & 0 & 2800 & 0 & 0 & 0 & 0 \\ 0 & 1400 & 0 & 0 & 0 & 0 & 2800 & 0 & 0 & 0 \\ 0 & 0 & 1226 & 398b & -548a & 0 & 0 & 3454 & 922b & 922a \\ 0 & 0 & 398b & 160b^2 & -168ab & 0 & 0 & 922b & 320b^2 & 252ab \\ 0 & 0 & 548a & 168ab & -240a^2 & 0 & 0 & 922a & 252ab & 320a^2 \end{bmatrix} \quad (5.25a)$$

$$[m_{21}] = \begin{bmatrix} 700 & 0 & 0 & 0 & 0 & 1400 & 0 & 0 & 0 & 0 \\ 0 & 700 & 0 & 0 & 0 & 0 & 1400 & 0 & 0 & 0 \\ 0 & 0 & 394 & 232b & -232a & 0 & 0 & 1226 & 548b & 398a \\ 0 & 0 & -232b & -120b^2 & 112ab & 0 & 0 & -548b & -240b^2 & -168ab \\ 0 & 0 & 232a & 112ab & -120a^2 & 0 & 0 & 398a & 168ab & 160a^2 \\ 1400 & 0 & 0 & 0 & 0 & 700 & 0 & 0 & 0 & 0 \\ 0 & 1400 & 0 & 0 & 0 & 0 & 700 & 0 & 0 & 0 \\ 0 & 0 & 1226 & 548b & -398a & 0 & 0 & 394 & 232b & 232a \\ 0 & 0 & -548b & -240b^2 & 168ab & 0 & 0 & -232b & -120b^2 & -112ab \\ 0 & 0 & -398a & -168ab & 160a^2 & 0 & 0 & -232a & -112ab & -120a^2 \end{bmatrix} \quad (5.25b)$$

$$[m_{21}] = \begin{bmatrix} 700 & 0 & 0 & 0 & 0 & 1400 & 0 & 0 & 0 & 0 \\ 0 & 700 & 0 & 0 & 0 & 0 & 1400 & 0 & 0 & 0 \\ 0 & 0 & 394 & -232b & -232a & 0 & 0 & 1226 & -548b & -398a \\ 0 & 0 & 232b & -120b^2 & 112ab & 0 & 0 & 548b & -240b^2 & -168ab \\ 0 & 0 & -232a & 112ab & -120a^2 & 0 & 0 & -398a & 168ab & 160a^2 \\ 1400 & 0 & 0 & 0 & 0 & 700 & 0 & 0 & 0 & 0 \\ 0 & 1400 & 0 & 0 & 0 & 0 & 700 & 0 & 0 & 0 \\ 0 & 0 & 1226 & -548b & 398a & 0 & 0 & 394 & -232b & -232a \\ 0 & 0 & 548b & -240b^2 & 168ab & 0 & 0 & 232b & -120b^2 & -112ab \\ 0 & 0 & 398a & -168ab & 160a^2 & 0 & 0 & 232a & -112ab & -120a^2 \end{bmatrix} \quad (5.25c)$$

$$[m_{22}] = \begin{bmatrix} 2800 & 0 & 0 & 0 & 0 & 1400 & 0 & 0 & 0 & 0 \\ 0 & 2800 & 0 & 0 & 0 & 0 & 1400 & 0 & 0 & 0 \\ 0 & 0 & 3454 & -922b & 922a & 0 & 0 & 1226 & -398b & -548a \\ 0 & 0 & -922b & 320b^2 & -252ab & 0 & 0 & -398b & 160b^2 & 168ab \\ 0 & 0 & 922a & -252ab & 320a^2 & 0 & 0 & 548a & -168ab & -240a^2 \\ 1400 & 0 & 0 & 0 & 0 & 2800 & 0 & 0 & 0 & 0 \\ 0 & 1400 & 0 & 0 & 0 & 0 & 2800 & 0 & 0 & 0 \\ 0 & 0 & 1226 & -398b & 548a & 0 & 0 & 3454 & -922b & -922a \\ 0 & 0 & -398b & 160b^2 & -168ab & 0 & 0 & -922b & 320b^2 & 252ab \\ 0 & 0 & -548a & 168ab & -240a^2 & 0 & 0 & -922a & 252ab & 320a^2 \end{bmatrix} \quad (5.25d)$$

For the RMPT application on composite plates element mass matrix is given by

$$[M]_e = \int \rho [N]^T \begin{bmatrix} h & 0 & 0 & 0 & 0 \\ 0 & h & 0 & 0 & 0 \\ 0 & 0 & h & 0 & 0 \\ 0 & 0 & 0 & \frac{h^3}{12} & 0 \\ 0 & 0 & 0 & 0 & \frac{h^3}{12} \end{bmatrix} [N] dA \quad (5.26)$$

The coefficient matrices of membrane and thick bending element are combined as R matrix,

$$[R] = \begin{bmatrix} 1 & -1 & -1 & 1 & 0 & 0 & 0 & 0 & 0 & 0 & 0 & 0 & 0 & 0 & 0 & 0 & 0 \\ 0 & 0 & 0 & 0 & 1 & -1 & -1 & 1 & 0 & 0 & 0 & 0 & 0 & 0 & 0 & 0 & 0 \\ 0 & 0 & 0 & 0 & 0 & 0 & 0 & 0 & 1 & -1 & -1 & 1 & 0 & 0 & 0 & 0 & 0 \\ 0 & 0 & 0 & 0 & 0 & 0 & 0 & 0 & 0 & 0 & 0 & 0 & 1 & -1 & -1 & 1 & 0 \\ 0 & 0 & 0 & 0 & 0 & 0 & 0 & 0 & 0 & 0 & 0 & 0 & 0 & 1 & -1 & -1 & 1 \\ 1 & 1 & -1 & -1 & 0 & 0 & 0 & 0 & 0 & 0 & 0 & 0 & 0 & 0 & 0 & 0 & 0 \\ 0 & 0 & 0 & 0 & 1 & 1 & -1 & -1 & 0 & 0 & 0 & 0 & 0 & 0 & 0 & 0 & 0 \\ 0 & 0 & 0 & 0 & 0 & 0 & 0 & 0 & 1 & 1 & -1 & -1 & 0 & 0 & 0 & 0 & 0 \\ 0 & 0 & 0 & 0 & 0 & 0 & 0 & 0 & 0 & 0 & 0 & 0 & 1 & 1 & -1 & -1 & 0 \\ 0 & 0 & 0 & 0 & 0 & 0 & 0 & 0 & 0 & 0 & 0 & 0 & 0 & 1 & 1 & -1 & -1 \\ 1 & 1 & 1 & 1 & 0 & 0 & 0 & 0 & 0 & 0 & 0 & 0 & 0 & 0 & 0 & 0 & 0 \\ 0 & 0 & 0 & 0 & 1 & 1 & 1 & 1 & 0 & 0 & 0 & 0 & 0 & 0 & 0 & 0 & 0 \\ 0 & 0 & 0 & 0 & 0 & 0 & 0 & 0 & 1 & 1 & 1 & 1 & 0 & 0 & 0 & 0 & 0 \\ 0 & 0 & 0 & 0 & 0 & 0 & 0 & 0 & 0 & 0 & 0 & 0 & 1 & 1 & 1 & 1 & 0 \\ 0 & 0 & 0 & 0 & 0 & 0 & 0 & 0 & 0 & 0 & 0 & 0 & 0 & 1 & 1 & 1 & 1 \\ 1 & -1 & 1 & -1 & 0 & 0 & 0 & 0 & 0 & 0 & 0 & 0 & 0 & 0 & 0 & 0 & 0 \\ 0 & 0 & 0 & 0 & 1 & -1 & 1 & -1 & 0 & 0 & 0 & 0 & 0 & 0 & 0 & 0 & 0 \\ 0 & 0 & 0 & 0 & 0 & 0 & 0 & 0 & 1 & -1 & 1 & -1 & 0 & 0 & 0 & 0 & 0 \\ 0 & 0 & 0 & 0 & 0 & 0 & 0 & 0 & 0 & 0 & 1 & -1 & 1 & -1 & 0 & 0 & 0 \\ 0 & 0 & 0 & 0 & 0 & 0 & 0 & 0 & 0 & 0 & 0 & 1 & -1 & 1 & -1 & 0 & 0 \end{bmatrix} \quad (5.27)$$

$$\delta = [1 \quad 1 \quad 1 \quad 1 \quad 1 \quad \xi \quad \xi \quad \xi \quad \xi \quad \xi \quad \eta \quad \eta \quad \eta \quad \eta \quad \eta \quad \xi\eta \quad \xi\eta \quad \xi\eta \quad \xi\eta \quad \xi\eta] \quad (5.28)$$

$$[N_1 \quad N_2 \quad N_3 \quad N_4] = \delta[R]^{-1} \quad (5.29a)$$

$$[N] = \begin{bmatrix} N_1 & 0 & 0 & 0 & 0 & N_2 & 0 & 0 & 0 & 0 & N_3 & 0 & 0 & 0 & 0 & N_4 & 0 & 0 & 0 & 0 \\ 0 & N_1 & 0 & 0 & 0 & 0 & N_2 & 0 & 0 & 0 & 0 & N_3 & 0 & 0 & 0 & 0 & N_4 & 0 & 0 & 0 \\ 0 & 0 & N_1 & 0 & 0 & 0 & 0 & N_2 & 0 & 0 & 0 & 0 & N_3 & 0 & 0 & 0 & 0 & N_4 & 0 & 0 \\ 0 & 0 & 0 & N_1 & 0 & 0 & 0 & 0 & N_2 & 0 & 0 & 0 & 0 & N_3 & 0 & 0 & 0 & 0 & N_4 & 0 \\ 0 & 0 & 0 & 0 & N_1 & 0 & 0 & 0 & 0 & N_2 & 0 & 0 & 0 & 0 & N_3 & 0 & 0 & 0 & 0 & N_4 \end{bmatrix} \quad (5.29b)$$

Finally, the mass matrix is obtained as

$$[M]_e = \rho_{ab} \begin{bmatrix} h & 0 & 0 & 0 & 0 \\ 0 & h & 0 & 0 & 0 \\ 0 & 0 & h & 0 & 0 \\ 0 & 0 & 0 & \frac{h^3}{12} & 0 \\ 0 & 0 & 0 & 0 & \frac{h^3}{12} \end{bmatrix} \int_{-1}^1 \int_{-1}^1 ([N]^T [N] d\eta) d\xi \quad (5.30)$$

$$[M]_e = \frac{\rho_{hab}}{9} \begin{bmatrix} [m_{11}] & [m_{12}] \\ [m_{12}] & [m_{11}] \end{bmatrix} \quad (5.31)$$

$$[m_{11}] = \begin{bmatrix} 4 & 0 & 0 & 0 & 0 & 2 & 0 & 0 & 0 & 0 \\ & 4 & 0 & 0 & 0 & 0 & 2 & 0 & 0 & 0 \\ & & 4 & 0 & 0 & 0 & 0 & 2 & 0 & 0 \\ & & & \frac{h^2}{3} & 0 & 0 & 0 & 0 & \frac{h^2}{6} & 0 \\ & & & & \frac{h^2}{3} & 0 & 0 & 0 & 0 & \frac{h^2}{6} \\ s & y & m. & & & 4 & 0 & 0 & 0 & 0 \\ & & & & & & 4 & 0 & 0 & 0 \\ & & & & & & & 4 & 0 & 0 \\ & & & & & & & & \frac{h^2}{3} & 0 \\ & & & & & & & & & \frac{h^2}{3} \end{bmatrix} \quad [m_{12}] = \begin{bmatrix} 1 & 0 & 0 & 0 & 0 & 2 & 0 & 0 & 0 & 0 \\ & 1 & 0 & 0 & 0 & 0 & 2 & 0 & 0 & 0 \\ & & 1 & 0 & 0 & 0 & 0 & 2 & 0 & 0 \\ & & & \frac{h^2}{12} & 0 & 0 & 0 & 0 & \frac{h^2}{6} & 0 \\ & & & & \frac{h^2}{12} & 0 & 0 & 0 & 0 & \frac{h^2}{6} \\ & & & & & 1 & 0 & 0 & 0 & 0 \\ s & y & m. & & & & 1 & 0 & 0 & 0 \\ & & & & & & & 1 & 0 & 0 \\ & & & & & & & & \frac{h^2}{12} & 0 \\ & & & & & & & & & \frac{h^2}{12} \end{bmatrix} \quad (5.32a)$$

The first step at stiffness achieving, these isotropic formulations of stiffness matrices are converted for orthotropic material properties.

So, for membrane stiffness A_{ij} matrix from equation 5.3a is used in equation 5.13,

$$[K]_m = \int [B_m]^T [A_{ij}] [B_m] dA \quad i, j = 1, 2, 6 \quad (5.33)$$

for bending stiffness D_{ij} matrix from equation 5.3d is used in bending stiffness matrix,

$$[K]_b = \int [B_b]^T [D_{ij}] [B_b] dA \quad i, j = 1, 2, 6 \quad (5.34)$$

for bending stiffness A_{ij} matrix from equation 5.3b is used in shear stiffness matrix,

$$[K]_s = \int [B_s]^T [A_{ij}] [B_s] dA \quad i, j = 4, 5 \quad (5.35)$$

and for membrane bending stiffness coupling effect B_{ij} matrix from equation 5.3c is used for coupling stiffness matrix,

$$[K]_{mb} = \int [B_m]^T [B_{ij}] [B_b] + [B_b]^T [B_{ij}] [B_m] dA \quad i, j = 1, 2, 6 \quad (5.36)$$

are found. The stiffness matrix of the element varies according to applied the theory.

If the KLPT is applied,

$$[K]_e = [K]_m + [K]_b + [K]_{mb} \quad (5.37)$$

$$B_m = \begin{bmatrix} \frac{\partial N_{mu}}{\partial x} & 0 & 0 & 0 & 0 \\ 0 & \frac{\partial N_{mv}}{\partial y} & 0 & 0 & 0 \\ \frac{\partial N_{mu}}{\partial y} & \frac{\partial N_{mv}}{\partial x} & 0 & 0 & 0 \end{bmatrix} \quad \text{and} \quad [B_b] = \begin{bmatrix} 0 & 0 & \frac{\partial^2 \partial N_b}{\partial x^2} \\ 0 & 0 & \frac{\partial^2 \partial N_b}{\partial y^2} \\ 0 & 0 & 2 \frac{\partial^2 \partial N_b}{\partial x \partial y} \end{bmatrix} \quad (5.38)$$

or the RMPT is applied,

$$[K]_e = [K]_m + [K]_b + [K]_s + [K]_{mb} \quad (5.39)$$

$$B_m = \begin{bmatrix} \frac{\partial N}{\partial x} & 0 & 0 & 0 & 0 \\ 0 & \frac{\partial N}{\partial y} & 0 & 0 & 0 \\ \frac{\partial N}{\partial y} & \frac{\partial N}{\partial x} & 0 & 0 & 0 \end{bmatrix} \quad (5.40)$$

$$[B^b] = \begin{bmatrix} 0 & 0 & 0 & 0 & -\frac{\partial N}{\partial x} \\ 0 & 0 & 0 & \frac{\partial N}{\partial y} & 0 \\ 0 & 0 & 0 & \frac{\partial N}{\partial x} & -\frac{\partial N}{\partial y} \end{bmatrix} \quad (5.41)$$

$$[B^s] = \begin{bmatrix} 0 & 0 & \frac{\partial N}{\partial x} & 0 & N \\ 0 & 0 & \frac{\partial N}{\partial y} & -N & 0 \end{bmatrix} \quad (5.42)$$

are used for element. In this thesis, a flat square composite plate non-dimensional natural frequencies are calculated with Mathematica 32x32 mesh size codes which are depending on the Kirchhoff and Mindlin's theories respectively. The composite flat plate is simply supported at four side. For the material, which has elastic properties as; $E_1/E_2=40$, $G_{12}=G_{13}=0.6 E_2$, $G_{23}=0.5 E_2$, $\nu_{12}=0.25$, calculated first non-dimensional frequency values are compared with Reddy & Phan (1985), in Table 5.1. For the thin plates, QLL method is applied on RMPT.

According to comparisons of CPT and FSDT with HSDT, for thick plates FSDT frequencies are actual levels of structures (Reddy & Phan, 1985). In examination of present study with FEM plate codes, if the KLPT is applied on composite thick plates in code, it can be seen that high differences from the other results and it is not suitable for thick plates in terms of neglecting transverse shear deformations. But modified Mindlin theory and the Kirchhoff FEM codes give very close results for thin composite plates.

Table 5.1 : Comparison of non-dimensional $\lambda = \omega (L^2/h) \sqrt{(\rho/E_2)}$ natural frequencies of the composite simply supported square plate with $[0^\circ/90^\circ]_s$.

2a/h	Present-Kirchhoff	Reddy & Phan-CPT (1985)	Present-Mindlin	Reddy & Phan- FSDT (1985)
2	15.828	15.830	5.528	5.492
5	18.317	18.215	10.989	10.820
10	18.595	18.652	15.469	15.083
20	18.990	18.767	17.830	17.583

6. FOLDED PLATES AND BOX BEAM

The folded plates are obtained by wrenching a plate or attaching end-to-end plates with a certain crank angle. The box beams are evaluated as 4 joining plate or 4 folded plates and can be analyzed same methods. These structures have widely applicable area on air vehicles like skins with wide crank angles, box beams in wing and empennages, helicopter blades etc. So, their vibration characteristics play more important role with used approaches in term of aerodynamic and structural integrity of air vehicles.

These plates are not located in the same plane as a result of crank angle effect. Therefore, this case creates difference between the global axes and the plate axes. The plate axes are called as local axes of the plates. The folded plates and box beams must undergo some processes before it can be analyzed using the finite element method.

Initial step is transformation of local axes to global axes. If considering the placement of the plates, when converting the local axes to the global axes, the plates should be relocated so that they are in one plane (ie, a kind of open dice). It shows necessity of the axial displacements consideration. Because 3 out of plane DOF on one face of plate may be in plane direction at global axes system. So, the structure examined with 5 DOF including 2 is in plane, 3 is out of plane like composite structures. Likewise, this transformation process reveals drilling DOF which is the rotation about the normal axis of plate, θ_z . It can be evaluated as transformation of one rotation of plate local axis to global axes system.

Secondly, adding of drilling DOF blows up the 5 DOF system to 6 DOF system and also blows up stiffness and mass matrix to 24x24 dimensions for 4 noded quadrilateral elements. Niyogi, et al. (1999), mentioned the θ_z terms in off-diagonal term is equal to zero but diagonal terms should be equaled to at least 1000 times smaller than the smallest term of diagonals at mass matrix in order to singularity does not occur. In this study diagonal terms of drilling degree are accepted as 0.0000001 and thus, singularity errors are avoided.

$$\begin{Bmatrix} u \\ v \\ w \\ \theta_x \\ \theta_y \end{Bmatrix} = \sum_{j=1}^4 N_j [I_5] \begin{Bmatrix} u_j \\ v_j \\ w_j \\ \theta_{xj} \\ \theta_{yj} \end{Bmatrix} \rightarrow \begin{Bmatrix} u \\ v \\ w \\ \theta_x \\ \theta_y \\ \theta_z \end{Bmatrix} \quad (6.1)$$

Finally, after the above operations are done separately for each face of folded plate, the elements of the plate are combined with the summation method and made into an assembly. General stiffness and mass matrices are obtained as if the folded plates are in a single flat plate on global axes with help of transform and they are used as the main matrices to find natural frequencies from eigenvalue problem. These matrices given by

$$[K]_g = [T]^T [K]_p [T] \quad (6.2)$$

$$[M]_g = [T]^T [M]_p [T] \quad (6.3)$$

where K_g and M_g are stiffness and mass matrices at global axes system when K_p and M_p are local ones and T is the transformation matrix that depends on crank angle. For 4-noded quadrilateral element, transformation data is shown as

$$[T] = \begin{bmatrix} R & 0 & 0 & 0 \\ 0 & R & 0 & 0 \\ 0 & 0 & R & 0 \\ 0 & 0 & 0 & R \end{bmatrix} \quad (6.4)$$

$$[R] = \begin{bmatrix} \cos[X, x] & \cos[Y, x] & \cos[Z, x] & 0 & 0 & 0 \\ \cos[X, y] & \cos[Y, y] & \cos[Z, y] & 0 & 0 & 0 \\ \cos[X, z] & \cos[Y, z] & \cos[Z, z] & 0 & 0 & 0 \\ 0 & 0 & 0 & \cos[X, x] & \cos[Y, x] & \cos[Z, x] \\ 0 & 0 & 0 & \cos[X, y] & \cos[Y, y] & \cos[Z, y] \\ 0 & 0 & 0 & \cos[X, z] & \cos[Y, z] & \cos[Z, z] \end{bmatrix} \quad (6.5)$$

where X , Y and Z are global axes, and x , y and z are local axes of the plate, their side-by-side use represents the angle between them (X, x). The R is the transformation submatrix. This matrix and angle relationship comes from vector calculation (Petyt, 1990).

$$\vec{u} = U\hat{X} + V\hat{Y} + W\hat{Z} \quad \text{and} \quad \hat{a}\hat{A} = \cos[A, a] \quad (6.6)$$

$$u = \hat{x}\vec{u} = \hat{x}(U\hat{X} + V\hat{Y} + W\hat{Z}) = U\cos[X, x] + V\cos[Y, x] + W\cos[Z, x] \quad (6.7)$$

$$\theta_x = \hat{u}\vec{u}, \quad v = \hat{y}\vec{u}, \quad \theta_y = \hat{v}\vec{u}, \quad w = \hat{w}\vec{u}, \quad \theta_z = \hat{w}\vec{u} \quad (6.8)$$

6.1. Folded Plates and Results

In this thesis, folded plates have 90° crank (folding) angle as β or α and different materials which are categorized by isotropic and orthotropic. Each fold length is equal to 2b dimension of rectangular plate and these edges are clamped. Plate length L is equal to 2a dimension of plate and these edges are free.

At the transformation submatrix, the angle between global and local axis is taken as 90° for first fold and 180° for the second fold. Since, the first face of folded plate is assumed at global axes. The transformation submatrices are given by

$$[R_1] = \begin{bmatrix} 1 & 0 & 0 & 0 & 0 & 0 \\ 0 & 1 & 0 & 0 & 0 & 0 \\ 0 & 0 & 1 & 0 & 0 & 0 \\ 0 & 0 & 0 & 1 & 0 & 0 \\ 0 & 0 & 0 & 0 & 1 & 0 \\ 0 & 0 & 0 & 0 & 0 & 1 \end{bmatrix} \quad (6.9a)$$

$$[R_2] = \begin{bmatrix} 1 & 0 & 0 & 0 & 0 & 0 \\ 0 & 0 & -1 & 0 & 0 & 0 \\ 0 & 1 & 0 & 0 & 0 & 0 \\ 0 & 0 & 0 & 1 & 0 & 0 \\ 0 & 0 & 0 & 0 & 0 & -1 \\ 0 & 0 & 0 & 0 & 1 & 0 \end{bmatrix} \quad (6.9b)$$

$$[R_3] = \begin{bmatrix} 1 & 0 & 0 & 0 & 0 & 0 \\ 0 & -1 & 0 & 0 & 0 & 0 \\ 0 & 0 & -1 & 0 & 0 & 0 \\ 0 & 0 & 0 & 1 & 0 & 0 \\ 0 & 0 & 0 & 0 & -1 & 0 \\ 0 & 0 & 0 & 0 & 0 & -1 \end{bmatrix} \quad (6.9c)$$

where R_1 is transformation submatrix of first face, R_2 is transformation submatrix of first fold (second face) and R_3 is transformation submatrix of second fold (third face).

The folded plates are shown in Figure 6.1. Their dimensions and boundary conditions are represented as one folded and two folded plates for both isotropic, orthotropic, thin and thick plates.

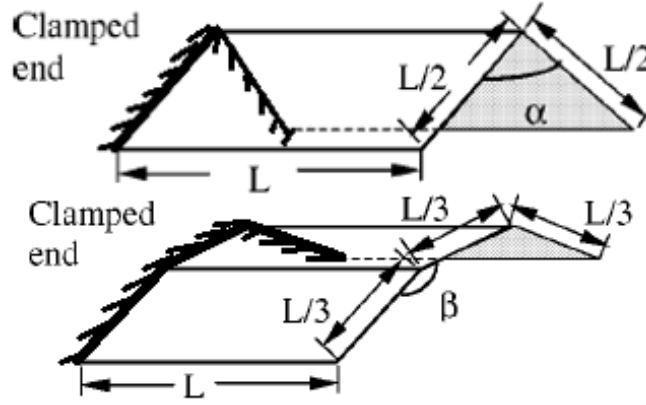


Figure 6.1 : Clamped one and two folded plate with crank angle α/β (Liu & Huang, 1992).

When the isotropic plates are considered, the KLPT and the RMPT can be applicable depending on length-to-thickness ratio of plate. For thin plates, the KLPT is preferred but if QLLL method is used on RMPT approach, these makes RMPT is applicable. Although RMPT is applicable for both of thin and thick plates, the KLPT is not suitable for thick ones because of neglecting shear effects which are through thickness of plate.

The orthotropic plates have composite laminated structure in this thesis. The KLPT and the RMPT are applied on different stacking sequenced composite plates with membrane effects which are mention in section 5.

6.1.1. The isotropic plates

The non-dimensional natural frequencies of one and two folded plates which are clamped at one side ($x=0$) and crank angle 90° are validated with developed FEM code in Mathematica. The folded plates are given in Figure 6.1. Two code studies are developed as one of these is based on the KLPT and the other one is RMPT with QLLL method.

At the same time, the natural frequencies of plate are obtained from mathematical modal in ABAQUS package program. For thin isotropic ones, its material and dimension properties are shown in Table 6.1. The one folded thin plate non dimensional frequency ($\lambda=L\omega\sqrt{(\rho(1-\nu^2))/E}$) results are compared with ABAQUS, Niyogi, et al., (1999) and Liu & Huang, (1992) results in Table 6.2 with $L=1.5\text{m}$ and the comparison for two folded plate is given in Table 6.3 with $L=2\text{m}$. Mode shapes of first 5 modes are represented in Figure 6.2 and Figure 6.3 for one folded and two folded cantilever isotropic thin plates respectively ($L/h>10$).

Table 6.1 : The thin plate properties (Niyogi, et al, 1999).

Plate Properties	Values
E	$10.92 \times 10^9 \text{ N/m}^2$
ρ	1000 kg/m^3
ν	0.3
h	$0.02 \times L$
2a	L
2b	L/2 for one fold L/3 for two fold
κ	5/6

Table 6.2 : Comparison of non-dimensional $\lambda = L\omega\sqrt{(\rho(1-\nu^2)/E)}$ natural frequencies of the 90° one folded thin clamped plate (L=1.5m).

Modes	Present-Kirchhoff (16x8)	Present-Mindlin (16x8)	Present-ABAQUS (16x8)	Liu & Huang (1992)	Niyogi, et al. (1999)
1	0.049	0.049	0.0487	0.0491	0.049
2	0.0972	0.0966	0.0970	0.0971	0.0971
3	0.1785	0.1792	0.1782	0.1786	0.1881
4	0.2089	0.2094	0.2085	0.2084	0.2183
5	0.3471	0.3566	0.3454	0.3558	0.3505

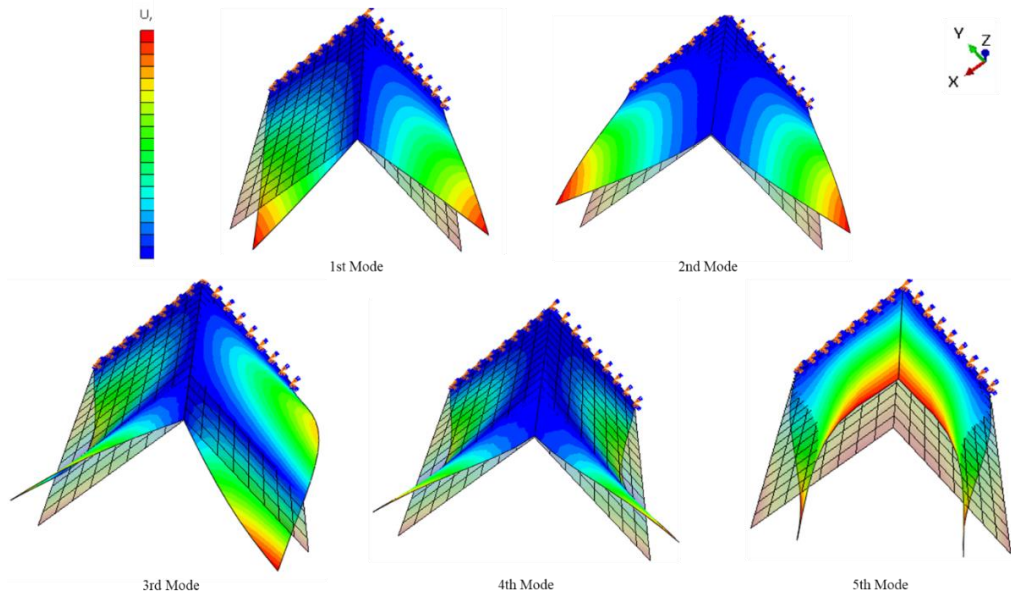


Figure 6.2 : Mode shapes of the cantilever one folded isotropic thin plate.

Table 6.3 : Comparison of the non-dimensional $\lambda=L\omega\sqrt{(\rho(1-\nu^2)/E)}$ natural frequencies of the 90° two folded thin clamped plate (L=2m).

Modes	Present-Kirchhoff (6x4)	Present-Mindlin (6x4)	Present-ABAQUS (6x4)	Liu & Huang (1992)	Niyogi, et al. (1999)
1	0.1249	0.1238	0.1234	0.1249	0.1249
2	0.1257	0.1252	0.1271	0.1252	0.1260
3	0.2579	0.2599	0.2678	0.2697	0.2579
4	0.2691	0.2727	0.2781	0.2830	0.2892
5	0.3277	0.3284	0.3165	0.3266	0.3286

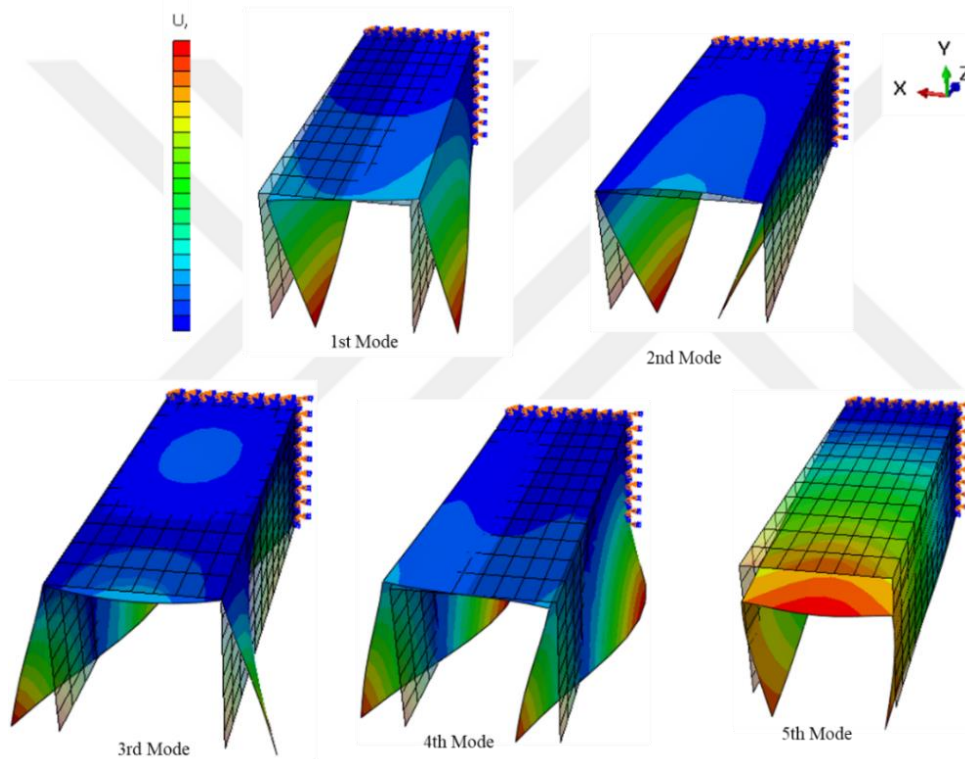


Figure 6.3 : Mode shapes of the cantilever two folded isotropic thin plate.

It can be seen from the above results that the Kirchhoff approach FEM code for an isotropic thin plate works better than others, even ABAQUS results. In addition, when shear locking is prevented by making necessary applications, the RMPT can also be used in thin folded plate FEM codes.

Then, in order to see the effect of thickness change on the natural frequency easily, the non-dimensional frequency values are given in terms of Hz in the Table 6.4.

Table 6.4 : Comparison of natural frequencies (Hz) of the folded thin plates.

Description of plate	Modes	Present-Kirchhoff	Present-Mindlin	Present-ABAQUS
90° one folded (L=1.5m)	1	18.02	17.76	17.91
	2	35.74	35.53	35.64
	3	65.63	65.91	65.51
	4	76.79	77.00	76.63
	5	127.58	131.08	126.94
90° two folded (L=2m)	1	34.43	34.13	34.03
	2	34.67	34.51	34.96
	3	71.10	71.66	71.88
	4	74.18	75.17	74.98
	5	90.33	90.54	87.25

Secondly, for the thick plates which have lower thickness ratio ($L/h < 10$) the code is prepared based on RMPT. The isotropic thick plate material and dimension properties are same with thin plate shown in Table 6.1 except the thickness of plate h . The plate thicknesses equal to $0.2 \cdot L$ for the thick folded plates. The thick folded plate code natural frequencies are compared with ABAQUS results in Table 6.5.

Table 6.5 : Comparison of natural frequencies (Hz) of the folded thick plates.

Description of plate	Modes	Present-Mindlin	Present-ABAQUS
90° one folded (L=1.5m)	1	119.3	118.98
	2	134.14	134.23
	3	233.31	233.15
	4	361.37	360.38
	5	469.62	469.16
	6	476.71	475.78
90° two folded (L=2m)	1	87.752	87.126
	2	95.619	94.665
	3	188.70	188.68
	4	281.78	280.12
	5	350.27	346.80
	6	396.78	395.54

Both of Mathematica code and ABAQUS solutions of the one folded plate use 32x16 mesh size and for two folded plate 12x8 mesh size is used. Mode shapes of first 5 modes are represented in Figure 6.4 and Figure 6.5 for one folded and two folded cantilever isotropic thick plates respectively. It can be seen that the Mindlin approach FEM code for an isotropic thick plate gives almost same results with ABAQUS program from the above results.

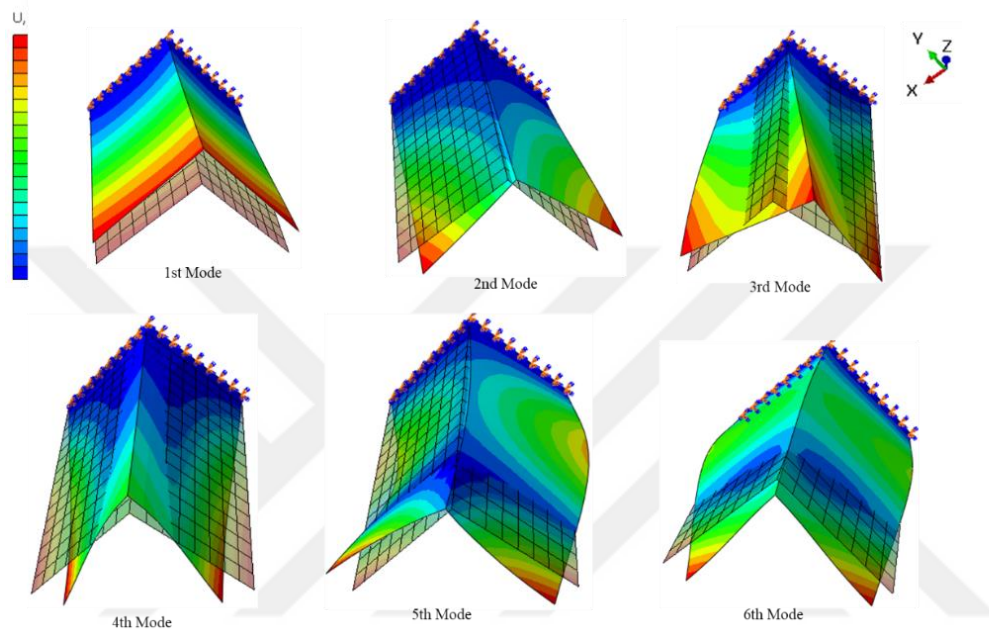


Figure 6.4 : Mode shapes of the cantilever one folded isotropic thick plate.

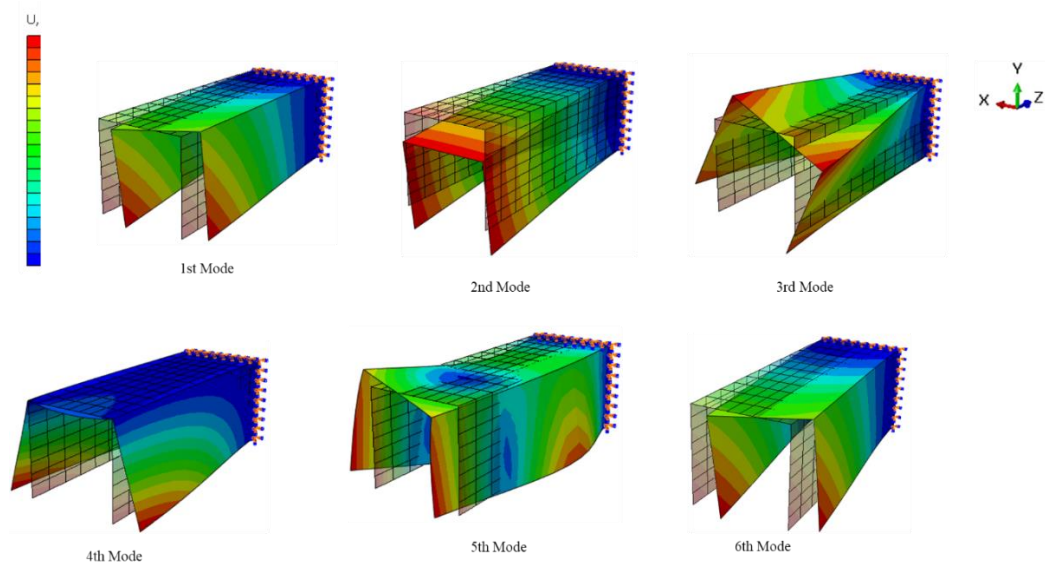


Figure 6.5 : Mode shapes of the cantilever two folded isotropic thick plate.

6.1.2. The composite laminated folded plates

The natural frequencies of one and two folded composite plates which are clamped at one side and crank angle 90° are validated with developed code in Mathematica. The composite laminated folded plates have same representation in Figure 6.1. Firstly, two code studies are developed as one of these is based on composite application of the KLPT and the other one is RMPT composite application with gauss integration method, for thin folded composite plates. At the same time, the natural frequencies of the plate are obtained from mathematical model on ABAQUS.

Table 6.6 : The composite plate properties with Material I (Niyogi, et al, 1999).

Plate Properties	Values
E_1	$60.7 \times 10^9 \text{ N/m}^2$
E_2	$24.8 \times 10^9 \text{ N/m}^2$
$G_{12}=G_{13}=G_{23}$	$12 \times 10^9 \text{ N/m}^2$
$\nu_{12}=\nu_{21}$	0.23
ρ	1300 kg/m^3
t_p	$h/3$
h	$0.02 \times L$
$2a$	L
$2b$	$L/2$
κ	$5/6$

For Material I, its material and dimension properties are shown in Table 6.6. Stacking sequence of the laminated plates is $[30^\circ/-30^\circ/30^\circ]$ and it can be seen in Figure 6.6. The composite laminated folded plate code results are compared with Niyogi, et al., (1999) non-dimensional frequencies ($\lambda=L\omega\sqrt{(\rho(1-\nu_{12}^2)/E_1)}$) in Table 6.7. The composite laminated folded plate code natural frequencies compare with ABAQUS results in Table 6.8. All solutions of the one folded composite plate use 32×16 mesh size and for two folded plates, 12×8 mesh size is used. Mode shapes of first 6 modes are represented in Figure 6.7 and Figure 6.8 for one folded and two folded cantilever composite plates respectively.

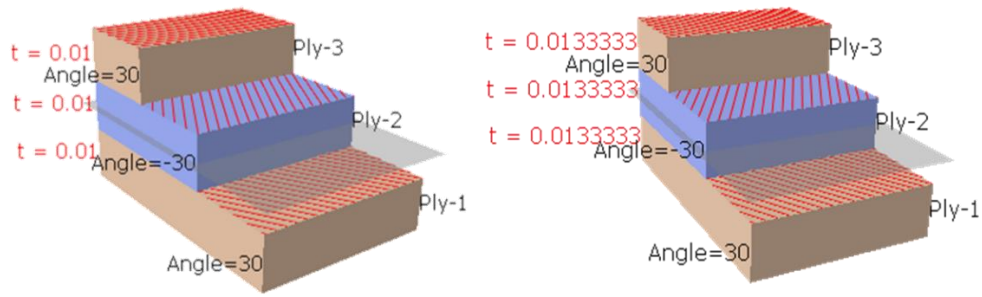


Figure 6.6 : Ply stacking $[30^\circ/-30^\circ/30^\circ]$ of one fold and two folded composite thin plate with reference surface ($z=0$) and thickness respectively.

Table 6.7 : Comparison of non-dimensional natural frequencies of the composite $[30^\circ/-30^\circ/30^\circ]$ clamped thin plate with Material I.

Description of plate	Modes	Present-Kirchhoff	Present-Mindlin	Present-ABAQUS	Niyogi, et al. (1999)
90° one folded (L=1.5m)	1	0.0416	0.0408	0.0412	0.0390
	2	0.0712	0.0712	0.0710	0.0712
	3	0.1500	0.1456	0.1476	0.1473
90° two folded (L=2m)	1	0.0915	0.0896	0.0896	0.0887
	2	0.1000	0.0977	0.0980	0.0992
	3	0.2116	0.2027	0.2073	0.2008

Table 6.8 : Comparison of natural frequencies (Hz) of the composite clamped thin plate with Material I $[30^\circ/-30^\circ/30^\circ]$ stacking sequence.

Description of plate	Modes	Present-Kirchhoff	Present-Mindlin	Present-ABAQUS
90° one folded (L=1.5m)	1	31.018	30.457	30.684
	2	53.084	53.037	52.943
	3	111.770	108.503	110.020
	4	123.220	123.780	124.53
	5	191.560	190.224	190.76
	6	211.340	212.107	211.41
90° two folded (L=2m)	1	51.125	50.071	50.092
	2	55.884	54.635	54.770
	3	118.26	113.298	115.88
	4	123.267	119.82	121.38
	5	149.847	148.845	146.83
	6	154.054	153.358	151.12

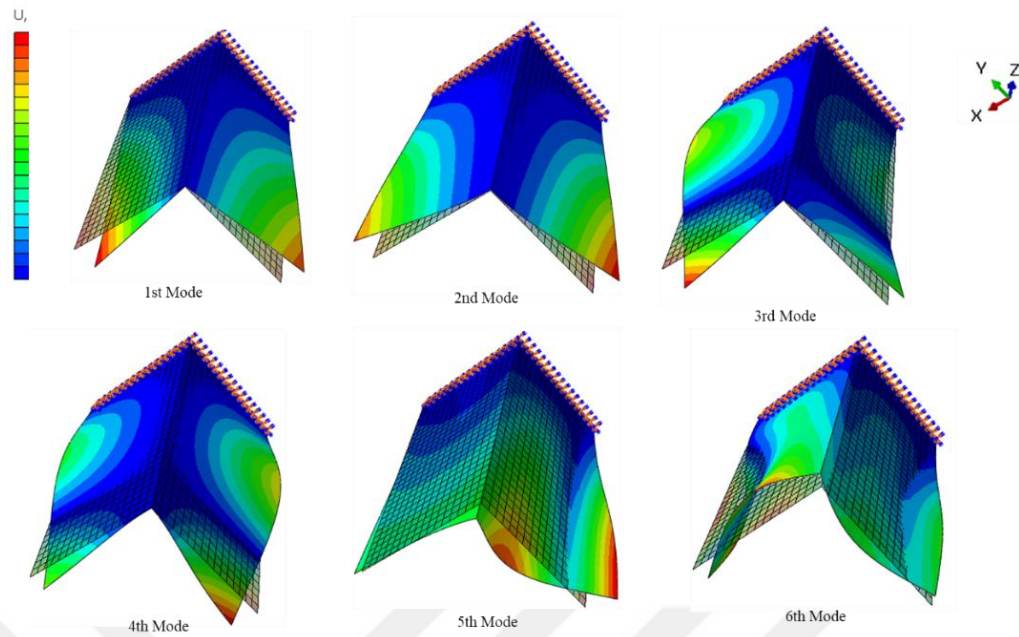


Figure 6.7 : Mode shapes of the one fold composite plate with Material I.

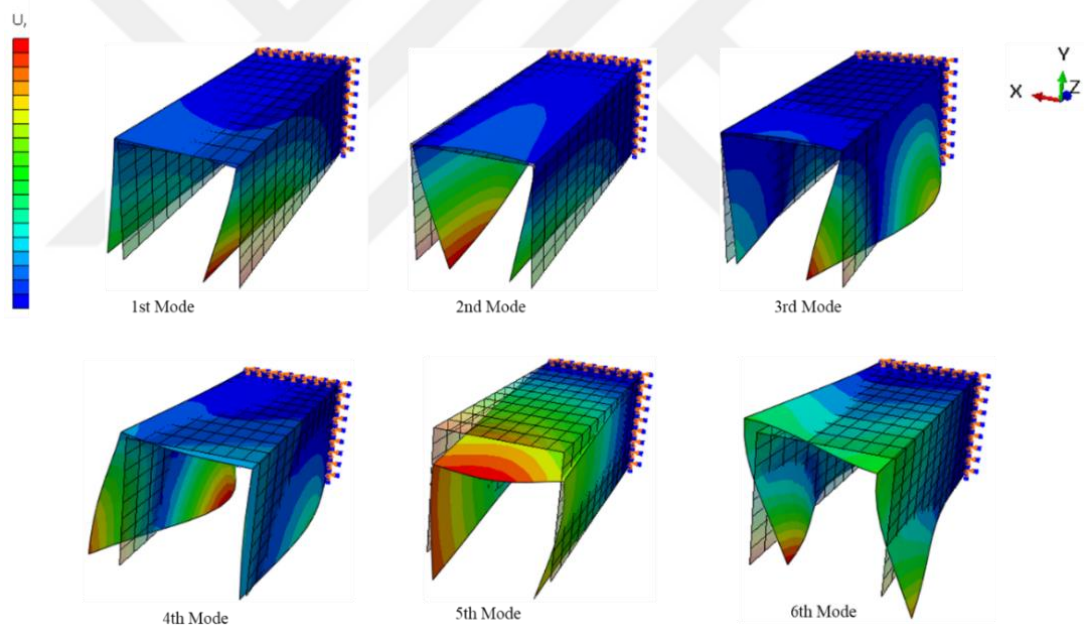


Figure 6.8 : Mode shapes of two fold composite plate with Material I.

For Material II, its material and dimension properties are shown in Table 6.9. The composite laminated one folded cantilever plate code results are compared with Halder & Sheikh (2005) and ABAQUS non-dimensional frequencies in Table 6.10. Stacking sequences of the laminated plates are $[0^\circ/90^\circ]$ and $[45^\circ/-45^\circ]$ respectively. All solutions of the one folded Material II composite plate use 16x8 mesh size is used.

Table 6.9 : The composite plate properties with Material II (Haldar & Sheikh, 2005).

Plate Properties	Values
E_1	$25 E_2 \text{ N/m}^2$
E_2	-
$G_{12}=G_{13}$	$0.5 E_2 \text{ N/m}^2$
G_{23}	$0.2 E_2 \text{ N/m}^2$
$\nu_{12}=\nu_{21}$	0.25
ρ	-
t_p	$h/2$
h	$0.01*L$
$2a$	L
$2b$	$L/2$
κ	$5/6$

Table 6.10 : Comparison of non-dimensional natural frequencies ($\lambda=L^2\omega\sqrt{(\rho/E_2)/h}$) of the one folded cantilever scomposite plate with Material II.

Description of plate	Modes	Present-Kirchhoff	Present-Mindlin	Present-ABAQUS	Haldar & Sheikh (2005)
90° one folded [0°/90°]	1	3.647	3.601	3.601	3.598
	2	9.976	9.901	9.681	9.663
	3	16.237	16.098	15.894	15.776
	4	19.394	19.194	18.894	18.771
	5	39.942	40.060	39.618	39.141
	6	41.830	41.615	41.159	40.186
90° one folded [45°/-45°]	1	5.876	5.666	5.518	5.527
	2	9.723	9.476	9.086	9.281
	3	19.459	18.585	17.887	18.216
	4	22.423	21.6	20.369	21.117
	5	33.338	32.447	31.404	31.695
	6	40.702	39.3327	36.842	38.141

It can be seen from the above results that the Mindlin approach FEM code for composite thin folded plates works better than others.

Secondly, for the thick folded composite plates which have lower thickness ratio ($L/h < 10$) the code is prepared based on RMPT with Material I again. Besides, the thickness of plate h equals to $2b/5$ and it consists of 6 ply which is $[30^\circ/-30^\circ/30^\circ/30^\circ/-30^\circ/30^\circ]$ stacking sequence and t_p equals to $h/6$.

The thick folded plate Mathematica FEM code natural frequencies are compared with ABAQUS results at Table 6.11. All solutions of the one folded cantilever composite plate use 32×16 mesh size and for two folded plates, 24×8 mesh size is used.

The following results gives that the Mindlin approach FEM code for the composite thick plate converges ABAQUS program in terms of natural frequencies values. The Kirchhoff FEM code, which diverges from the actual natural frequency values when the thickness ratio of the plate is higher, is not applied on the plate.

Table 6.11 : Comparison of natural frequencies (Hz) of the composite cantilever thick plate with Material I $[30^\circ/-30^\circ/30^\circ/30^\circ/-30^\circ/30^\circ]$ sequence.

Description of plate	Modes	Present-Mindlin	Present-ABAQUS
90° one folded ($2a=1.5$ m, $2b=0.75$ m, $h=0.15$ m)	1	140.71	139.79
	2	180.99	178.27
	3	335.51	331.00
	4	377.61	373.46
	5	496.19	494.39
	6	551.07	546.85
90° two folded ($2a=2$ m, $2b=0.667$ m, $h=0.133$ m)	1	95.99	93.89
	2	157.69	154.18
	3	175.83	167.79
	4	286.04	281.99
	5	323.97	307.42
	6	363.35	350.72

6.2. Box Beams and Results

In this thesis, each of fold length is equal to $2b$ or $2c$ of rectangular plate dimension, box length is equal to $2a$ dimension of plate and plate thickness is equal to h . The box beam and their dimensions are represented in Figure 6.9. Property tables are given in related sections for both isotropic and orthotropic box beams with different materials and boundary conditions.

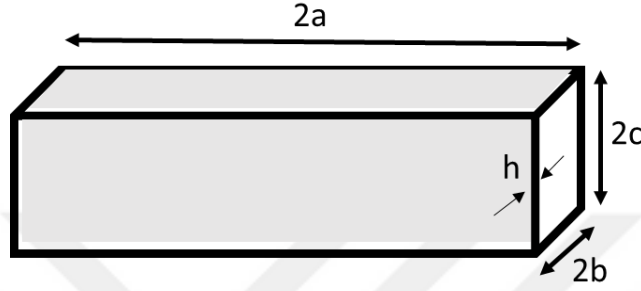


Figure 6.9 : The box beam representation.

At the transformation submatrix, the angle between global and local axis are is taken as 90° for first fold, 180° for the second fold and 270° for the third fold. Because the first face of folded plate is assumed on global axes. The transformation submatrices R_1 , R_2 and R_3 are given in equations 6.9a, 6.9b and 6.9c. The transformation submatrix for 270° given by

$$[R_4] = \begin{bmatrix} 1 & 0 & 0 & 0 & 0 & 0 \\ 0 & 0 & 1 & 0 & 0 & 0 \\ 0 & -1 & 0 & 0 & 0 & 0 \\ 0 & 0 & 0 & 1 & 0 & 0 \\ 0 & 0 & 0 & 0 & 0 & 1 \\ 0 & 0 & 0 & 0 & -1 & 0 \end{bmatrix} \quad (6.10)$$

where R_4 is transformation submatrix of bottom face (third fold) of box.

The isotropic box beam study is considered both the KLPT and the RMPT. For thin boxes Gauss integration scheme method is used on RMPT. The composite laminated box beams, the RMPT are applied on different stacking sequenced composite plates with membrane effects which are mention in section 5 due to consideration of transverse shear deformation effects through composite laminate.

6.2.1. The isotropic box beam

The non-dimensional natural frequencies of box beams which are clamped at one side and also have crank angle 90° are validated with developed code in Mathematica. Two code studies are developed as one of these is based on the KLPT and the other one is RMPT with Gauss selective integration scheme method. At the same time, the natural frequencies of box beams are obtained from mathematical modal in ABAQUS.

First study is examination of the thin isotropic box beams which have Material III. Its material and dimension properties are shown in Table 6.12.

Table 6.12 : The isotropic thin box beam properties with Material III (Ramkumar & Kang, 2013).

Plate Properties	Values
E	$210 \times 10^9 \text{ N/m}^2$
ρ	7850 kg/m^3
ν	0.3
h	0.004 m
2a	0.75m
2b=2c	0.15m
κ	5/6

The comparison of Mathematica code results, ABAQUS results and Ramkumar & Kang (2013) for Material III can be seen in Table 6.13. Two different type boundary conditions are applied on box beams: clamped-free (cantilever) and clamped-clamped. The mesh size 32x8 is used for all the face of box.

Mode shapes of first 6 modes are represented in Figure 6.10 and Figure 6.11 for cantilever and clamped-clamped isotropic box beams with Material III respectively. The mesh size is used as 150x30 at ABAQUS and deformed shapes are shown with undeformed shape of box beam in order to realize of changing.

Table 6.13 : Comparison of natural frequencies (Hz) of the thin isotropic box beam with Material III.

Boundary Condition	Modes	Present-Kirchhoff (32x8)	Present-Mindlin (32x8)	Present-ABAQUS (32x8)	Present-ABAQUS (150x30)	Ramkumar & Kang (2013)
Clamped-Free	1	277.36	277.68	277.09	276.78	277
	2	277.36	277.68	277.09	276.78	277
	3	309.69	311.30	311.45	308.86	309
	4	438.92	444.50	449.35	438.37	438
	5	475.18	479.52	485.54	474.84	475
	6	546.33	548.74	556.86	546.26	547
Clamped-Clamped	1	457.31	463.20	466.62	457.48	457
	2	518.01	522.48	527.60	518.66	518
	3	617.25	621.20	628.28	618.84	618
	4	647.34	658.00	665.59	647.02	646
	5	647.34	658.00	665.59	647.02	646
	6	730.97	743.88	753.97	732.19	730

The result tables give The Kirchhoff FEM code works better than the modified Mindlin FEM code for the thin box beam and converges ABAQUS program which is divided into more elements in terms of actual Ramkumar & Kang (2013) natural frequencies values. The modified Mindlin FEM code also closes the 32x8 mesh ABAQUS results and almost as good as the Kirchhoff. Besides, the different boundary condition effects on vibration of box beams can be seen.

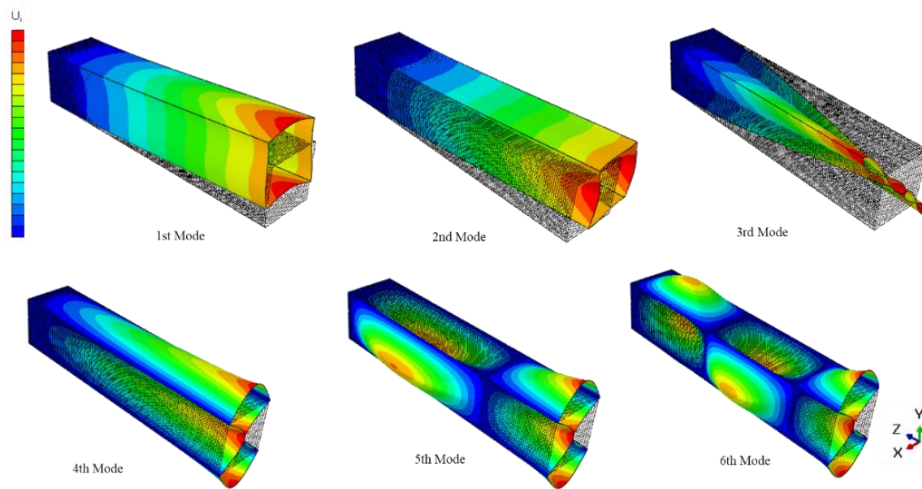


Figure 6.10 : Mode shapes of the clamped-free thin Material III isotropic box beam with deformed and undeformed shapes.

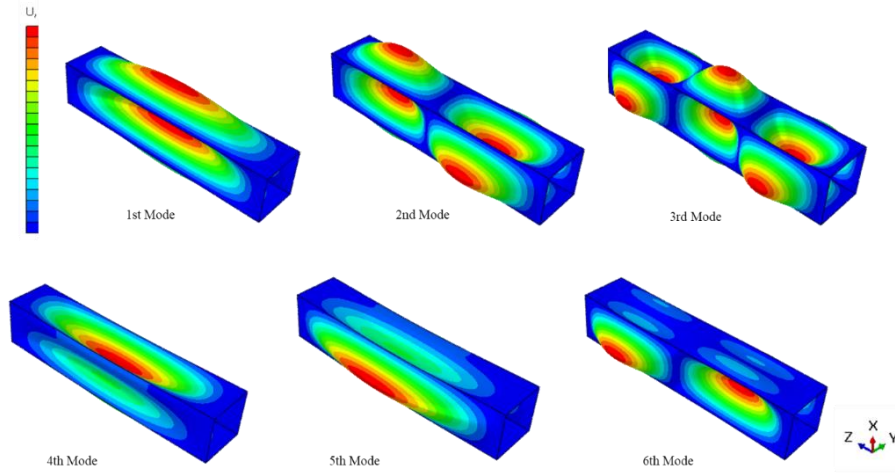


Figure 6.11 : Mode shapes of the clamped-clamped thin isotropic box beam with Material III.

After that, the thick isotropic box beam which has Material III is analyzed h taken as 0.04 m. Only RMPT is applied on it because of thickness to length ratio of plate ($L/h < 10$). The comparison of Mathematica code results and ABAQUS results are compared each other in Table 6.14. The mesh size is used as 16×4 for all of the box faces. Their mode shapes that obtained by ABAQUS can be seen in Figure 6.12 and Figure 6.13.

Table 6.14 : Comparison of natural frequencies (Hz) of the thick isotropic box beam with Material III.

Boundary Condition	Modes	Present-Mindlin (32x8)	Present-ABAQUS (32x8)	Present-ABAQUS (75x15)
Clamped-Free	1	291.45	290.30	290.46
	2	291.45	290.30	290.46
	3	958.50	958.52	957.86
	4	1294.98	1291.1	1288.2
	5	1294.98	1291.1	1288.2
	6	1728.75	1728.5	1728.2
Clamped-Clamped	1	1203.98	1202.1	1196.9
	2	1203.98	1202.1	1196.9
	3	1926.42	1929.2	1924.2
	4	2497.13	2498.0	2472.9
	5	2497.13	2498.0	2472.9
	6	2581.07	2541.2	2513.0

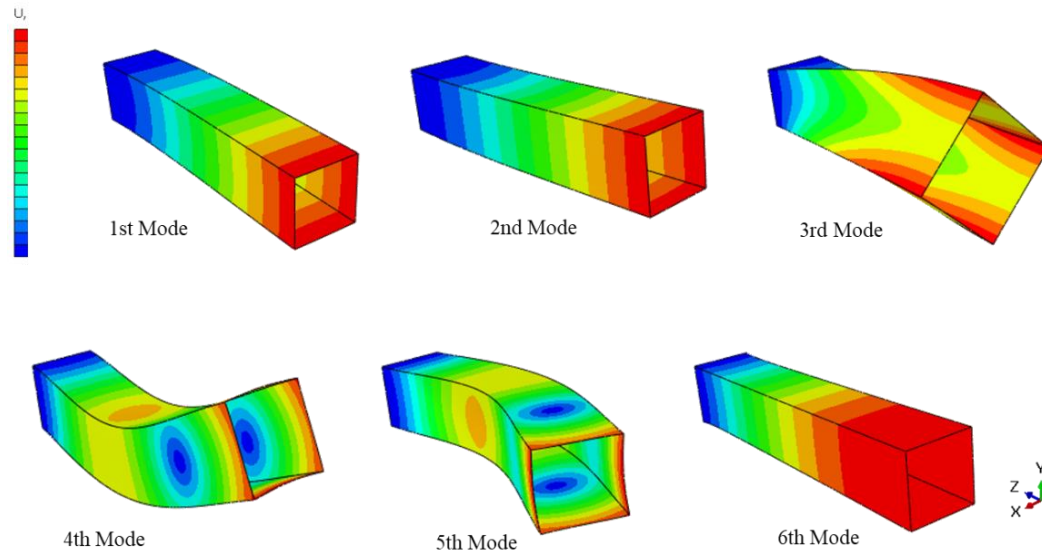


Figure 6.12 : Mode shapes of the thick clamped-free Material III isotropic box beam.

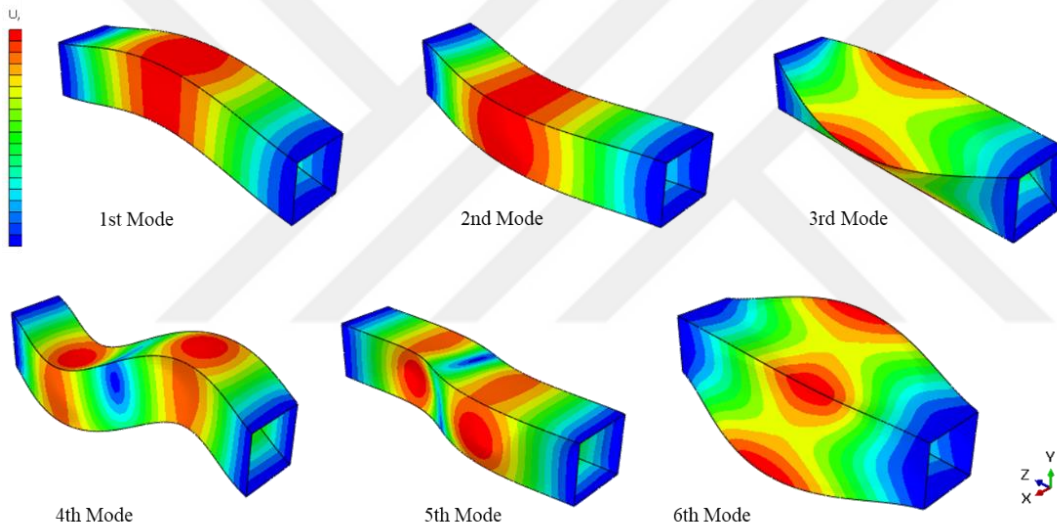


Figure 6.13 : Mode shapes of thick clamped-clamped Material III isotropic box beam.

6.2.2. The composite laminated box beam

The composite laminated plate thickness is equal to h while one ply thickness is equal to t_p . The different stacking sequences and boundary conditions are evaluated for examination of composite box beam vibration characteristics. The natural frequencies of composite laminated box beams which have crank angle 90° are validated with developed code in Mathematica.

Two code studies are developed as one of these is based on the KLPT and the other one is RMPT with Gauss selective integration scheme method for thin composite box beams. For the thick composite box beam, only one FEM code developed based on RMPT.

Table 6.15 : The composite laminated thin box beam properties with Material IV (Ramkumar & Kang, 2013).

Plate Properties	Values
Material	Glass/Epoxy
E_1	37.78 GPa
E_2	10.9 GPa
$G_{12}=G_{13}= G_{23}$	4.91 GPa
$\nu_{12}= \nu_{21}$	0.3
ρ	1870 kg/m ³
t_p	$h/5$ m
h	0.004 m
$2a$	0.75m
$2b=2c$	0.15m
κ	5/6

The composite box beam, which is made with Material IV, is examined with different stacking sequences and compared. Its material and dimension properties are shown in Table 6.15. The comparison of Mathematica code results, ABAQUS FEM results and Ramkumar & Kang (2013) for Material IV can be seen in Table 6.16.

Two different type boundary conditions are applied on box beams. One of them is clamped-free ends and the other is clamped at both ends. The mesh size has 2 type as 16x4 and 32x8 for all the face of box.

The first 5 ABAQUS mode shapes of thin box beams, which has material IV, are examined as using Figure 6.14, Figure 6.15, Figure 6.16 and Figure 6.17 at different boundary conditions and stacking sequence. For instance, the first and second modes of cantilever box beam column bending which have the same natural frequency because of the symmetry. The third mode is column torsion, fourth mode is a first plate bending mode and the rest of the modes are higher plate bending modes.

Table 6.16 : Comparison of natural frequencies (Hz) of the composite thin box beam with Material IV.

Stacking Sequence	Boundary Condition	Modes	Present-Kirchhoff (16x4)	Present-Mindlin (16x4)	Present-Mindlin (32x8)	Present-Abaqus (32x8)	Ramkumar & Kang (2013)
[45/45/45/ 45/45]	Clamped-Free	1	147.81	148.65	146.02	146.7	146.7
		2	147.81	148.65	146.02	146.7	146.7
		3	168.63	172.65	166.22	170.25	168.68
		4	251.13	267.08	252.19	260.91	255.71
		5	286.00	297.87	285.32	295.44	289.19
	Clamped-Clamped	1	267.61	283.75	269.70	279.68	274.27
		2	317.25	329.06	317.05	328.53	321.56
		3	360.19	398.32	365.51	378.85	368.69
		4	360.19	398.32	365.51	378.85	368.69
		5	392.59	402.76	390.75	405.41	395.52
[90/90/90/ 90/90]	Clamped-Free	1	135.61	135.84	134.97	133.41	133.5
		2	135.61	135.84	134.97	133.41	133.5
		3	228.05	234.93	227.39	228.34	226.1
		4	367.67	392.34	370.78	373.56	366.49
		5	374.69	400.66	379.22	383.89	376.85
	Clamped-Clamped	1	370.75	396.30	374.44	378.63	371.61
		2	382.89	410.17	389.24	396.44	389.48
		3	405.83	437.13	416.59	428.21	421.08
		4	442.59	473.98	451.73	456.58	449.36
		5	442.59	473.98	451.73	456.58	449.36

The modified Mindlin FEM code for thin composite box structure gives closer results to Ramkumar & Kang (2013) natural frequencies values than ABAQUS results and the Kirchhoff FEM code when divided into more elements. In addition, the different boundary conditions and angle orientation of plies affect vibration of box beams. The 45° ply laminates have more natural frequency in first bending modes but other modes are higher for 90°. As a result of this, bending coupling effects are estimated in terms of angle ply or cross ply usage.

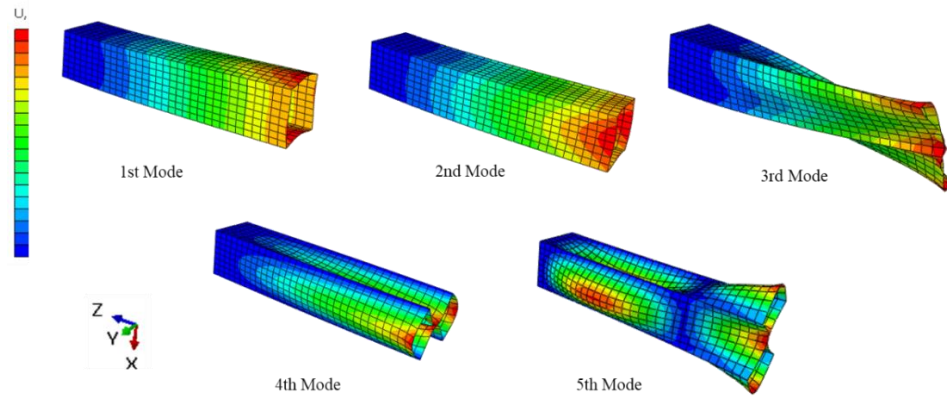


Figure 6.14 : Mode shapes of the [45/45/45/45/45] composite clamped-free box beam.

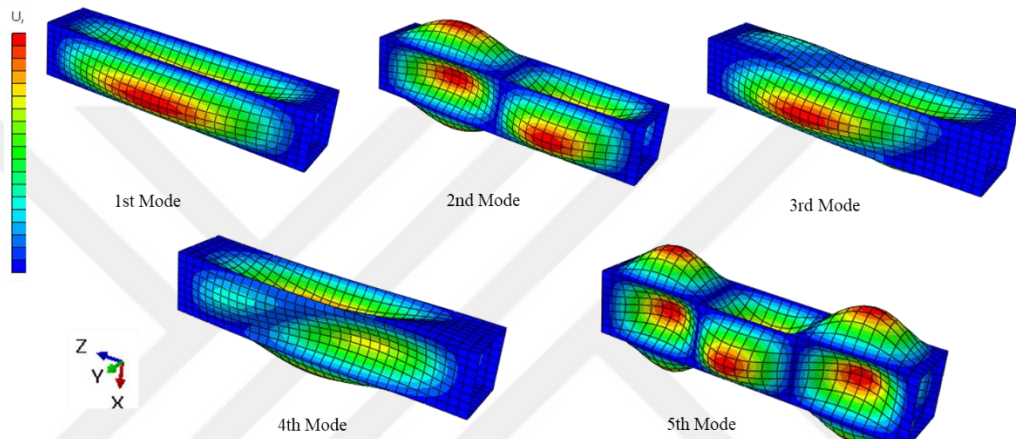


Figure 6.15 : Mode shapes of the [45/45/45/45/45] composite clamped-clamped box beam.

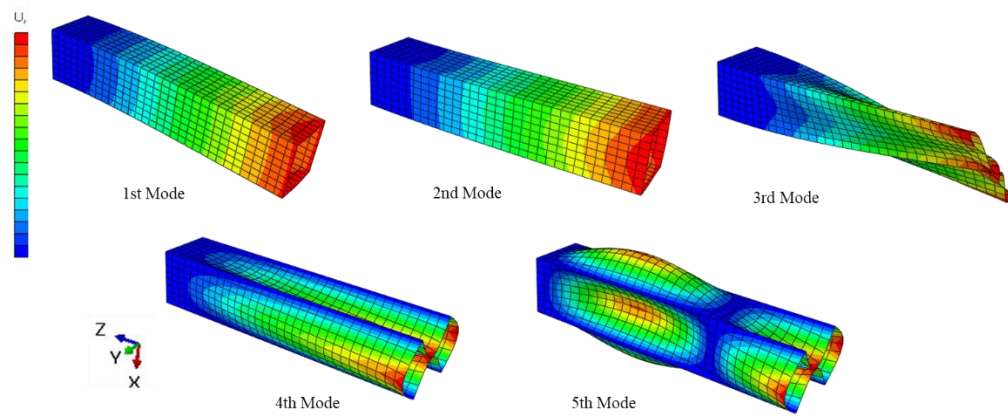


Figure 6.16 : Mode shapes of the [90/90/90/90/90] composite clamped-free box beam.

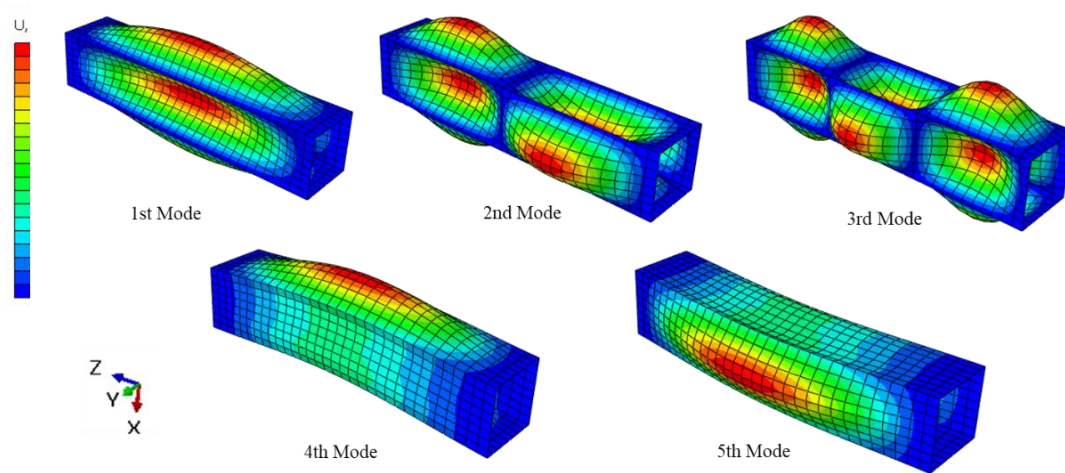


Figure 6.17 : Mode shapes of the [90/90/90/90/90] composite clamped-clamped box beam.

The cantilever thin composite box beam which is made with Material V is examined according to its material and dimension properties are shown in Table 6.17. The stacking sequence of this cantilevered composite box beam is $[0_3/90_2/0_3]$.

The comparison of Mathematica code results and ABAQUS results for Material VI can be seen in

Table 6.18. The mesh size is 16x4 for all the face of box.

Table 6.17 : The composite laminated box beam properties with Material V.

Plate Properties	Values
Material	Graphite/Epoxy
E_1	23.69 GPa
E_2	7.63 GPa
$G_{12}=G_{13}= G_{23}$	3.37 GPa
ν_{12}	0.26
ρ	1985 kg/m ³
t_p	0.00025 m
2a	0.655 m
2b	0.057 m
2c	0.019 m
κ	5/6

Table 6.18 : Comparison of natural frequencies (Hz) of the composite thin box beam with Material V $[0_3/90_2/0_3]$.

Modes	Present-Kirchhoff	Present-Mindlin	Present-ABAQUS
	(16x4)	(16x4)	(16x4)
1	35.50	35.50	35.14
2	80.97	80.97	80.20
3	206.67	207.58	202.73
4	313.44	314.67	309.82
5	461.25	461.88	458.75

The modified Mindlin FEM code and the Kirchhoff FEM code for thin cantilever composite box structure give closer results each other and their tolerances are better than ABAQUS. The mode shapes of first 6 modes are represented in Figure 6.18 for cantilever composite box beams with Material V.

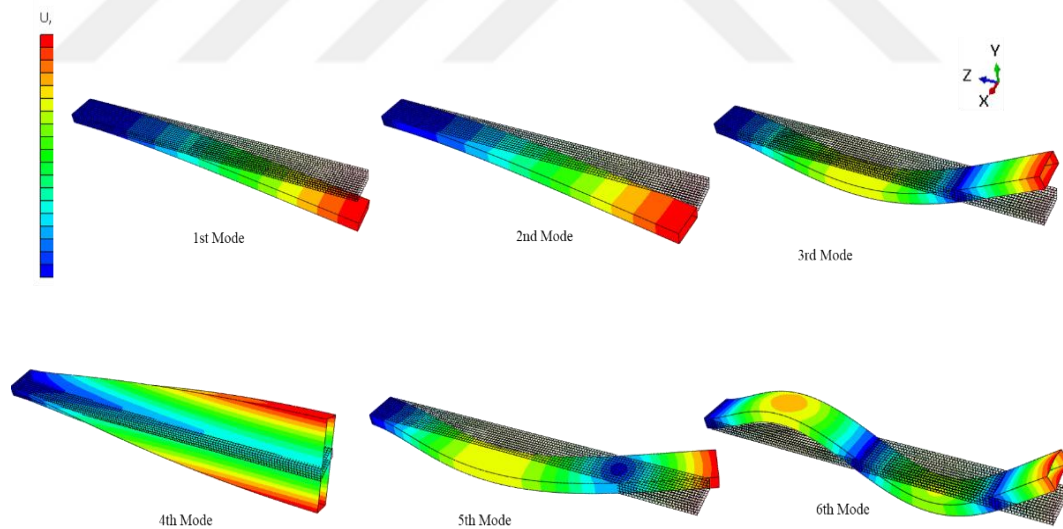


Figure 6.18 : Mode shapes of the thin cantilever Material V composite box beam with undeformed and deformed shapes.

After that, the thick composite box beam, which has material V, properties and stacking sequence are shown in Table 6.17 except t_p equals to 0.0005 m. The RMPT is applied as a result of higher thickness to length ratio. The Mathematica code results and ABAQUS results are compared each other in Table 6.19. The mesh size is 24x6 for all of the box faces.

Table 6.19 : Comparison of natural frequencies of the composite thick box beam with Material V $[0_3/90_2/0_3]$.

Modes	Present-Mindlin (Hz)	Present-ABAQUS (Hz)
1	34.74	35.42
2	79.20	81.11
3	203.53	204.13
4	325.51	324.96
5	451.42	459.19
6	519.85	509.85

The RMPT FEM code is used for thick cantilever composite box structure due to better tolerances on composites and high thicknesses. For the same lattice sizes, Mathematica FEM code appears to work better than ABAQUS when comparing box beam results. Their mode shapes that obtained by ABAQUS can be seen in Figure 6.19.

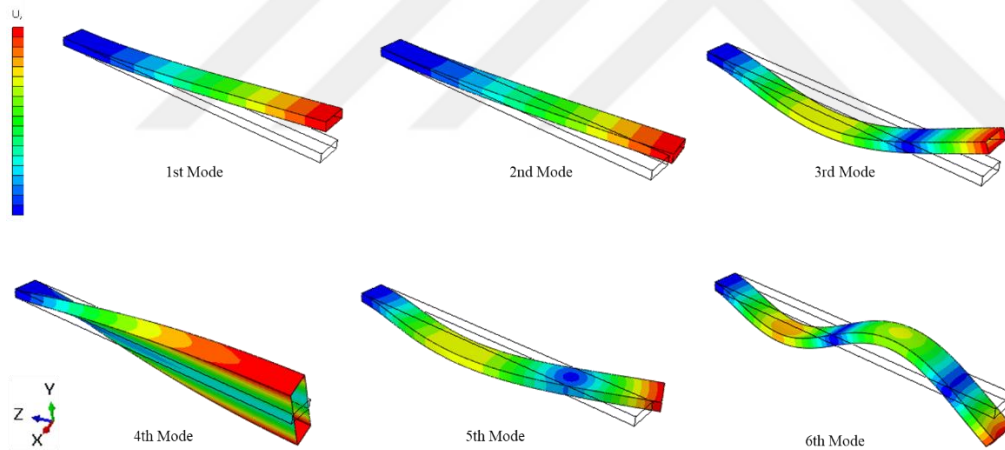


Figure 6.19 : Mode shapes of the thick cantilever Material V composite box beam with undeformed and deformed shapes.

7. CONCLUSIONS AND RECOMMENDATION

In this thesis, the flat plates, folded plates and box beams are examined to know the influence of altered thickness and boundary conditions on behavior of structures in terms of frequency. Examination of the vibration is evaluation process of the isotropic and composite plates that have different length-to-thickness ratio under different boundary conditions. However, the plates and plate theories are specified according to changed length to thickness ratio. In order to obtain more precise results, research is made on folded plates and box sections with the same geometric parameters or material properties based on the comparison factor.

From the studies on folded plates and box beams, the following conclusions can be drawn about effect on frequencies, such as:

- For plates, folded plates and box beams which have low length to thickness ratio ($L/h < 10$ -thick), the RMPT approach FEM code is better than the other compared theories. The KLPT FEM code diverges from the actual natural frequency for this plates.
- For thin plates ($L/h > 10$) the KLPT approach FEM code is more applicable but the modified Mindlin can be used and gives almost close results.
- It can be seen from the comparing results that the RMPT approach FEM code works better than others as a result of taking into account the changing transverse shear deformation effects across the laminate for composite folded plates.
- The isotropic box beams are investigated, for thick ones RMPT FEM gives closer to actual natural frequencies of structure. Also, for thins modified RMPT FEM code and the KLPT FEM code are almost at same accuracy.
- The composite laminated box beams are considered, the RMPT FEM gives best results. In addition, for thins modified RMPT FEM code and the KLPT FEM have better tolerances than ABAQUS.

- The different boundary condition effects on vibration of box beams can be seen that clamped condition increases the natural frequencies when compared clamped-clamped and cantilever box beam frequencies. So, it can be concluded that the increase in the restricted DOF affects the frequency to increase the frequency because of the effect of altered stiffness, inertia terms. These effects can also be examined on the mode shapes.
- The stacking sequence and angle orientations affect the natural frequency. For this evaluation, it can be compared that angle ply and cross ply orientations. The angle ply laminates have more natural frequency in first bending mode as a result of bending coupling like 45° plies.
- Especially, ABAQUS diverges at high modes of box beams. For the same lattice sizes, Mathematica FEM code appears to work better on the composite boxes.
- There is a frequency fall with decreasing thickness of plate which means the slender structure would have failure at lower vibration levels like local vibrations.
- The variances between the theories rely on many parameters such as angle orientations, stacking sequences, thickness, and BCs.
- The transverse shear terms play significant role in analyzing folded and box structures especially composite ones to achieve better accuracy. At the same time, the membrane effects cannot be neglected for this type structures owing to the fact that the stiffness and mass matrices are transformed as planar.

Consequently, the various end conditions, lay-ups and materials have been appeared to response differently as above. Folding is observed with little differences by both of the theories for isotropic structures but for composites, RMPT can be preferred to obtain better accuracy on behavior.

It may be recommended to consider aeroelastic effects in future studies. Aerodynamic formulations can be implemented in this work. Also, Circumferentially Asymmetric Stiffness/Circumferentially Uniform Stiffness Configuration thin walled beams examination with above methods can be another recommendation. The rotation can be added to evaluate vibration characteristics of structures such as helicopter blades.

REFERENCES

- Augarde, C. E.** (2004). Generation of shape functions for rectangular plate elements. *Communications in Numerical Methods in Engineering*, 20(8), pp. 655-663. doi:10.1002/cnm.703
- Chakraverty, S.** (2009). *Vibration of Plates*. Boca Raton, Florida: CRC Press.
- Cook, R. D., Malkus, D. S., Plesha, M. E., & Witt, R. J.** (2001). *Concepts and Applications of Finite Element Analysis*. Wiley.
- Haldar, S., & Sheikh, A. H.** (2005). Free Vibration Analysis of Isotropic and Composite Folded Plates Using A Shear Flexible Element. *Finite Elements in Analysis and Design*, 208-226.
- Hinton, E., & Bicanic, N.** (1979). A Comparison of Lagrangian and Serendipity Mindlin Plate Elements for Free Vibration Analysis. *Computers & Structures*, 10, 483-493.
- Irie, T., Yamada, G., & Kobayashi, Y.** (1984). Free vibration of a cantilever folded plate. *J. of Acoustical Society of America*, 1743-1748.
- Liu, W. H., & Huang, C. C.** (1992). Vibration Analysis of Folded Plates. *Journal of Sound and Vibration*, 157(1), 123-137.
- Nettles, A. T.** (1994). *Basic Mechanics of Laminated Composite Plates*. Alabama: NASA.
- Nguyen-Van, H., Mai-Duy, N., & Tran-Cong, T.** (2008). Free vibration analysis of laminated plate/shell structures based on FSDT with a stabilized nodal-integrated quadrilateral element. *Journal of Sound and Vibration*, 205-223. doi:10.1016/j.jsv.2007.11.043
- Niyogi, A. G., Laha, M. K., & Sinha, P. K.** (1999). Finite element vibration analysis of laminated. *Shock and Vibration*, 273-283.
- Noor, A. K.** (1972). Free Vibrations of Multilayered Composite Plates. *AIAA Journals*.
- Oñate, E.** (2013). *Structural Analysis with the Finite Element Method* (Vols. Beams, Plates and Shells). Barcelona, Spain: Springer.
- Petyt, M.** (1990). *Introduction to Finite Element Vibration Analysis*. Cambridge, United Kingdom: Cambridge University Press.
- Ramkumar, K., & Kang, H.** (2013). Finite element based investigation of buckling and vibration behaviour of thin walled box beams. *Applied and Computational Mechanics*, 155-182.
- Rao, S. S.** (1993). *Mechanical Vibrations*. Prentice Hall.

- Reddy, J. N., & Phan, N. D.** (1985). Stability and Vibration of Isotropic, Orthotropic and Laminated Plates According to A Higher-Order Shear Deformation Theory. *Journal of Sound and Vibration*, 98(2), 157-170.
- Reed, R. E.** (1965). *Comparison of Methods in Calculating Frequencies of Corner-Supported Rectangular Plates*. California: NASA Ames Research Center.
- Seegerlind, L. J.** (1984). *Applied Finite Element Analysis*. Canada: John Wiley and Sons.
- Szilar, R.** (2004). *Theories and applications of plate analysis: classical, numerical and engineering methods*. John Wiley & Sons.
- Thai, C. H., Nguyen-Xuan, H., Nguyen-Thanh, N., Le, T.-H., Nguyen-Thoi, T., & Rabczuk, T.** (2012). Static, free vibration, and buckling analysis of laminated composite Reissner–Mindlin plates using NURBS-based isogeometric approach. *International Journal for Numerical Methods in Engineering*. doi:10.1002/nme.4282

CURRICULUM VITAE



Name Surname : Buse Tuğçe TEMUÇİN
Place and Date of Birth : Bahçelievler 13.10.1994
E-Mail : tugcetemucin94@gmail.com

EDUCATION

:

- **B.Sc.** : 2017, Istanbul Technical University, Faculty of Aeronautics and Astronautics, Aeronautical Engineering
- **M.Sc.** : 2020, Istanbul Technical University, Faculty of Aeronautics and Astronautics, Aeronautical and Aerospace Engineering

PROFESSIONAL EXPERIENCE AND REWARDS:

- 2017-Turkish Aerospace Industry Structural Design Engineer

OTHER PUBLICATIONS, PRESENTATIONS AND PATENTS:

- **Temuçin, B.T., Özdemir, Ö.** (2018). Yeni Nesil Helikopter Pallerinin Yapısal İncelemesi, *VII. ULUSAL HAVACILIK VE UZAY KONFERANSI* UHUK-2018-056